



Aus der Kinderklinik und Kinderpoliklinik im Dr. von Haunerschen Kinderspital des  
Klinikums der Ludwig-Maximilians-Universität München

Direktor: Prof. Dr. med. Dr. sci. nat. Christoph Klein

**Generation and functional characterization of induced pluripotent  
stem-cell-derived keratinocytes as an *in-vitro* model for Cockayne  
Syndrome, Xeroderma Pigmentosum and UV-sensitive Syndrome**

Dissertation

zum Erwerb des Doktorgrades der Medizin

an der Medizinischen Fakultät der  
Ludwig-Maximilians-Universität zu München

vorgelegt von

Tobias Gabriel Prell

aus

München

2022

Mit Genehmigung der Medizinischen Fakultät  
der Universität München

Berichterstatter: Prof. Dr. med. Dr. sci. nat. Christoph Klein

Mitberichterstatter: PD Dr. rer. hum. biol. Robert Besch  
Prof. Dr. med. Lucie Heinzerling, M.P.H.  
Prof. Dr. med. Ortrud Steinlien

Mitbetreuung durch den  
promovierten Mitarbeiter:

Dekan: Prof. Dr. med. Thomas Gudermann

Tag der mündlichen Prüfung: 23.03.2022

# Eidesstattliche Versicherung

Tobias Gabriel Prell

Ich erkläre hiermit an Eides statt,  
dass ich die vorliegende Dissertation mit dem Titel:

**Generation and functional characterization of induced pluripotent stem-cell-derived keratinocytes as an *in-vitro* model for Cockayne Syndrome, Xeroderma Pigmentosum and UV-sensitive Syndrome**

selbständig verfasst, mich außer der angegebenen keiner weiteren Hilfsmittel bedient und alle Erkenntnisse, die aus dem Schrifttum ganz oder annähernd übernommen sind, als solche kenntlich gemacht und nach ihrer Herkunft unter Bezeichnung der Fundstelle einzeln nachgewiesen habe.

Ich erkläre des Weiteren, dass die hier vorgelegte Dissertation nicht in gleicher oder in ähnlicher Form bei einer anderen Stelle zur Erlangung eines akademischen Grades eingereicht wurde.

München, 04.04.2022

Ort, Datum

Tobias Prell

Tobias Prell

## Table of contents

<b>Summary .....</b>	<b>3</b>
<b>Zusammenfassung.....</b>	<b>4</b>
<b>1. Introduction.....</b>	<b>5</b>
1.1. General Outline.....	5
1.2. Biochemical and clinical description of diseases examined.....	12
1.2.1. Xeroderma pigmentosum.....	12
1.2.2. Cockayne Syndrome.....	16
1.2.3. UV-Sensitive Syndrome.....	19
1.3. Research objectives.....	23
1.3.1. Creation and use of iPS cell models of UV light sensitive syndromes.....	23
1.3.2. Differentiation of iPS cells and opportunities for application in clinical setting.....	24
1.3.3. Standardized induction of DNA damage and meaning for translational medicine.....	25
<b>2. Materials and methods.....</b>	<b>27</b>
2.1. Induction of pluripotency into cells from a patient with Cockayne Syndrome.....	27
2.2. Specific genomic knockdown by CRISPRi technology.....	31
2.3. Implementation of an effective iPS cell-to-Keratinocyte differentiation protocol.....	44
2.4. Comparison of cell lines WTC, C5, ERCC3, ERCC6, E1S and UVSSA.....	55
2.4.1. Basic comparison on iPS cell level.....	55
2.4.2. Comparison on iPS cell level and differentiated level using UV light and H <sub>2</sub> O <sub>2</sub> .....	57
<b>3. Results .....</b>	<b>62</b>
3.1. Induction of pluripotency into cells from a patient with Cockayne Syndrome.....	62
3.2. Specific genomic knockdown by CRISPRi technology.....	63
3.3. Implementation of an effective iPS cell-to-Keratinocyte differentiation protocol.....	72

---

3.4. Comparison of cell lines WTC, C5, ERCC3, ERCC6, EIIS and UVSSA.....	86
3.4.1. Basic comparison on iPS cell level.....	86
3.4.2. Comparison on iPS cell level and differentiated level using UV light and H <sub>2</sub> O <sub>2</sub> .....	88
<b>4. Discussion.....</b>	<b>99</b>
4.1. Implementation of an iPS cell-to-Keratinocyte differentiation protocol.....	99
4.2. Difficulties of gene knockdown in iPS cells.....	101
4.3. Translational medicine based on this research.....	102
<b>5. References.....</b>	<b>105</b>
<b>6. List of abbreviations .....</b>	<b>112</b>
<b>7. Appendix.....</b>	<b>115</b>
<b>Permission of data usage.....</b>	<b>115</b>
<b>Danksagung.....</b>	<b>116</b>
<b>謝辭.....</b>	<b>117</b>

**Summary**

Recent progress in induced pluripotent stem-cell (iPS) research and genome editing has enabled the development of new approaches in clinical research for previously incurable diseases. Using these new technologies, I sought deeper understanding of a group of related diseases, namely Cockayne syndrome, xeroderma pigmentosum, and UV-sensitive syndrome. The shared features in these diseases are their heredity aspect and the insufficiency of repair systems for DNA damage. The impairment of DNA repair systems leads to successive accumulation of genomic mutations, which often greatly elevate the risk of cancer and neuronal damage, and the skin's sensitivity to ultraviolet (UV) light exposure. The specific differences among these related diseases are unknown. Effective therapies have also not yet been discovered. In this study, I used Clustered Regularly Interspaced Short Palindromic Repeats interference (CRISPRi), a method that can specifically and efficiently suppress genes of interest in undifferentiated and differentiated iPS cells. I developed a system to elucidate molecular mechanisms that cause the specific characteristics of the diseases. For instance, when I suppressed *ERCC6*, a gene responsible for Cockayne syndrome, cell proliferation of iPS cells was impaired. A similar phenotype was observed using iPS cells generated from a Cockayne syndrome patient, suggesting that CRISPRi can reproduce the diseases' phenotypes. This thesis will discuss differences and commonalities in phenotypes among the three diseases at the cellular and molecular levels. My work is based on suppressing the genes that are responsible for the diseases by testing iPS cells and iPS-cell-derived keratinocytes. Based on these findings new ideas for implication as therapy may be considerable, which I will discuss at the end of this thesis.

## Zusammenfassung

Die Fortschritte der Forschung an induzierten pluripotenten Stammzellen (iPS cells) sowie im Bereich des Genom-Editing ermöglichen zahlreiche neue Herangehensweisen an bisher unheilbare Krankheiten. Mit diesen neuen Technologien habe ich versucht, ein tieferes Verständnis über eine Gruppe solcher Krankheiten mit schlechter Prognose zu erlangen – namentlich das *Cockayne*-Syndrom, *Xeroderma Pigmentosum* und das *UV-Sensitive*-Syndrom. Die Gemeinsamkeiten dieser drei Krankheiten sind deren Heredität und die Insuffizienz von DNA-Reparaturmechanismen. Aufgrund der beeinträchtigten Reparatursysteme akkumulieren sich sukzessive Schäden im Erbgut, was das Risiko der Tumorentwicklung erhöht, neuronale Schäden verursachen kann und oft zu Hypersensitivität gegenüber ultravioletter Strahlung führt.

Allerdings sind die genauen Unterschiede dieser Krankheiten bislang genauso wenig bekannt wie effektive Therapieansätze. In dieser Studie habe ich die Methode der *CRISPR interference* (CRISPRi) genutzt, mit der spezifisch und hocheffizient die Transkription bestimmter Genloci unterdrückt werden kann, sei es in undifferenzierten oder in ausdifferenzierten iPS-Zellen. Mit diesen Modellzellen habe ich ein experimentelles Setting entwickelt, um die jeweiligen Unterschiede im Phänotyp der Krankheiten auf molekularer Ebene besser zu verstehen.

So ist es mir gelungen, mit CRISPRi die Expression von *ERCC6*, dessen Ausfall zum *Cockayne*-Syndrom führt, zu unterdrücken und habe hierbei einen Rückgang in der Proliferationsrate dieser modifizierten iPS-Zellen beobachtet. Diese und andere Tendenzen zeigten sich auch in iPS-Zellen, hergestellt aus somatischen Zellen eines tatsächlichen Patienten mit dem *Cockayne*-Syndrom. Dies impliziert, dass meine Zellen als Modell geeignet sind.

In diesem Forschungsprojekt werde ich mithilfe der Modellzellen die Unterschiede und Gemeinsamkeiten der oben genannten Krankheiten auf molekularer wie auch zellulärer Ebene diskutieren und auf Grundlage dieser Erkenntnisse versuchen, Vorschläge für neue Herangehensweisen in der Therapie zu erarbeiten.

## 1. Introduction

### 1.1. General outline

One of the basic principles of life is the relative stability of genetic material. The equilibrium between small changes in the blueprint of life, which lead to diversity and adaptation to environmental challenges, and the perpetuation of genetic information on the other side is fundamental for evolution<sup>1</sup>. In maintaining this stability of genomes, nature has evolved several mechanisms to prevent and repair DNA damage. Damaging factors may be exogenous, such as ultraviolet light, carcinogenic aerosols due to air pollution, and intake of carcinogenic pesticides or heavy metals<sup>2</sup>. Endogenous factors, on the other hand, include oxidative stress and mistakes during reproduction of the genome for cell division; stochastic estimates suggest that spontaneous mutations occur naturally in about a third of the  $10^7$  cells that are dividing every second<sup>3</sup>. The human body provides several repair systems to face these mutations and to protect the human genome from changes.

These repair systems are categorized into a group of mechanisms that take care of double-strand breaks, and another group in charge of single-strand DNA damage. The latter is based on cutting out the erroneous site of the DNA strand and then replacing it with correctly arranged base pairs. Because of this principle, it is named the “excision repair system”<sup>4</sup> and it is classified into three main pathways: DNA mismatch repair (MMR), base excision repair (BER) and nucleotide excision repair (NER). MMR targets mismatched Watson-Crick base pairs, whereas BER recognizes specific non-bulky lesions in the DNA consisting of damaged bases, which are removed by specific glycosylases<sup>5</sup>. NER plays its main role in the excision of damage induced by ultraviolet (UV) light. This damage causes bulky DNA adducts, mostly thymine dimers and 6,4-

photoproducts. If an adduct of this kind is recognized by the system, a single-strand segment of several base pairs – including the lesion – will be removed, whereas the undamaged single-strand DNA remains as a template<sup>6</sup>. DNA polymerase then synthesizes the complementary sequence according to this template, followed by ligation to complete the corrected double strand.

There are two sub-pathways of NER: global genomic NER (GG-NER), which differs from the transcription-coupled NER (TC-NER) regarding the site of damage recognition. As implied by the name, GG-NER is able to recognize damage anywhere in the genome, while TC-NER occurs during transcription, therefore only in exons. However, both GG-NER and TC-NER end in a common final path of excision, repair and ligation<sup>7</sup>. Figure 1 shows some of the proteins involved and their interactions, summarized in a simplified pathway.

Several monogenic diseases have been linked to irregularities in the pathway of nucleotide excision repair (NER). That was why I sought to gain deeper insight into its mechanisms. The syndromes I examined are a group of autosomal recessive hereditary diseases: Cockayne syndrome (CS) (subtype CSA to C), xeroderma pigmentosum (XP) (subtypes XPA to G and XPV) and UV-sensitive syndrome (UVSS) (subtype *UVSSA*). Table 1 shows further details. The diseases are all associated with certain inefficiencies in either the GG-NER or the TC-NER sub-pathway, or both.

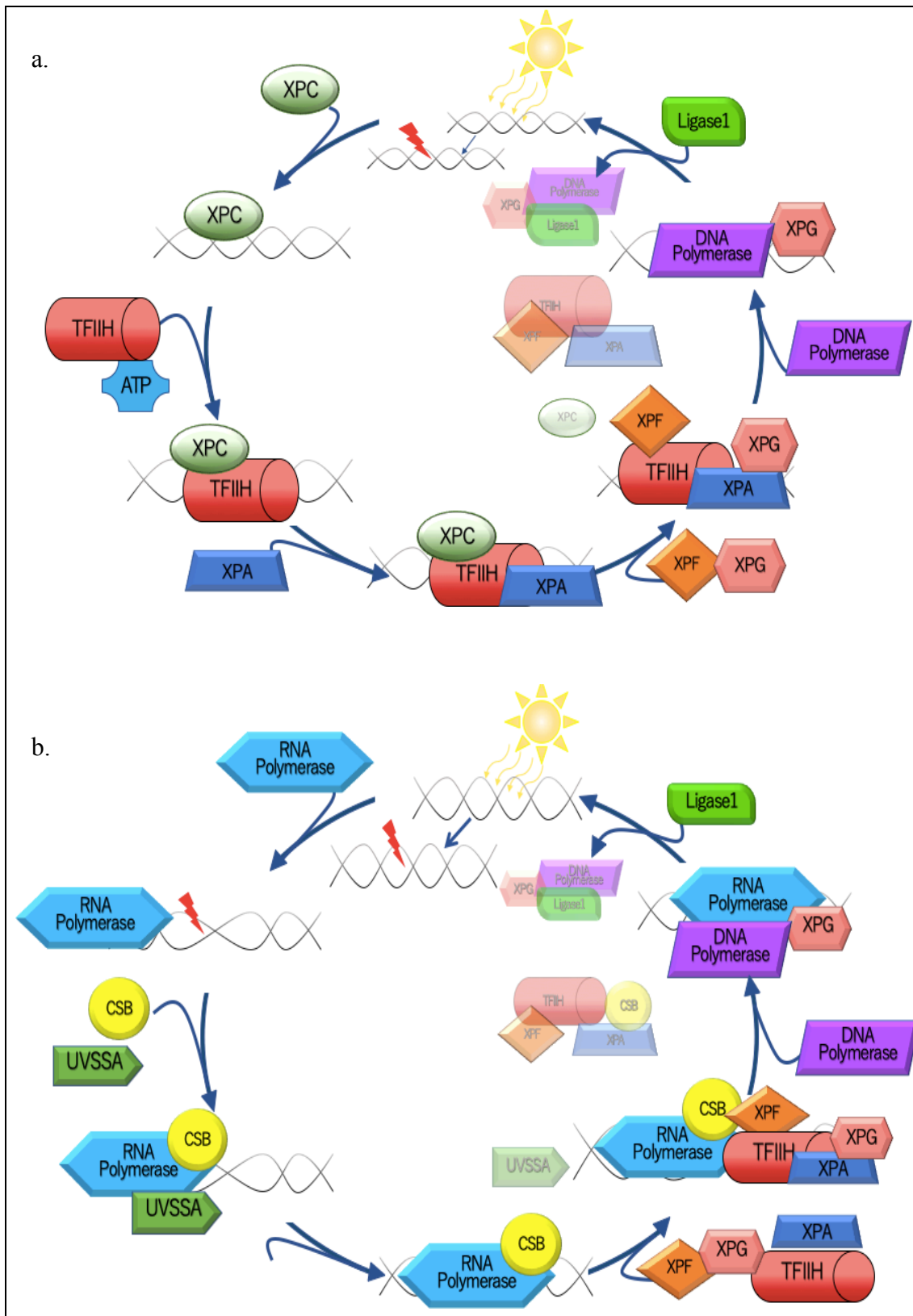


**Figure 1. Schematic overview of nucleotide excision repair.** Interaction of proteins involved in the biochemical process of **a.** global genomic nucleotide excision repair (GG-NER) and **b.** transcription-coupled nucleotide excision repair (TC-NER) after UV-light-induced genomic damage.

XP: Xeroderma Pigmentosum Protein subtypes A, C, E, F, G; UVSSA: UV-sensitive syndrome protein A; CSB: Cockayne Syndrome Protein subtype B TFIIH: Transcription Factor IIIH

I selected three subtypes and designed model iPS cell lines by knocking down the loci listed in Table 1 (*ERCC3*, *ERCC6*, *UVSSA*). The technology I used was Clustered Regularly Interspaced Short Palindromic Repeats interference (CRISPRi).

**Table 1.** Summary of three skin related hereditary diseases caused by insufficiency of DNA repair systems, their subtypes and their loci<sup>8</sup>.

Disease type	Gene	Locus
Cockayne Syndrome group A	CSA, ERCC8	5q12.1
<b>Cockayne Syndrome group B</b>	<b>CSB, ERCC6</b>	<b>10q11.23</b>
Cockayne Syndrome group C	CSC	None known
Xeroderma Pigmentosum group A	XPA, ERCC1	9q22.3
<b>Xeroderma Pigmentosum group B</b>	<b>XPB, ERCC3</b>	<b>2q21</b>
Xeroderma Pigmentosum group C	XPC	3p25
Xeroderma Pigmentosum group D	XPB, ERCC2	19q13.2-q13.3, 10q11
Xeroderma Pigmentosum group E	XPE, DDB2	11p12-p11
Xeroderma Pigmentosum group F	XPF, ERCC4	16p13.3-p13.13
Xeroderma Pigmentosum group G	XPG, ERCC5	13q33
Xeroderma Pigmentosum group V	XPV, POLH	6p21.1-p12
<b>UV-Sensitive Syndrome group A</b>	<b>UVSSA</b>	<b>4p16.3</b>
Bold: Subtypes I derived from iPS cells by genomic knockdown using CRISPRi.		

The basis for CRISPR technology was discovered by Ishino et al. (1987) in *E. coli* cells<sup>9</sup>. Since then, the world of science has explored its mechanisms and applications for the human genome. Unlike most scientific findings, CRISPR has received public acclaim due to high-profile events like the Breakthrough Prize Awards, which honored two leading scientists in the field of CRISPR in 2015 (Jennifer Doudner and Emmanuelle Charpentier)<sup>10</sup>. Other headlines were made by Chinese scientist He Jiankui, who claimed

to be the first person to genetically edit human embryos, in 2018<sup>11</sup>, which has raised public concern and led to a fundamental ethical debate.

The method of knocking down genes in human cells by CRISPR technology was reliably established in 2013. It uses the Cas9 protein, first found as part of the bacterial adaptive immune system<sup>12</sup>. This protein has two main abilities: first, it can attach specifically to a certain sequence of the genome if provided with an appropriate template of the targeted sequence; second, it has endonuclease activity<sup>13</sup>. As the specific attachment is the core of genome editing through CRISPR, the latter had to be disabled to prevent the targeted DNA from being cleaved. Therefore, Cas9 protein's catalytic activity was deactivated by inserting two point mutations (D10A, H840A) in the encoding gene<sup>14</sup> – now called dead Cas9 or dCas9. This tracking protein can then be used to screen the genome for a specific sequence and visually displaying it by attaching fluorescent marker to the protein<sup>15</sup>. Alternatively, it can be used to increase or decrease the translation of a certain exon, either by activating (CRISPRa) or interfering (CRISPRi) with its promoter<sup>16</sup>. For activation and interfering, either an activation or a repression domain is linked to the dCas9 protein<sup>17</sup>. The easiest handling and best outcome in repression during the improvement of CRISPRi technology was achieved by fusing a repressor to dCas9, called the Krüppel-associated box (KRAB)<sup>18</sup>, which can result in knockdown rates of up to 99%.

To integrate the dCas9 protein into the cell's proteome, a safe harbor site was needed that would not affect the surrounding genes and could itself provide stable and robust expression. A well-studied region, the adeno-associated virus integration Site 1 (AAVS1), shows such characteristics<sup>19</sup>. In addition to the dCas9 DNA, a reverse transcriptional activator (rtTA) and a highly effective constitutive promoter, CAG, ensure the

transcription<sup>20</sup>. To retain control of the expression of the implemented dCas9 system, the sequence is put under transcriptional control of a tetracycline-responsive element (in my system: Doxycycline). The advantage of such a chemical “switch” to turn transcription on and off, is that one can easily check on the functionality of the implemented dCas9 system. This technique also enables comparative experiments more easily, as the cells compared have identical genomes with proteomes differing only in the one knocked-down protein examined. This chemical “switch” is the doxycycline-specific transcriptional response element (TRE). If treated with doxycycline in the presence of a specific artificial guide RNA (gRNA) brought into the iPS cell’s nucleus, the dCas9-KRAB system uses the gRNA as a template to bind the correspondent genomic site and suppresses its transcription. (This is contingent on the gRNA being designed thoroughly.) In the absence of doxycycline, the transcription proceeds unaffected.

The appropriate template – the gRNA mentioned above – that must be provided to dCas9 to enable the intentional tracking of certain sequences of the genome is a single-stranded artificial RNA-primer that is complementary to the sequence targeted. The design of this gRNA depends on the aim of the intervention and the specific conditions in the DNA segment being targeted. In CRISPRi, an ideal gRNA template would enable the KRAB repressor to reach the promotor region of the gene that is aimed for knockdown. It should also be unique in the whole genome, so there would be no off-target sites that dCas9 could accidentally bind to. In reality, there is no ideal template. However, even if dCas9 binds to a non-target, the odds of a noticeable effect on the cell are low. This is because less than 2% of the genome is transcribed<sup>21</sup> and the non-target would have to be located in a position close enough to a promotor region to affect transcription. In addition, as

described in the methodology of this work, quite a high level of uniqueness is predictable by analyzing databanks on the human genome, such as the Genome Browser I referred to provided by the University of California Santa Cruz<sup>22</sup>. Assuming a low variability of human genomes regarding the sequence of promoter regions, the genome analyzed to design the gRNA resembles the DNA of any human iPS cells well enough to be used and to prevent off-target effects. Figure 2 shows an overview of how CRISPRi works.

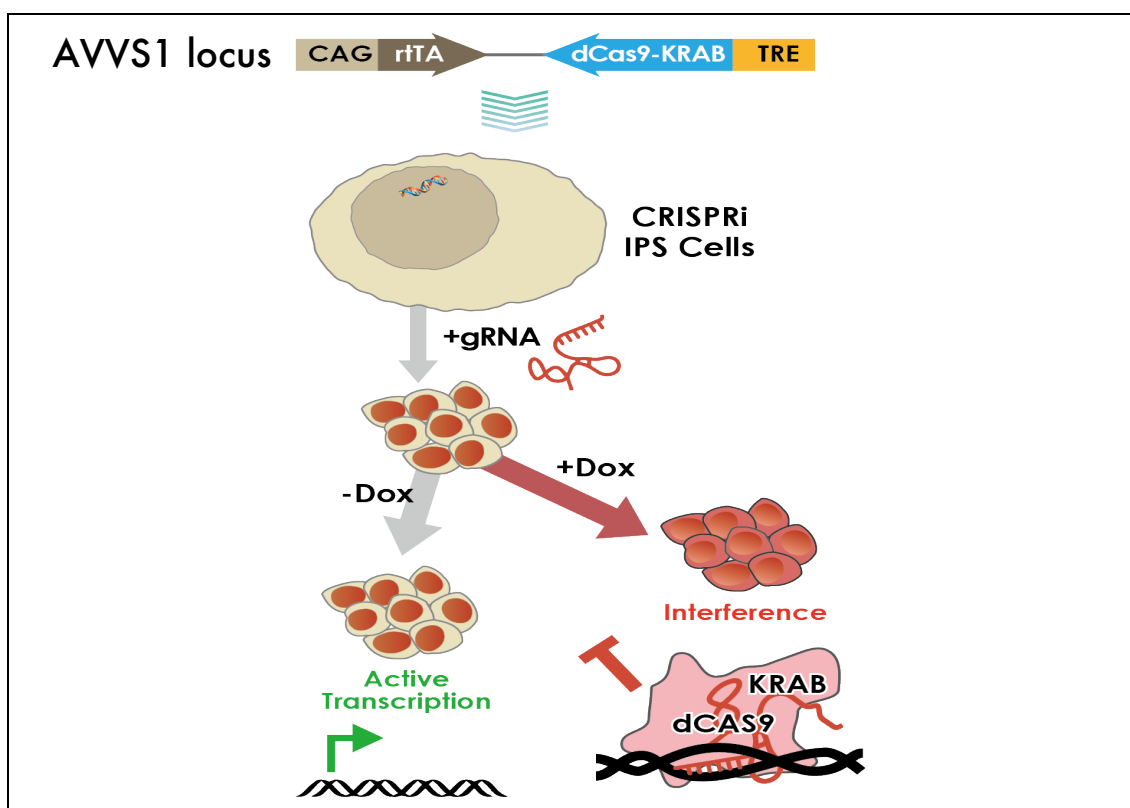


**Figure 2. Schematic overview of the principle of the CRISPRi method.** The AAVS1 locus is used to implement a dCas9-KRAB system. The system is provided with the tracking system “dCas9-KRAB” that can either be used to knock in or knock down certain genomic regions, after being transcribed and translated. To assure transcription, a reverse transcriptional activator (rtTA) controlled by doxycycline (dox) is placed immediately downstream the strong constitutive promoter CAG. The “switch” to turn on/off transcription is the dox-specific transcriptional response element (TRE). If treated with doxycycline (+dox) in the presence of an artificial gRNA brought into the iPS cell’s nucleus, the dCas9-KRAB system uses the gRNA as a template to bind the corresponding genomic site. It suppresses transcription, if the gRNA was designed thoroughly. In the absence of doxycycline (-dox), the transcription will proceed unaffected<sup>20</sup>.

In addition to the three edited cell lines for which the loci of ERCC3, ERCC6 or UVSSA were knocked down by CRISPRi, I also created iPS cells of a Cockayne syndrome patient (gene affected: *ERCC6*). The purpose was to obtain a “non-artificial” comparison model for my knockdown cells so I could check their resemblance at the morphologic and biochemical level.

The final aim of my research was to gain deeper understanding of common and unique mechanisms leading to the different syndromes, and to develop new ideas for medical support of these as-yet incurable diseases. The diseases generally become manifest during the first decade of life, making it impossible for these young patients to enjoy a carefree childhood, and most of them die before reaching adulthood.

## **1.2. Biochemical and clinical description of diseases examined**

### **1.2.1. Xeroderma pigmentosum**

The need of strict restriction of exposure to sunlight and its damaging UV effects from an early age, and an overall survival beyond 20 years for fewer than 40% of patients<sup>23</sup> are the main features of XP. The condition has been adopted in popular culture with movies like “The Dark Side of the Sun” (1988) starring Brad Pitt and “太陽の歌” (*Taiyou no Uta*, meaning “Song of the Sun”, 2006). The latter gained popularity in Japan and was adopted by Hollywood in 2018 as “Midnight Sun”. In addition, articles have appeared in the press, such as *The New York Times Magazine* article called “Midnight’s Children”<sup>24</sup>. It focused on Camp Sundown, a summer camp in New York for XP children who otherwise would never have the opportunity to enjoy a summer camp.

As tragic as the disease is, due to the media interest, public awareness has increased over the years. This has accelerated research and institutional help for these children, making XP the best understood of the three rare diseases presented in this thesis.

With some individual variation, the average age at which patients start to show symptoms is about two years<sup>25</sup>. As the disease's name implies, dry skin (Latin *xeroderma*) and distinct freckling (*pigmentosum*) are the main features. The disease has an incidence of ca. 2.3 per one million live births in Western Europe and only 0.9 per one million if only the autochthonic population is referred to<sup>26</sup>. Its prevalence is higher in the US (1:250.000) and even higher in North Africa and East Asia, with the highest rate in Japan (1:20.000<sup>27</sup>). In perspective of its rareness, these first symptoms seldom lead to the correct diagnosis of XP. Symptoms will then worsen, and ongoing exposure to sunlight can cause agonizing blisters or even lead to precancerous lesions. It is often at this point that a doctor provides the correct diagnosis.

A first diagnostic attempt is often made with a method called unscheduled DNA synthesis (UDS). The patient's cells are collected by biopsy and a panel of characterized XP cells are exposed to UV C light (wavelength 100-290 nm) and then compared for their ability to recover. This UDS test cannot clarify the specific subtype and screens only for GG-NER, not for TC-NER. It is thus not applicable for certain phenotypes with a strong component of TC-NER insufficiency but only for typical GG-NER activity that sometimes presents in patients<sup>28</sup>. Fortunately, the cost of direct high-volume DNA sequencing has been falling since the human genome project. This scenario is boosting the database for specific information on the subtypes and will ease the differential diagnosis of CS, which sometimes presents as clinically similar to XP<sup>29</sup>.

A Caucasian has a statistical probability of 0.6% to develop skin cancer between birth and the age of 49 years; the risk increases to 1.8% for individuals above 70 years<sup>30</sup>. Insufficient repair mechanisms for DNA damage accelerate the accumulation of damaged cells, elevating the risk for skin cancer up to 10 000-fold<sup>25</sup>. Thus, XP patients are required to undergo monthly skin examinations and surgical excisions of critical lesions, often several times each year. For highly exposed body parts, particularly the hands, neck and face, the cosmetic results can be devastating for young people's mental health. Furthermore, corneal cells are likely to be hypersensitive to sun rays. About half of XP patients experience symptoms such as conjunctival injections or even blindness in adolescence<sup>31,32</sup>. In addition to dermatological problems, progressive neurological abnormalities are seen in about 30% of XP patients<sup>33</sup>, ranging from restricted intellectual development to motor difficulties or loss of hearing.

The expected lifespan can be greatly improved by early diagnosis and stringent preventive measures against the progression of the disease; nonetheless, overall survival remains less than 30 years<sup>34</sup> (less than 40% reaching the age of 20<sup>23</sup>). If neurological disorders occur, the prognosis is even poorer.

As explained above, there are eight subtypes of XP (A to G and V). They all have some kind of insufficiency in GG-NER in common, as well as insufficiency in the TC-NER. Table 2 summarizes the eight genes by which the subtypes are distinguished.

**Table 2.** Details on genes causing Xeroderma Pigmentosum<sup>25</sup>.

Gene	Exon count	Chromosomal location	Protein size (aa)	Protein function	Defective pathway
XPA	6	9q22.33	273	Damage verification	NER
XPB/ <i>ERCC3</i>	15	2q14.3	782	Helicase	NER
XPC	16	3p25.1	940	Damage recognition	NER (GGR)
XPD/ <i>ERCC2</i>	23	19q13.32	760	Helicase	NER
XPE/ <i>DDB2</i>	10	11p11.2	427	Damage recognition	NER (GGR)
XPF/ <i>ERCC4</i>	11	16p13.12	916	Nuclease	NER
XPG/ <i>ERCC5</i>	15	13q33.1	1186	Nuclease	NER
XPV/ <i>POLH</i>	11	6p21.1	713	Polymerase	TLS
Abbreviations: NER: Nucleotide excision repair, GGR: global genome repair sub-pathway, TLS: translation synthesis.					

I tried to create model cells from the two most common subtypes, A and B. However, despite experimenting with different sequences and in several attempts, I could not effectively knock down the XPA locus. I managed to effectively knock down the *ERCC3* gene in the available iPS cells and I thus focused on subtype B for my XP research. *ERCC3* deficiency causes XPB, which is also the name of the expressed protein. Figure 3 shows how the process operates, simplified.

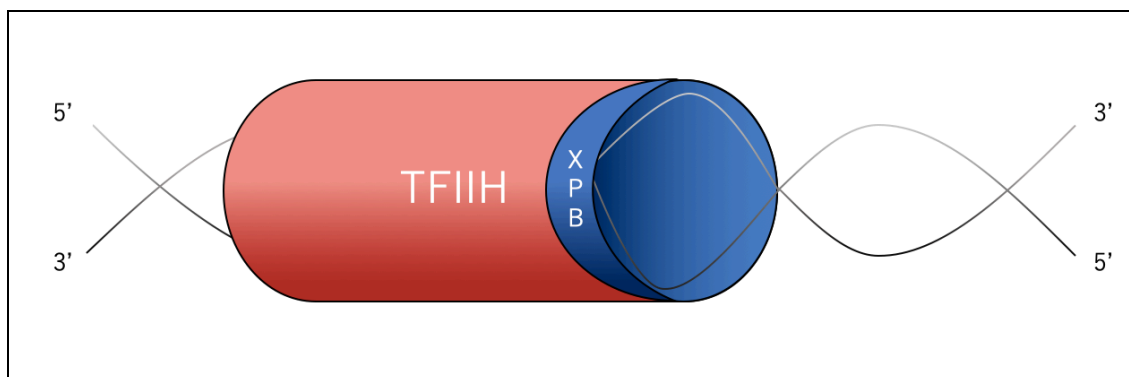


**Figure 3. Schematic image showing how the XP protein B (XPB) is assembled to transcription factor IIIH (TFIIH) to repair DNA damage.** By using energy provided by ATP, the helicase XPB loosens the binding of several consecutive base pairs to enable TFIIH to access DNA, which then initiates the transcription. As TC-NER depends on transcription, this enzyme complex is a core feature of the whole repair system. By contrast, if recruited to a site of damage by XPC in the context of GG-NER, the complex is essential for XPA (for example) and DNA-polymerase to access the base pairs, as shown in Figure 1.

After the XPB protein is folded into its tertiary structure, it becomes part of the quaternary structure of the biomolecular complex called transcription factor IIIH (TFIIH). It then fulfills its function as an ATP-dependent helicase of 3'-5' polarized DNA<sup>35,36</sup>. Because it performs such an essential role in both GG-NER and TC-NER, it is easy to imagine an insufficiency can lead to severe symptoms as described above.

### 1.2.2. Cockayne Syndrome

CS is less well-known than XP. As with XP, the incidence differs by ethnic group and region. In Western Europe there are 2.7 cases of CS per million live births, 1.8 per million interpolated for the autochthonic European population<sup>26</sup> and 2.77 per million in Japan. The prevalence is 1 in 2 500 000<sup>37</sup>. British pediatric expert Edward Alfred Cockayne – whose name is eponymous with the disorder – defined CS as a rare disease with specific cardinal symptoms: impaired development of the nervous system, dwarfism, notable facial characteristics and pigmentary retinopathy<sup>38</sup>. Recent research has differentiated the

three genetic subtypes A, B and C, depending on the mutation's location (refer to Table 3).

**Table 3.** Details of genes causing Cockayne syndrome<sup>39,40,37</sup>.

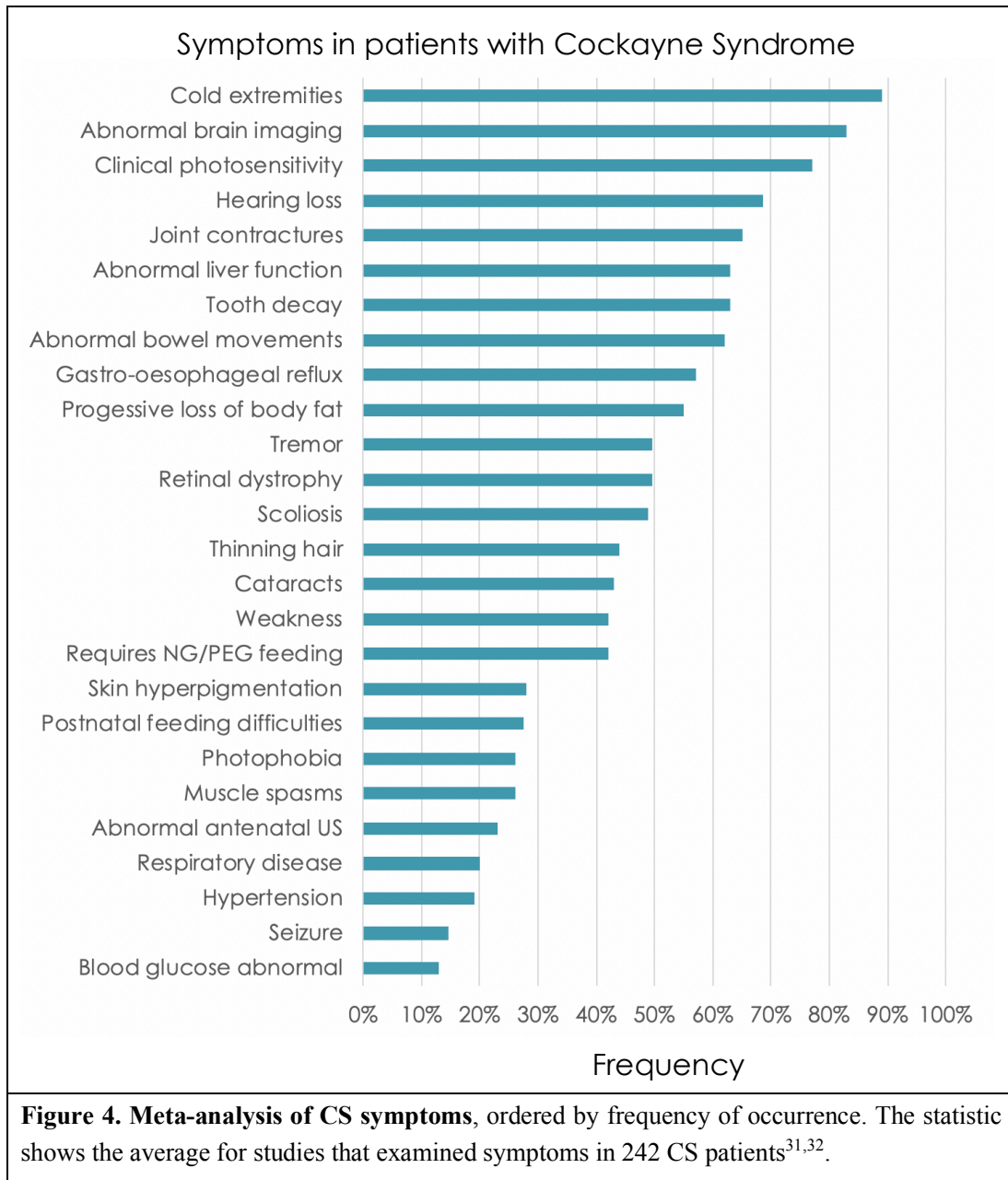
Gene	Exon count	Chromosomal location	Protein size (aa)	Protein function	Defective pathway
CSA, <i>ERCC8</i>	13	5q12.1	396	subunit of RNA polymerase II transcription factor IIIH (TFIIH)	TC-NER
CSB, <i>ERCC6</i>	23	10q11.23	1493	ATP-dependent helicase	TC-NER
CSC	unknown	unknown	unknown	unknown	TC-NER

More than 100 exons scattered across eight genes have been described as involved in XP. By contrast, there are just two specific loci described as causing CS, which makes direct sequencing the best standard diagnostic method in case of clinical suspicion<sup>29</sup>. Depending on the severity of onset and its timing, three phenotypes have been classified: Average onset (CS I), early onset (CS II) and late onset (CS III).

CS I (80%) is the classical form, with symptoms first appearing during their second year of life and patients surviving up to 20 years. CS II (18%) is normally diagnosed directly after delivery and has an even worse prognosis. In contrast, the rare CS III patients first show light-sensitive symptoms in their adolescence, and might have normal life expectancy<sup>41</sup>.

The symptoms are led by cerebral abnormalities like microcephaly, increasing calcification in the area of the basal ganglia and widening ventricles. Additional symptoms are neurological dysfunction, photosensitivity, tooth decay and hypertension.

The variety, as well as the severity of the symptoms listed in Figure 4 implicate the vital importance of the CSA and CSB proteins.



According to current research, CSA is the substrate recognizing part of the CSA complex, which also contains the proteins RBX1, DDB1 and CUL4A. These work together as a DCX (DDB1-CUL4-X-box) E3 ubiquitin-protein ligase complex, important for the

clearance of damaged or misfolded proteins. Furthermore, the complex interacts closely with the TFIIH sub-unit, a necessary interaction to recognize damaged sites during exon translation<sup>39,42</sup>. CSB is an essential partner for the RNA polymerase II complex. As the polymerase starts translation, the ATP-stimulated ATPase CSB is recruited, providing the ability to change the translated DNA strings' conformation by wrapping it around itself. This improves the accessibility of the base pairs, enabling the TC-NER pathway to initiate its function. There is also evidence CSB recruits the CSA complex, further NER-proteins and the histone acetyltransferase p300 to the RNA-polymerase blocking lesions, showing its importance in the NER-pathway initiation<sup>40,43</sup>.

### **1.2.3. UV-Sensitive Syndrome**

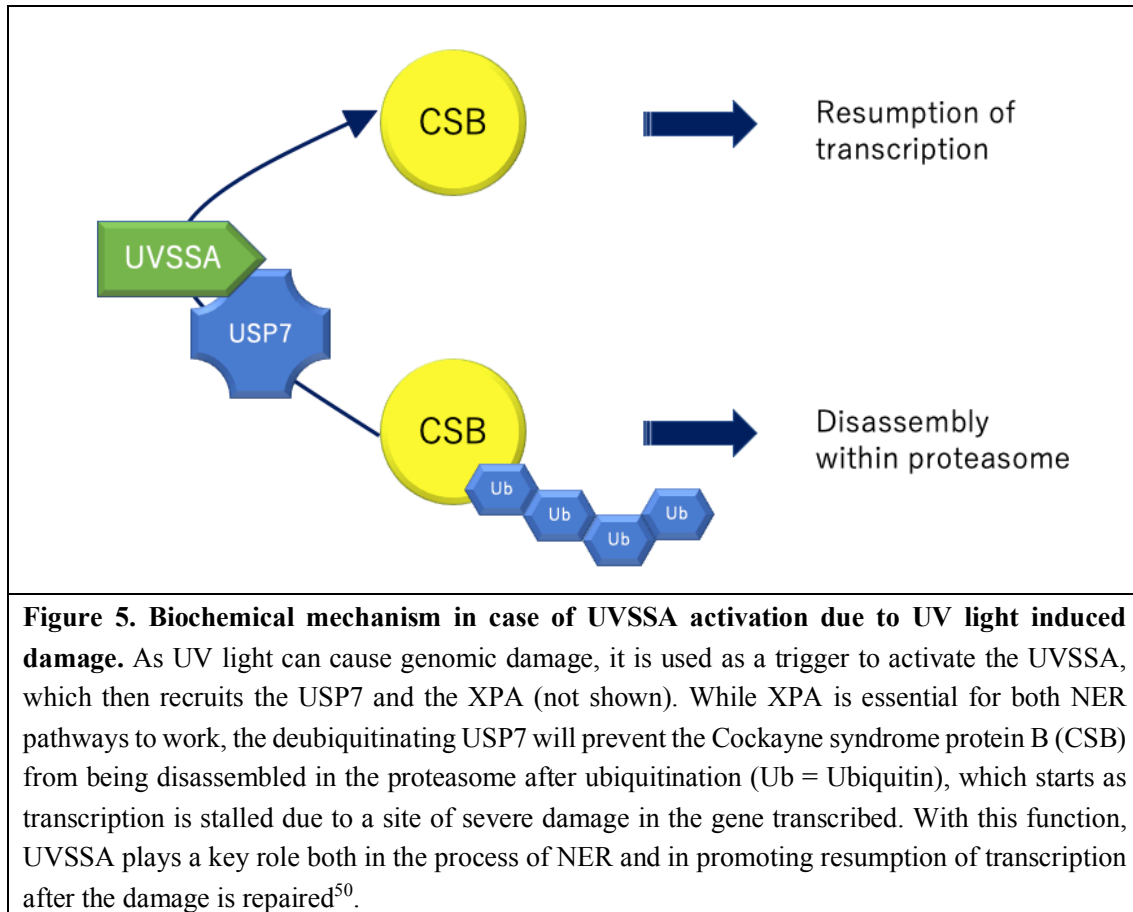
In contrast to XP and CS, UVSS is a relatively recently defined disease<sup>44</sup> that yet has many unknown aspects. Hence, data on this disease is limited, making it difficult to deduce any firm conclusions about the incidence or prevalence. The organization *Orphanet*, an information base for rare diseases, estimates the prevalence of UVSS lower than 1 in a million births<sup>45</sup>.

As the syndrome's name implies, this disease is characterized by exaggerated sensitivity to UV exposure. The spectrum of symptoms is broad, ranging from skin dryness and freckles to extraordinary changes in pigmentation or so-called telangiectasia (enlarged blood vessels in the epidermis). Patients show a general tendency to develop sunburn even with small amounts of sun exposure. In contrast to XP and CS, there is no elevated risk for skin cancer or neurological disorders. The life expectancy also appears to be normal, according to the current sparse data<sup>38</sup>. The relatively unspecific symptoms and

the relatively low level of suffering among patients suggest that the number of unreported cases is probably high. Patients might think of their problems as an individual reactivity to sunlight more than a disease. I included this syndrome in my studies because this light-related symptom raises the question of why mutations in TC-NER-related genes differ so much in their clinical presentation. There are three complementary groups, with the actual *UVSSA* locus – but also certain mutations in the *ERCC8* (*CSA*) and the *ERCC6* (*CSB*) loci – being thought to present as UV-sensitive syndrome<sup>46</sup>.

The *UVSSA* locus encodes the UV-stimulated scaffold protein A. As the name implies, this protein is activated by UV light radiation. The activated UVSSA has two functions to resume the transcription if the RNA polymerase II is stalled at a damage site. First, UVSSA recruits xeroderma protein A (*XPA*) to the site, which then can initiate the TC-NER. For the second function it has to build a complex with ubiquitin-specific peptidase 7 (*USP7*)<sup>47</sup> that regulates the *CSB* protein, which is part of the *TFIIH* complex as explained above. If the RNA polymerase II is stalled, the *CSB* protein is disassembled in the proteasome after ubiquitination, the *TFIIH* complex loses access to genomic information and transcription would eventually be impossible. However, as the recruited *XPA* initiates TC-NER and the repair of the damaged site, the UVSSA-*USP7*-complex cuts the ubiquitin off the *CSB* protein and enables the resumption of the transcription<sup>48,49</sup>.

The process is shown in Figure 5.



First, it was expected that similar to XP and CS mutations in several genes could lead to insufficiency of the UVSSA protein, but so far only one locus has been defined (Table 4).

**Table 4.** Details about gene that causes UV-sensitive syndrome<sup>51,52</sup>

Gene	Exon count	Chromosomal location	Protein size (aa)	Protein function	Defective pathway
<i>UVSSA</i>	25	4p16.3	709	Regulation of RNA Polymerase II, Stabilization of CSB	TC-NER

A plausible and currently unrefuted hypothesis is that UVSSA plays a major role only in the algorithm for damage distorting the DNA helix. According to this concept, UVSSA does not act in oxidative damage nor in the regular RNA transcription (as CSA and CSB

do) and therefore UVSSA causes a milder phenotype<sup>53</sup>. Congruent with this hypothesis is that genomic damage in the cell compartment mitochondrion, which is exposed to the most extreme oxidative stress, leads to similar symptoms as CS; hence, mitochondrial DNA damage could be a key difference leading to the broad variety of phenotypes of CS and UVSSA. Mitochondriopathies like the LHON diseases or the MELAS syndrome show the crucial role of mitochondria for the nervous system and thriving of the human organism with undeniable similarities to the typical CS symptoms and their age of onset. LHON causes sudden blindness in the patient and the MELAS syndrome presents with **myopathy, encephalopathy, lactate acidosis and stroke-like episodes** as cardinal symptoms, as well as restricted thrive, dwarfism and amblyacousia, with an onset during childhood in 65% to 76% of patients<sup>54</sup>. It was shown that the CS proteins, mainly CSB, are crucial for the repair of certain oxidative lesions (e.g. 7,8-dihydroxyguanine)<sup>55</sup> and for promoting mitochondrial autophagy in case of severe damage<sup>56</sup>. None of these mechanisms have been implied for UVSSA-deficient cells to date. This suggests a major role of oxidative stress, especially in mitochondria, for the severe CS phenotype – unlike UVSS. Even XP patients do not often show symptoms of the nervous system or thrive (roughly 30%)<sup>33</sup>.

UVSS and XP are phenotypically closer to each other in comparison to UVSS and CS. Although biochemically UVSSA prevents the degradation of CSB and is thus expected to resemble the CS phenotype. An explanation might be found in two previous studies on this topic. Schwertman et al. noted that lesions that cause a helix distortion will cause a prolonged transcriptional arrest, as relatively minor lesions caused by oxidative stress lead to short and transient arrests<sup>46</sup>. Although the CSA-CSB-dependent pathway remains

stable enough to repair oxidative lesions even without deubiquitinating of CSB by UVSSA, it is not stable enough to repair the greater UV-induced helix distortions, as CSB would be degraded in the proteasome too quickly.

Experiments by Hanawalt et al. show that if RNA polymerase is restrained while transcribing due to a DNA lesion, it can still be ubiquitinated and degraded by the proteasome in a CSA-CSB-dependent pathway. This occurs even without the presence of UVSSA, providing other DNA-repair mechanisms with access to the lesion and preventing the gene from becoming unreadable for other RNA polymerases due to the stalled one. However, if CSA or CSB is absent and only UVSSA is present, the stalled RNA polymerase II would not be degraded and would remain stalled. The lesion would not be repaired<sup>57</sup>, hence the gene transcription would remain impossible, eventually resulting in a more severe phenotype.

### **1.3. Research objectives**

#### **1.3.1. Creation and use of iPS cell models of UV light sensitive syndromes**

My research aims to gain new insights into the spectrum of UV light sensitive syndromes by using the new experimental approach of iPS cell models. To my best knowledge there was yet no (publicized) use of iPS cell methods made on *ERCC3*, *ERCC6* or *UVSSA* at the time I conducted my studies. By using these methods, I was able to imitate and observe the impacts of loss of function mutations in each of the genes introduced above starting from the earliest stage of a human body's development all the steps through a differentiated keratinocyte.

Setting up eligible, low-cost, practical and reproducible conditions for the creation and analysis of iPS cell models for these three genes – model cells we gladly share with other institutes, if needed – will contribute to improve the access to this new approach in NER-related research.

### **1.3.2. Differentiation of iPS cells and opportunities for application in clinical setting**

A crucial part of this project was not just the creation of XP, CS and UVSS model iPS cells by CRISPRi knockdown. In fact, by developing an efficient protocol to differentiate iPS cells into keratinocytes, I was furthermore able to follow the whole course of events from the stem cell stage to the fully differentiated skin cell. Skin cells, or keratinocytes, play a key role in the symptoms attributed to the three syndromes.

Similar to established protocols for differentiation of iPS cells into, for example, neurons, this work builds a foundation for follow-up research on skin cells, as there is still much to understand. Because many other tissues besides the skin are involved in the phenotype of XP, CS and UVSS it will be as essential as this study to establish differentiation protocols for further effected cell types in order to gain a holistic understanding of this diseases and offer an integral and/or causal therapy.

I developed an efficient differentiation protocol from iPS cell to keratinocyte, based on promising research published to date aiming to fine-tune this protocol to increase its efficiency. Such iPS-cell-derived keratinocytes could find broad application in various fields. iPS cells have a high proliferation rate and therefore could provide the many keratinocytes needed for artificial 3D-skin other researchers are working on recently. Eventually such patient derived artificial skin could provide autologous skin transplants

for patients suffering from severe medical conditions such as high-grade burns, Staphylococcal scalded skin syndrome or toxic epidermal necrolysis. A vision for the future would be that such a patient arrives at the ICU, is stabilized as far as possible and temporarily provided with artificial skin replacements. Meanwhile, patient cells are taken from healthy tissue (e.g. a blood draw), then these cells are transformed to iPS cells, which are then multiplied massively in vitro before being differentiated into keratinocytes. Eventually these are used for 3D-skin to create an autologous transplant for the patient, which replaces the artificial skin. This scenario could replace current therapies like the homologous skin transplantation using mashed skin from healthy skin and therefore causing iatrogenic damage, or heterologous skin transplantations, which are associated with poor healing and the risk of a host vs. graft reaction. If this vision is realized, the patient's outcome will certainly be improved, days spent in the ICU and length of hospitalization would drop, and so would the associated costs. For these reasons an efficient iPS cell to keratinocyte protocol, as I tried to implement, has a high potential for translational use in various clinical settings.

### **1.3.3. Standardized induction of DNA damage and meaning for translational medicine**

Regarding the NER-related diseases I examined, in addition to my observations during differentiation, I devised settings to induce DNA damage. This was mainly through exposure to UV light and oxidative stress applied by H<sub>2</sub>O<sub>2</sub>, which I standardized for various stages of differentiation in my model cells. A standardized protocol of how to apply genomic damage to cells and finding parameters to measure the damage applied

(e.g. expression of reactive oxidative species, ROS, as a parameter for oxidative stress) enabled me to screen various remedies. I chose different kind of remedies that I thought might alleviate the damage caused by UV light and H<sub>2</sub>O<sub>2</sub>. As this screening is still far from being completed, my protocol will also be useful as reference for follow-up research. An advantage of using iPS cells for remedy screening is their strong capacity for proliferation. This means many remedies can be tested in a short period, which was always a challenge in testing cell samples from diseases with a low incidence, such as XP, CS and UVSS.

The clinical reality of having nothing but symptomatic treatment for these patients and a severely limited life expectation for most of them, urges researchers to seek further understanding. Previously gained knowledge was summarized in the last section. Ongoing studies seek more precise insight into the mechanisms of NER, which could eventually lead to the functional identification of new syndromes and a more distinct classification of their subentities. Such a better understanding, which this study aims to contribute to, can eventually disclose new opportunities for therapeutic approaches.

## 2. Materials and Methods

### 2.1. Induction of pluripotency in somatic cells from a patient with CS

#### 2.1.1. Materials

Materials	Source
Phosphate-buffered saline, PBS	Wako
2%, 80% Fetal Bovine Serum, FBS	Gibco
1 mM, 2 mM EDTA	Sigma-Aldrich (Merck)
FcR Blocking Reagent	miltenyi biotec
MACS Buffer (0,5% BSA + 2 mM EDTA + PBS)	miltenyi biotec
Human ES Medium, hES Medium	Thermo Fischer
Stem-Pro 34, with Cytokine mix E	Life-Technologies
20% DMSO	Sigma-Aldrich (Merck)
plasmid hul (= L-myc) plasmid hosp (= Oct3/4) plasmid hsk (= Sox2, Klf4) plasmid ebna plasmid GFP	Addgene
Cell Banker	Nippon Zenyaku Kogyo
Equipment	Source
BD Vacutainer Cell Preparation Tube	BD Biosciences
Hemocytometer Thoma	SLGC
6-well ultra-low attachment plate (ULA plate)	Corning
LONZA Nucleofector <sup>®</sup> Kits for Human CD34+ Cells	LONZA

#### 2.1.2. Methods

Blood was drawn from a 61-year-old female patient in ambulant care at Osaka Medical Collage after declaring her informed consent following detailed explanations by Prof. Dr. Shunichi Moriwaki about the analysis and research projects performed with her blood in accordance to the Declaration of Helsinki. The result of the analysis by complementation

test lead to the diagnosis Cockayne Syndrome (CS) late-onset subtype III (Type: CS B, affected gene: *ERCC6*). At the time her blood was drawn, she presented with increased photosensitivity, unsteady gait, dysarthria, dementia, and demyelination. The latter was evident in MRI of the brain, which also showed calcification of the cerebrum.

After gently inverting the BD Vacutainer Cell Preparation Tubes with the collected blood (9.0 mL) six times, we centrifuged the blood samples for 20 min at RCF of 1650 g, in a horizontal rotor at RT. Mononuclear cells and platelets appeared as a white layer below the plasma layer (“buffy coat”). After aspirating more than half of the plasma, taking care not to disturb the white layer, we collected the mononuclear cells and platelets using a Pasteur Pipette and transferred them to a 50 mL conical centrifuge tube with cap. After filling the tube to 45 mL by adding PBS + 2% FBS + 1.0 mM EDTA and inverting it five times, we centrifuged it at an RCF of 300 g for 15 min. Next, we aspirated the supernatant without disturbing the pellet, resuspended the cells by tapping, added PBS to make up a volume of 45 mL again, inverted the tube five times, and performed a cell count. We then centrifuged the tube again for 10 min at an RCF of 300 g, and finally filled up the tube again with filter-sterilized MACS buffer to yield a dilution of  $1.0 \times 10^8$  cells.

We then separated 300  $\mu$ L of this dilution and added 100  $\mu$ L of FcR blocking reagent, pipetted a few times, and added up to 100  $\mu$ L of CD34 MicroBeads before pipetting again. The suspension was then incubated at 4°C for 30 min, with gentle shaking every 10 min. After adding 10 mL of MACS before resuspending the mix in 500  $\mu$ L of MACS buffer (on ice) again, we placed the LS column on a magnetic separator and rinsed it with 3 mL of cold MACS buffer. Finally, we added the cell suspension into the column. By placing a new 15 mL conical tube under the column, we collected the flow-through containing

the unlabeled cells. The cells were washed with MACS buffer with 3 mL three times, and this flow-through was added to the unlabeled cells. The flow-through was placed on ice and later used for cryopreservation of the PBMC (see below).

Next, we placed the column on a new 15 mL tube, added 5 mL of the MACS buffer, and immediately flushed out the magnetically labeled cells by firmly pushing the provided plunger into the column. After counting the gained CD34<sup>+</sup> cells (CD34: specific for hematopoietic stem cells), we centrifuged for 5 min at an RCF of 400 g and then discarded the supernatant, carefully leaving ca. 50  $\mu$ L on top of the pellet. After resuspending the cells, we added hematopoietic expansion medium to make a final cell concentration of about  $7.0 \times 10^5$  cells per 3 mL.

The next step was to dispense 3 mL of this CD34<sup>+</sup> cell enriched suspension per well of the ULA plate and this was cultured for 3 to 6 days (37°C, 5% CO<sub>2</sub>, medium: Stem-Pro 34, with cytokine mix E). If the confluence per well exceeded 80%, we separated the cells into two new wells. For the cryopreservation, we centrifuged the flow-through for 10 min at an RCF of 300 g, aspirated as much supernatant as possible without disturbing the pellet, and resuspended the cell pellet in heat-activated 100% FBS (1 mL FBS per  $2 \times 10^7$  cells). By dispensing 0.5 mL of this suspension into pre-cooled cryovials and adding 0.5 mL of 20% DMSO and 80% heat-activated FBS, we obtained a final concentration of  $1 \times 10^7$  cell. The tubes were inverted three times. Finally, we transferred the tubes to a -80°C refrigerator overnight, then placed the frozen tubes into a liquid gen tank.

While the cultured cells grew to an adequate number (1 million cells were required for each nucleofection), I prepared the plasmid cocktail to provide 4  $\mu$ g for each episome. The cocktail was hul 2.3  $\mu$ L + hosp 1.9  $\mu$ L + hsk 1.0  $\mu$ L + ebna 1.0  $\mu$ L, and as a control

GFP 2  $\mu$ L mixed with 1  $\mu$ L of ebna. I then referred to the Amaxa<sup>®</sup> Human CD34+ Cell Nucleofector<sup>®</sup> Kit protocol<sup>58</sup> and selected the U-008 program of the LONZA transfection machine.

After incubation at 37°C overnight, green fluorescent protein (GFP) activity was observed in about 50% of the control cells. These were discarded as successful transfection was assumed. Two days after transfection, I replated 20 000 cells from each condition onto 10-cm dishes containing feeder cells (3 million SNLs/plate), and added 5 mL of human ES medium (KO DMEM + 20% KSR + Glutamax + NEAA + PS + bME + 4.0 ng/mL FGF), 5 mL of hematopoietic medium and 10  $\mu$ L Rock Inhibitor (also known as Y-27632). Seven days after daily medium exchange (only hES medium), I picked up suitable colonies that were visible without a microscope and not confluent with other colonies. I plated each of them in separate wells of a 24-well plate. After characterizing their eligibility, I stocked high-quality clones by freezing them at -80°C using Cell Banker. Figure 6 summarizes the workflow.

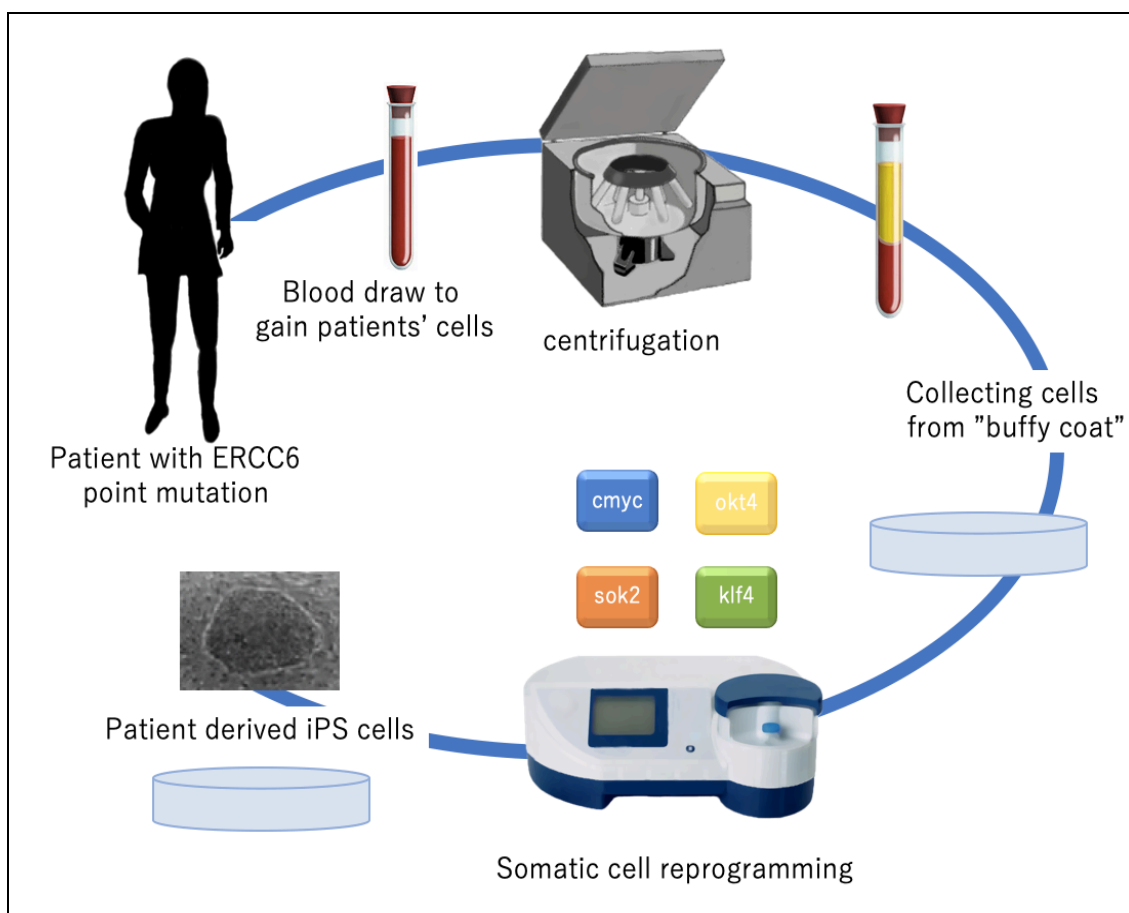


**Figure 6. Schematic overview of the workflow to create patient-derived iPS cells.** After centrifugation of the patient's blood, the leucocytes concentrated in the "buffy coat" are singularized and cultivated on a plate as single-clone colonies. The single clones of these somatic leucocytes are then reprogrammed with plasmids that contain the reprogramming factors *cmc*, *okt4*, *sok2* and *klf4* transfected by the LONZA Nucleofactor<sup>®</sup>. These transfected single clones are tested for successful induction of pluripotency and cultivated for further research.

## 2.2. Specific genomic knockdown using CRISPRi technology

### 2.2.1. Material

Material	Source
Predefined guide RNA (gRNA) oligoprimer	Eurofins
pQM-u6g-CNKB vector	Made in our laboratory
2X T4 DNA Ligase Buffer	Takara/Clontech
NEB Turbo competent cells ( <i>E. coli</i> )	NEB
Ampicillin containing medium	Sigma-Aldrich (Merck)
Plasmid Mini Kit	QIAGEN

Dilution Buffer: 125mM Tris-HCl, 5mM MgCl/DDW (pH 9.0)	Mixed in our laboratory
BigDye	Thermo Fisher
ddH <sub>2</sub> O	Merk
125 mM EDTA	Sigma-Aldrich (Merck)
99.5% Nuclease free Ethanol	Wako
70% Nuclease free Ethanol	Wako
3M acetic acid	Sigma-Aldrich (Merck)
Hi-Di formamide	Thermo Fisher
iPS cell line with Doxycycline inducible dCas9 activity ("C5")	Gladstone Institute
Human Stem Cell Nucleofector <sup>®</sup> Kit 1	LONZA
StemFit	Takara
Blastocytidine	Nacalai tesque
Doxycycline	Sigma-Aldrich (Merck)
ERCC6/CSB	Santa Cruz
ERCC3/XPB	abcam
UVSSA	GeneTex
RNAzol <sup>®</sup>	Molecular Research Center, Inc.
RNAse free water	Molecular Research Center, Inc.
RNAse free 75% Ethanol	Wako
RNAse free 70% Isopropanol	Wako
5xPrimeScript Buffer (for RealTime PCR)	Takara/Clontech
PrimeScriptRT Enzyme Mix I	Takara/Clontech
Oligo dT primer (50 μM)	Takara/Clontech
Random 6mers (100 μM)	Takara/Clontech
Probe qPCR Mix 2x	Takara/Clontech
PCR forward primer (10 μM)	Eurofins
PCR reverse primer (10 μM)	
TaqMan Probe	Thermo Fisher
Rox Reference Dye (50x)	Thermo Fisher
cDNA template	Thermo Fisher

Sodium dodecyl sulfate–polyacrylamide gel electrophoresis (SDS-PAGE) sample buffer containing 1% protease inhibitor	Wako
Dithiothreitol (DTT)	Wako
Sodium orthovanadate	Wako
Sodium Fluoride (NaF)	Wako
Methanol 100%	Wako
Tris-buffered saline (TBS)	Wako
Tween 20	Thermo Fisher
HRP-conjugated secondary antibodies	SouthernBiotech
2% skimmed milk	Nacalai Tesque
Luminata Western HRP substrate	Merck Millipore
<b>Equipment</b>	<b>Source</b>
Dry Thermo Unit	TAITEC
Ampicillin containing agarose plates	Nacalai tesque
DNA Sequencer 3130	Applied Biosystems
StepOnePlus Real-Time PCR System	Life Technologies
LONZA Nucleofactor <sup>®</sup>	LONZA
LONZA Human Stem Cell Nucleofactor <sup>®</sup> Kit 1	LONZA
Semi-dry blotting system	Bio-Rad
Polyvinylidene fluoride (PVDF) membrane	Merck Millipore, Billerica, MA
Densitometry system LAS3000	Fujifilm

### 2.2.2. Methods

Following the general procedure of CRISPRi as described in the introduction, I started by designing suitable guide-RNA-primers (gRNA) that would be integrated into the cell's genome upstream of the promotor of the gene aimed for knockdown. Using the database Genome Browser provided by the University of California Santa Cruz<sup>22</sup> and its dataset Human Assembly: February 2009 (GRCh37/hg19), I looked up the following genomic sequences:

•*ERCC3 (Homo sapiens excision repair cross-complementing rodent repair deficiency, complementation group 3)*

•*ERCC6 (Homo sapiens excision repair cross-complementing rodent repair deficiency, complementation group 6)*

•*XPA (Homo sapiens xeroderma pigmentosum, complementation group A, transcript variant 1)*

•*UVSSA (Homo sapiens UV stimulated scaffold protein A)*

I copied 200 bp upstream of the transcription start site, and 50 bp downstream. Using the Massachusetts Institute of Technology design tool for CRISPRi<sup>59</sup>, I analyzed each of these 250-bp sets for three suitable 20-bp segments. A high score implies specificity and uniqueness of the sequence of the targeted area, with low likelihood of off-target bindings. I prevented the segments from overlapping. Figure 7 illustrates this analysis using the example of ERCC3.



**Figure 7. Analysis of 200 bp upstream and 50 bp downstream in the promotor area of the ERCC3 to create gRNA for CRISPRi technology.** **a.** The extract shows the ERCC3 gene and its surrounding in the Human Assembly: February 2009 (GRCh37/hg19). **b.** Shown here are 1000 bps upstream the promotor and an extract of the sequence downstream, with a set of 250 bps marked in the first exon. **c.** The ranking suggests sequences in the 250 bps suitable to use for gRNA, based on a score mainly determined by uniqueness, which indicates a low chance of off-target binding sites with similar sequences (max.: 100). I chose five (ERCC6) or three (ERCC3, UVSSA, XPA) sequences based on high rankings and location in the promotor. I avoided overlapping sequences and tried to include sequences read in opposite directions.

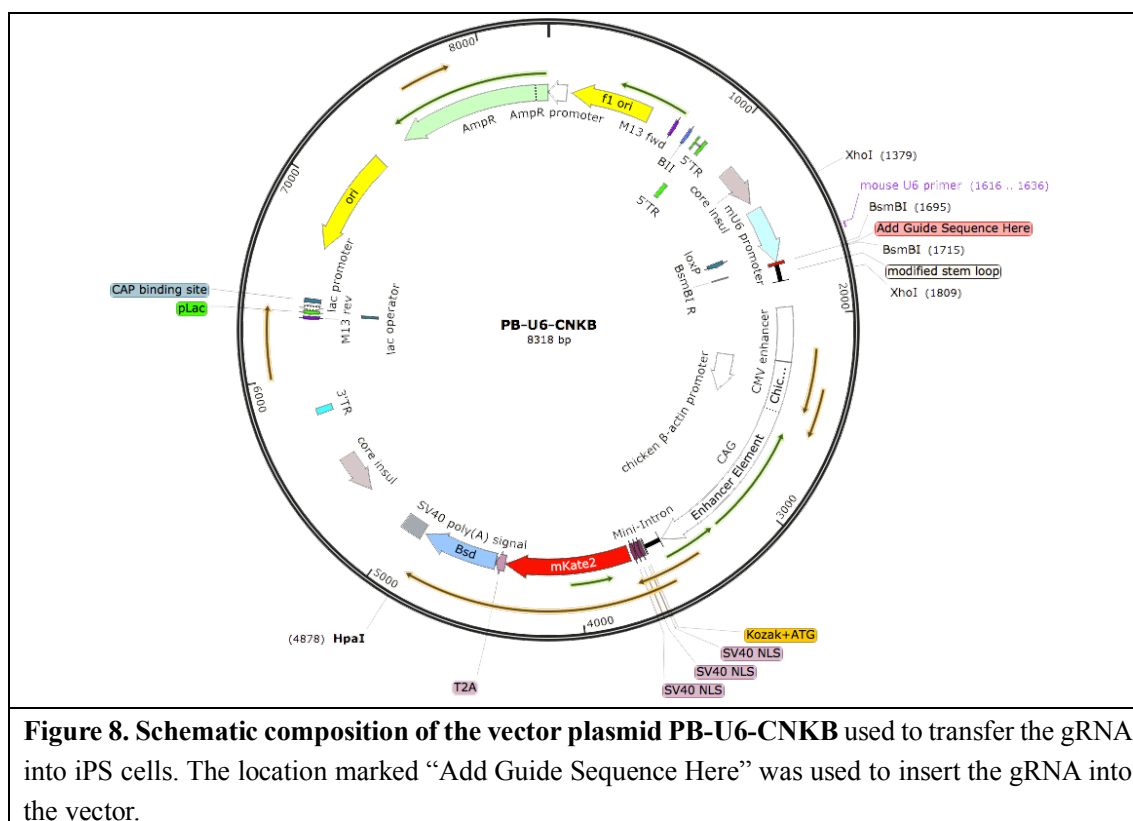
The software Snapgene<sup>60</sup> was a convenient tool with which to edit and document the total of 16 sets of primers. Before ordering the forward (F) and reverse (R) oligoprimer, I added a TTGG-overhang to the 5' end of the forward primers and an AAAC-overhang to the 5' end of the reverse primers (Table 5).

**Table 5.** Sequence of order-made oligoprimer containing guide RNA (5'-3')

Primer Name	Ordered Sequence
ERCC6 CRISPRi gRNA1 F	ttggttctactgcgtgcgagc
ERCC6 CRISPRi gRNA1 R	aaacgctcgcacgcaagtagaaa
ERCC6 CRISPRi gRNA2 F	ttggttctactgcgtgcgagca
ERCC6 CRISPRi gRNA2 R	aaactgctcgcacgcaagtagaa
ERCC6 CRISPRi gRNA3 F	ttggaagcacgggcaagaccacg
ERCC6 CRISPRi gRNA3 R	aaaccgtggttggcccgtgctt
ERCC6 CRISPRi gRNA4 F	ttggcgggcaagaccacgtgggt
ERCC6 CRISPRi gRNA4 R	aaacaaccacgtggttggccc
ERCC6 CRISPRi gRNA5 F	ttggtgctcgcacgcaagtagaa
ERCC6 CRISPRi gRNA5 R	aaacttctactgcgtgcgagca
ERCC3 CRISPRi gRNA1 F	ttgggcacgagctaacagatcgg
ERCC3 CRISPRi gRNA1 R	aaacccgatctgtagctcgtgc
ERCC3 CRISPRi gRNA2 F	ttggttaattcgcgcactacac
ERCC3 CRISPRi gRNA2 R	aaacgtgtagtgcgcgaattaa
ERCC3 CRISPRi gRNA3 F	ttggcccacatcacggcgcctag
ERCC3 CRISPRi gRNA3 R	aaacctaggcggcgtgatgtggg

UVSSA CRISPRi gRNA1 F	ttggggccgcgctcagcggtaggta
UVSSA CRISPRi gRNA1 R	aaacacctaccgctgacgcggcc
UVSSA CRISPRi gRNA2 F	ttggcgcgccggttcgggtcccg
UVSSA CRISPRi gRNA2 R	aaaccggggaccgaaccggcgcg
UVSSA CRISPRi gRNA3 F	ttggtggttacgctgccggcgcg
UVSSA CRISPRi gRNA3 R	aaaccgcccggcagcgtaacca
XPA CRISPRi gRNA1 F	ttgggtctgggtatgcgcggaca
XPA CRISPRi gRNA1 R	aaactgtccgcgataccagac
XPA CRISPRi gRNA2 F	ttgggagcgctgcgcagttaag
XPA CRISPRi gRNA2 R	aaaccttaactgcgcaggcgctc
XPA CRISPRi gRNA3 F	ttggccgagccccttaactgcgc
XPA CRISPRi gRNA3 R	aaacgcgcagttaaggggctcgg
Abbreviations: F = Forward primer, R = reverse primer.	

The oligoprimers above were annealed by mixing 1  $\mu$ L of the reverse oligos with 1  $\mu$ L of the forward ones (100  $\mu$ M each) with 8  $\mu$ L of ddH<sub>2</sub>O. I performed a PCR on the mix, with the following settings: 37°C for 30 min, 95°C for 5 min, and then dropping down to 25°C at a rate of 5°C/min. Using the annealed oligoduplex, I continued with its ligation into the targeting vector PB-U6-CNKB (Figure 8), which also contained an Ampicillin-resistant locus (ligation for 2h at room temperature).



To increase the amount of vector, I transformed the ligated vector into NEB Turbo competent cells (*E. coli*) by mixing the full 3  $\mu\text{L}$  of the mix above (Table 6) with 5  $\mu\text{L}$  of bacteria. The mixtures were incubated on ice for 30 min before being placed into the Dry Thermo Unit, preheated to 42°C, for 45 sec. After that I placed them back on ice.

**Table 6.** Mixture used to insert gRNA into the vector plasmid

Digested PB-U6-CNKB (100 ng)	1 $\mu\text{L}$
Phosphorylated and annealed oligoduplex (1:100 dilution)	1 $\mu\text{L}$
2X T4 DNA Ligase Buffer	1 $\mu\text{L}$
Total	3 $\mu\text{L}$

To be sure to grow only transformed bacteria, I plated them on Ampicillin-containing plates overnight at 37°C. The following day I detected two colonies for each gRNA-

primer, making a total of 24 colonies to be analyzed before using them for CRISPRi. For this purpose, I first grew them overnight in 5 mL of Ampicillin-containing medium at 37°C, under constant shaking and with O<sub>2</sub> access (not closing the cap completely). To extract the plasmid, I used the QIAGEN Plasmid Mini Kit according to its protocol. I started the sequencing with a PCR reaction of the mix, as described in Table 7.

**Table 7.** Mixture used to perform PCR reaction.

Plasmid DNA	1 µL (<200 ng)
Primer	1µL (3.2 pmol)
Dilution Buffer: 125mM Tris-HCl, 5mM MgCl/DDW (pH 9.0)	3.5 µL
ddH <sub>2</sub> O	3.5 µL
BigDye	1 µL
Total	10 µL

I used the following setting for the PCR machine:

95°C for 3 min → 25 cycles (90°C for 30 sec → 50°C for 15 sec → 60°C for 4 min) → 4°C without time limit.

The next step was to purify the DNA. I added 1 µL of 125-mM EDTA, 25 µL of 99.5% nuclease-free ethanol and 1 µL of 3-M acetic acid to the PCR product. I then vortexed the mixture before transferring it to an Eppendorf tube. After waiting 10 min, I centrifuged the tubes at RCF of 21 500 g for 15 min (RT), aspirated the supernatant, and washed it with 150 µL of 70% nuclease-free ethanol. I vortexed it again, spun it down at an RCF of 21 500 g for 5 min (RT), aspirated the supernatant carefully, and resuspended the DNA in

15  $\mu$ L of Hi-Di formamide by vortexing. I placed the mixture into a preheated 95°C Thermo Dry Unit for 2 min before immediately cooling the samples down in ice.

I then placed the samples into a 96-well plate suitable for the DNA Sequencer 3130, which I used according to the protocol provided by Applied Biosystems. After I had ensured that all single gRNA primers had been integrated into the digested PB-U6-CNKB vector successfully and without mutations, I transfected these vectors into the iPS cell line C5. This was derived from a healthy proband and the dCas9-KRAB system was already integrated into its genome.

For the transfection procedure, I used essentially the same technology as described in section 2.1. I induced pluripotency by transfection of plasmids using the LONZA product. Based on the purpose and cell type, I used the LONZA Human Stem Cell Nucleofector® Kit 1 and set the program of the Nucleofector to A23. After successful transfection of one type of each primer set per disease (number of primer sets: ERCC6:  $n = 5$ ; ERCC3, UVSSA, XPA:  $n = 3$ ), I plated ca.  $1 \times 10^3$  cells to a 10-cm plate each, and ca.  $1.5 \times 10^4$  to one well of two 6-well plates each (Medium StemFit). After incubating these plates overnight, I added Ampicillin to the medium and changed it every two days. For the 6-well plate, I added doxycycline to one of the corresponding wells to induce the activity of dCas9; this in turn would induce the knockdown of the locus I targeted with my gRNA. When the cells on the 6-well plate reached about 60% confluence, I analyzed the knockdown efficiency by analyzing the cells' transcription. Referring to the RNAzolRT protocol<sup>61</sup>, I collected the cells of each well and cleaned up these samples until only pure RNA remained. As the next step, I performed a qPCR reaction to transform the RNA into cDNA so it was stable enough for analysis. For this purpose I used the protocol provided

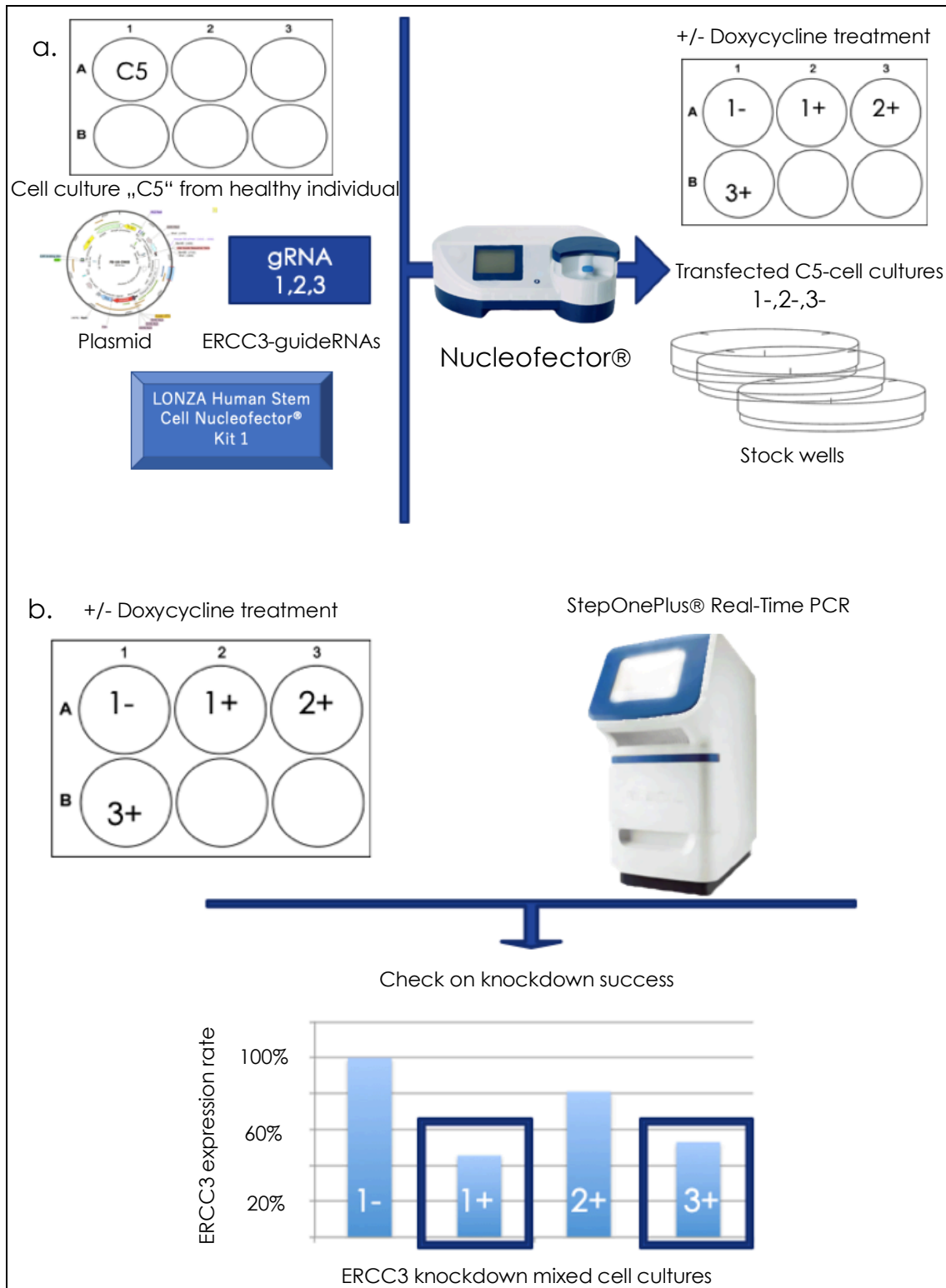
by TAKARA<sup>62</sup>, suitable for the StepOnePlus Real-Time PCR System, and continued following this TAKARA<sup>63</sup> protocol.

The results showed which of the five (ERCC6), respectively three (ERCC3, UVSSA, XPA) wells per targeted genomic locus was the most effective for suppressing the expression of that locus. I then selected five types of single-cell colonies from the referring 10-cm plate, repeated the culturing (doxycycline +/-) and checked on the expression rate for these single colonies again with the rtPCR (Figure 10).

To be sure the knockdown worked properly at the protein level, I transferred the clone with the most effective knockdown on transcription level to a 6-well plate. I then performed a follow-up analysis by western blotting on these cells after a week. The cells were lysed in SDS-PAGE sample buffer containing 1% protease inhibitor, 1  $\mu$ M dithiothreitol, 0.5  $\mu$ M sodium orthovanadate and 0.5  $\mu$ M NaF. They were then boiled at 100 °C for 5 min, and the lysates were stored at -80 °C until used. Protein concentrations of the lysates were estimated by staining lysate spots on a paper with Coomassie brilliant blue dye.

Approximately equivalent amounts of proteins were loaded for each sample and resolved by SDS-PAGE. The gel was placed into a semi-dry blotting system, and was electrophoretically transferred to a PVDF membrane that was presoaked in 100% methanol. Then the membrane was blocked with 2% skimmed milk in TBS containing 0.1% Tween 20 (TBST) and probed overnight at 4 °C, with antibodies as indicated below. Blots were washed with TBST, incubated for 1 h with HRP-conjugated secondary antibodies in TBST supplemented with 2% skimmed milk at room temperature, and then washed again with TBST. Blots were developed using a Luminata Western HRP substrate.

Signals were detected and documented with the densitometry system LAS3000. The primary antibody dilution rate was 1:100 for *ERCC3* and 1:1000 for *ERCC6* (*UVSSA* not yet performed). I then froze all the high-quality clones with knockdown rates over 85%.



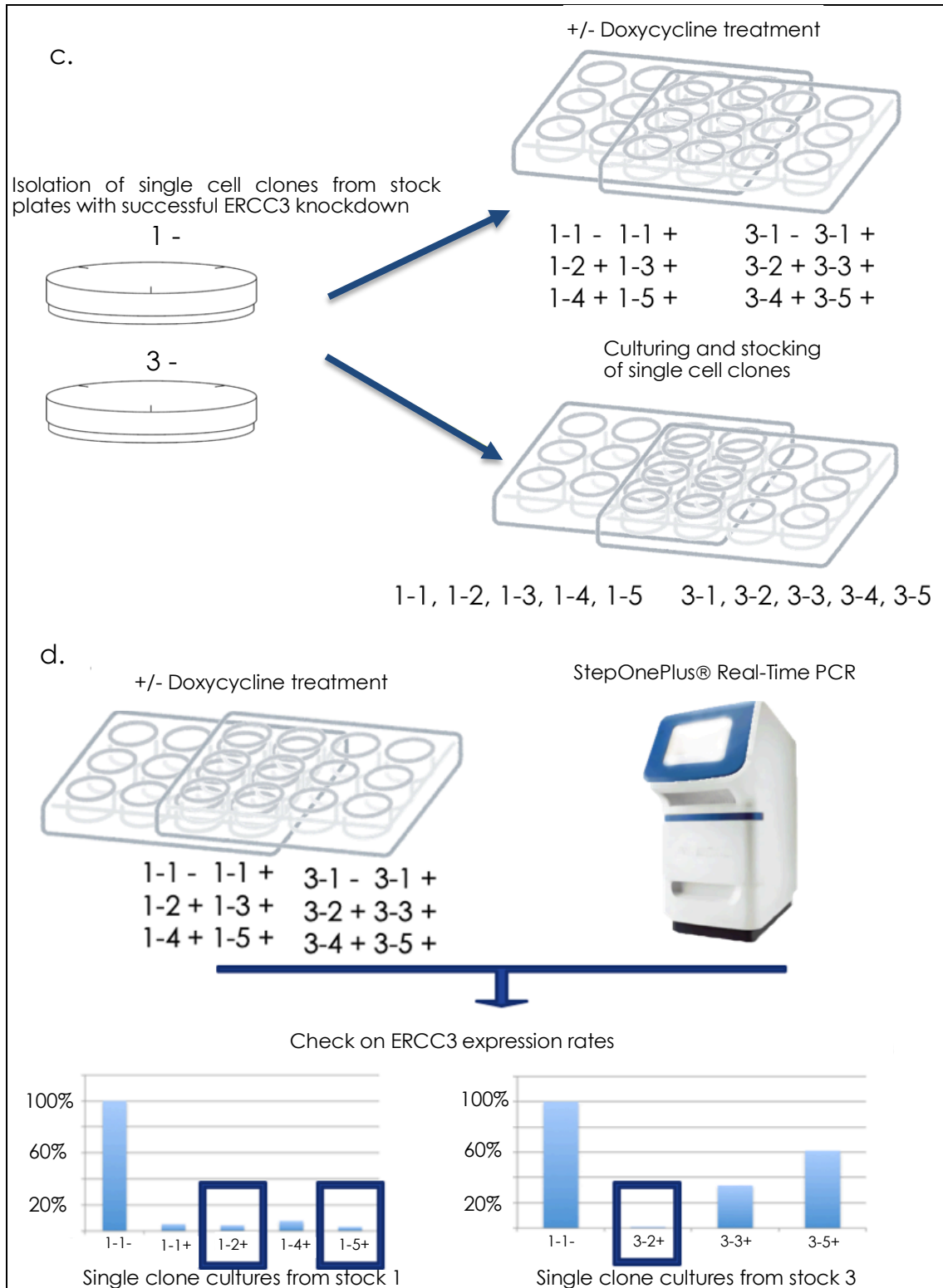


**Figure 9. Workflow of targeted genomic knockdown using CRISPRi.** **a.** After cultivating the C5 cell line gained from a healthy person, I used a plasmid vector to integrate the three ERCC3 gRNAs into the genome of cells via Nucleofector®. I cultivated them separately under doxycycline treatment, with one reference well containing gRNA 1-cells untreated with doxycycline as reference for the rtPCR. I also plated a few of each gRNA-cell on a 10-cm plate to cultivate single clone colonies. **b.** Next, I performed the rtPCR on my dox-treated cells in relation to the untreated cells to determine which gRNA had knocked down the ERCC3 gene most efficiently. **c.** As gRNA 1 and 3 seemed the most efficient at ERCC3 knockdown, I selected single clone colonies from the 10-cm

plates and plated five colonies each, under the procedure described for mixed colonies. **d.** Analyzing these single clone colonies resulted in the determination of three clones (marked with blue frames) with ERCC3 transcription rates lower than 5%, which I then cultivated (clone 3-2) and stocked in our liquid nitrogen tank (clone 1-2, 1-5, 3-2) and discarded the others. The wells of clones 1-3, 3-1 and 3-4 were in poor condition so I excluded them from rtPCR analysis.

### 2.3. Implementing an effective iPS cell-to-keratinocyte differentiation protocol

#### 2.3.1. Materials

Material	Source
Coating Matrix Kit, Buffer and Matrix, mainly type 1 Collagen	ThermoFisher Scientific
Collagen, type 2, Collagen from chicken sternal cartilage	Sigma-Aldrich (Merck)
Collagen, type 4, Collagen Type IV from human cell culture	Sigma-Aldrich (Merck)
Laminin, iMatrix 511 silk	nippi
Geltrex	ThermoFisher Scientific
Atelocollagen Bovine dermispepsin-solubilized type I Collagen solution	Koken
Acetic acid (0.1 M)	Sigma-Aldrich (Merck)
Retinoic acid	Sigma-Aldrich (Merck)
Bone morphogenetic protein 4 (BMP4)	Peprtech
StemFit AK02N	Takara
Defined Keratinocyte-Serum Free Medium, DKFSM	ThermoFisher Scientific
CnT-Prime, Epithelial Culture Medium	CELLnTEC
DAPT (N-[N-(3,5-difluorophenacetyl)-1-alanyl]-S-phenylglycine t-butyl ester)	Sigma-Aldrich (Merck)
Accutase	Innovative Cell Technologies Inc.
Phosphate Buffered Saline	Wako
Epidermal Growth factor	Gibco
Rock-Inhibitor, Y-27632	Focus Bio Molecules

CHIR 99021, 10mM	Wako
4% Paraformaldehyde Phosphate	Nacalai tesque
100% Methanol	Wako
0.1% Triton	0.1% Triton
DAPI	Sigma-Aldrich (Merck)
<b>Primary Antibodies</b>	
Keratin 8/18	Cellsignal
Keratin 14	Arigobio
p63	abcam
Involucrin	abcam
<b>Second Antibodies</b>	
SAB4600353 Anti-Mouse IgG1 ( $\gamma$ 1), CF <sup>TM</sup> 647 antibody produced in goat	Sigma
SAB4600238 Anti-Mouse IgG1 ( $\gamma$ 1), CF <sup>TM</sup> 488A antibody produced in goat	Sigma
SAB4600030 Anti-Rabbit IgG (H+L), CF <sup>TM</sup> 488A antibody produced in chicken	Sigma
SAB4600212 Anti-Rabbit IgG (H+L), CF <sup>TM</sup> 750 antibody produced in goat	Sigma
<b>Equipment</b>	<b>Source</b>
LAF (Lamina Airflow) bench	Sanyo
CO <sub>2</sub> Incubator MCO-170AIC	Panasonic
Pipet-Aid XP	Drummond
Pipetman	Gibson
BioLite 10cm/6well/12well/24well/96well Multidish	Thermofisher Scientific
Cell Lifter, TR9002 1.9 cm blade	TrueLine
Cell Scraper, No.179693, 1.55 cm blade	Nunc
Centrifuge KN-70 for 15ml (r=166mm)	Kubota
All-in-One Fluorescence Microscope Keyence XZ-710 (Lenses: CFI PlanFluor DL x4 NA 0.13 PhL field (um) 3623x2728, CFI PlanFluor DL x10 NA 0.30 PhL field	Keyence

(um) 1449x1091, CFI PlanFluor DL x20 NA 0.45 PhL)	
OP-87762 BZX Filter DAPI Excitation wavelength 360/40, Emission wavelength 460/50	Keyence
OP-87763 BZX Filter GFP, Excitation wavelength 470/40, Emission wavelength 525/50	Keyence
OP-87765 BZX Filter TexasRed, Excitation wavelength 560/40, Emission wavelength 630/75	Keyence
OP-87766 BZX Filter Cy5 Excitation wavelength 620/60, Emission wavelength 700/75	Keyence

### 2.3.2. Methods

I reviewed previous research, referred to later in this paper. Based on this review, I composed a blueprint that combined the most promising methods with my ideas for improvement, and decided which proteins to use as markers for successful differentiation (Figure 11). As a cell line, I used wildtype C (WTC) human iPS cells derived by Miyaoka et al.<sup>64</sup>.

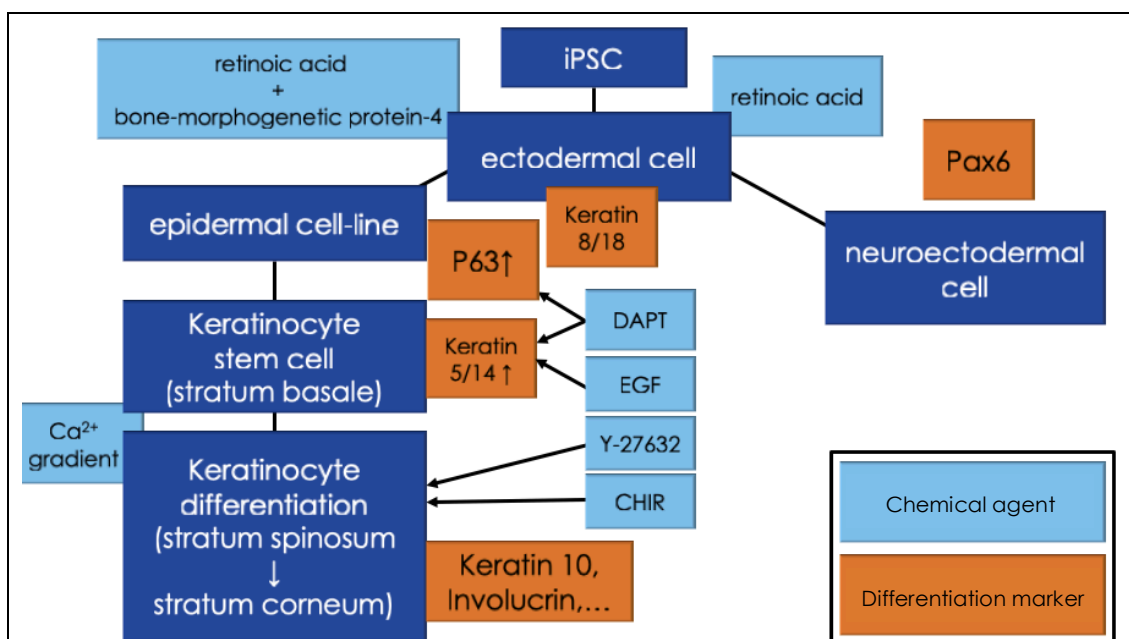


**Figure 10. Flow chart of keratinocyte cell differentiation** under influence of defined chemicals and overview of protein markers at each step of differentiation.

I used a modified protocol according to Kogut et al. (2014)<sup>65</sup>. Coating was performed overnight (at least 6 h), as shown in Table 8.

**Table 8.** Summary of optimal coating conditions to cultivate Keratinocytes.

	Collagen I Buffer	Collagen I Matrix	Collagen IV (10µg/mL)	iMatrix (0.5 µg/µL)
24-well plate	200 µL	2 µL	5 µL	3.5 µL
12-well plate	400 µL	4 µL	10 µL	7 µL
6-well plate	850 µL	8.5 µL	20 µL	11 µL

After aspirating the coating fluid from the well, I washed it twice with PBS and added a suitable amount of Y-27632 containing StemFit. I then transferred the iPS cells to the plate. I noticed that a certain density of cells per area was necessary for a smooth differentiation, and summarized the optimal cell count per well as shown in Table 9

**Table 9.** Summary of optimal cell count per well to cultivate Keratinocytes.

	24-well plate	12-well plate	6-well plate
Optimal cell count	$2 \times 10^5$	$5 \times 10^5$	$10 \times 10^5$

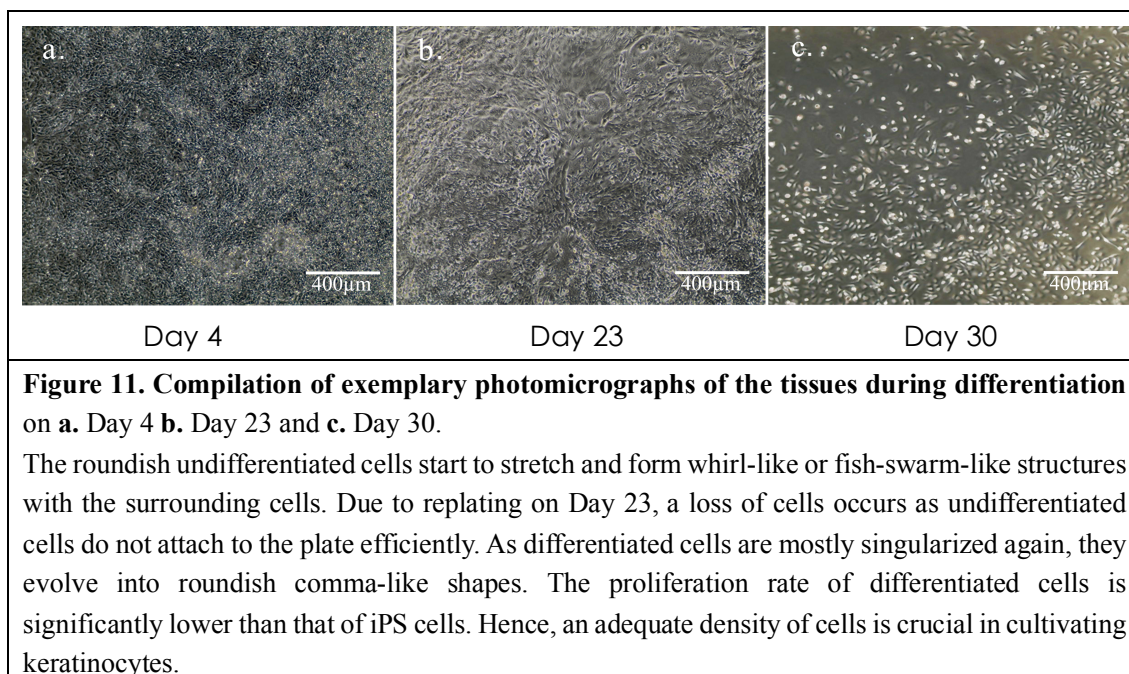
I recommend allowing the cells to attach to the plate overnight, before starting the differentiation process. The following instructions refer to a 22-mm diameter well of the standardized 12-well plate. I placed 3 mL of pre-warmed DKFSM into a conical tube, added 3  $\mu$ L of 1-mM RA to achieve a 1- $\mu$ M working concentration, and added 3  $\mu$ L of 25-ng/mL BMP4 to achieve a 25-ng/mL dilution<sup>65</sup> by mixing well. I aspirated and exchanged 1 mL of the medium on the plate with the differentiation mixture (described above) and incubated the cells for 48 h. I repeated this step on Day 2, so the differentiation mixture was allowed to take effect for four days.

For the next step, I prepared a new medium by mixing 30 mL of DKFSM with 30  $\mu$ L of 5-mM DAPT (N-[N-(3,5-difluorophenacetyl)-1-alanyl]-S-phenylglycine t-butyl ester, also known as GSI-IX or LY-374973)<sup>66</sup> and 6  $\mu$ L of 100- $\mu$ g/ml EGF<sup>67</sup>. On Day 5, I exchanged the old medium for the DKFSM-based medium and thereafter exchanged it every day.

On Day 23 after starting the differentiation, I prepared the transfer of cells to a new well by repeating the same coating as mentioned above. The next day, I used a modified version of the rapid-attachment passaging described by Kogut et al.<sup>65</sup> The process involves aspirating the DKFSM medium, washing the well with PBS once, adding 1 mL of Accutase, incubating for 4 min (using either the Cell Lifter or Cell Scraper depending on the size of the well) and scraping off the cells not yet detached. Then I transferred the

floating cells into a 15-mL tube. To be sure to remove all cells from the plate, I washed the well with 4 mL of DKFSM and transferred this fluid into the 15-mL tube as well. (This procedure also dilutes and weakens the Accutase, which to some extent damages suspended cells).

Next, I spun down the cells at an RCF of 475 for 5 min, aspirated the supernatant, added 1.5 mL of DKFSM, and re-suspended the pellet by pipetting up and down to break the clumps and singularize the cells. Then I aspirated the coating fluid before adding the full amount of 1.5 mL cell suspension. I allowed the cells to attach for 25 min before aspirating the medium and cells which had not yet attached to the plate (Figure 12). This rapid method of attachment aims to separate undifferentiated from differentiated cells, as the latter have a better chance of adhering to the stratum-basale-like coating on the plates.



Kogut et al. showed that statistically, K14 positive cells are more likely to attach to the plate in this restricted period than are undifferentiated iPS cells. Thus, using this

procedure I aimed to raise the ratio of differentiated cells to undifferentiated ones. Implementing the results of Kajiwara et al.<sup>68</sup>, I added EGF after the rapid attachment to the DKFSM medium (concentration: 20 ng/ml); I also added 10 mM of Y-27632 in a 1:1000 dilution and calcium in a 0.05-mM concentration. I renewed this medium every day. To increase the cells' condition and accelerate their growth, I furthermore added CHIR (1  $\mu$ M) to the medium.

When the plate was confluent with cells by over 80% and the tissue looked much like skin tissue, I performed the next passage. The coating method remained the same. For the passage method, I used Accutase for 4 min, unhitched the cells from the plate by using either Cell Lifter or Cell Scraper, and continued singularizing the cells by pipetting. I then transferred the suspension to a 15-mL conical tube. As described above, I added 4 mL of DKFSM to the well to ensure that all cells were removed from the plate, and transferred this medium to the same 15-mL tube. Next, I performed a spin-down at an RCF of 475 g for 6 min, aspirated the supernatant, suspended the pellet in 1 mL of DKFSM, and passaged the total amount to the new coated well (Figure 12).

For the final step in the cells' differentiation, I imitated the microenvironment of the human epidermis. This environment differs from the deeper skin layers mainly through a rising calcium concentration level, leading to a "calcium switch" above 0.1 mM<sup>69</sup> up to concentrations of 0.4 mM in the stratum corneum (Figure 13). I used involucrin as a

characteristic marker protein expressed in keratinocytes of the stratum granulosum and stratum corneum. This protein is located intracellularly throughout the whole cytoplasm.

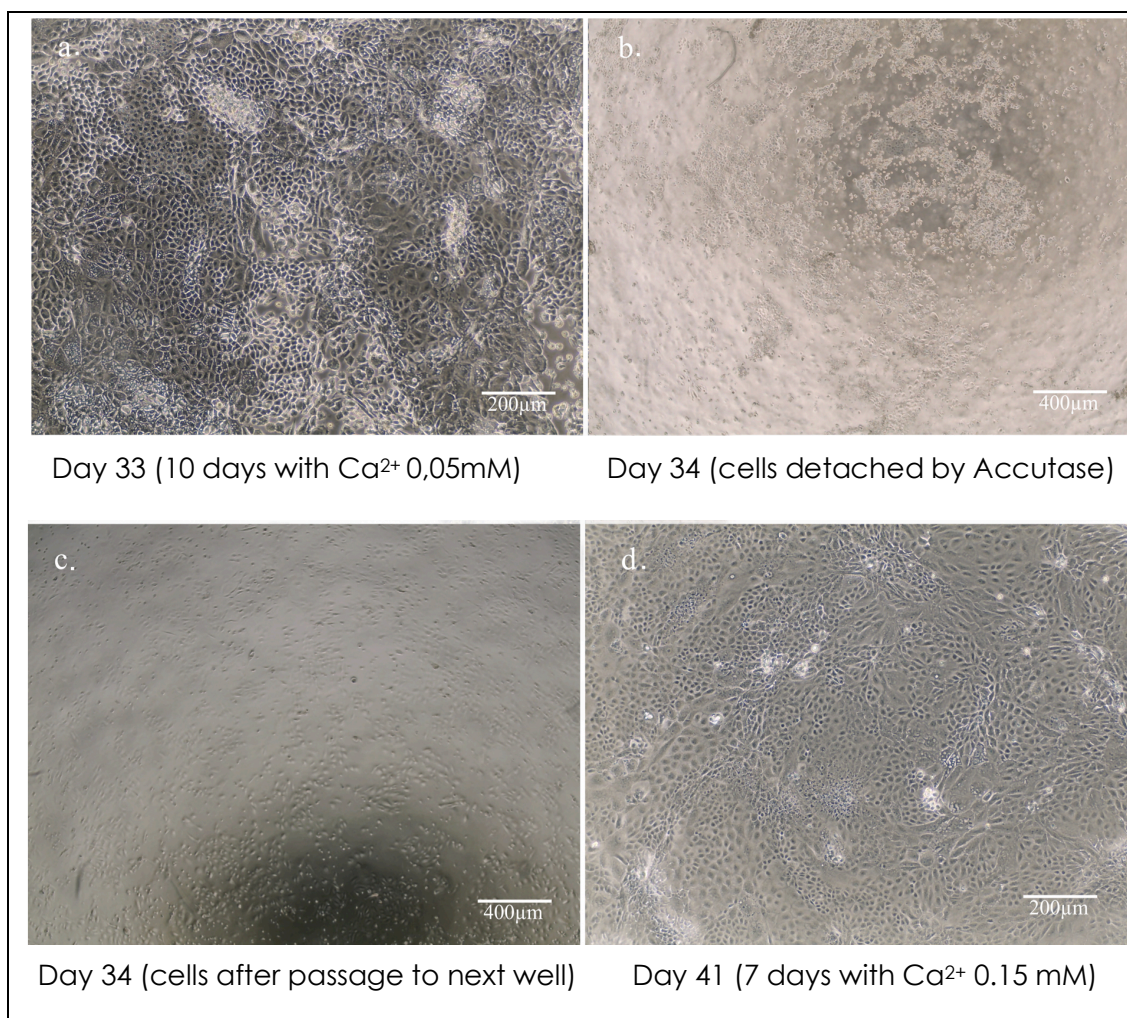


**Figure 12. Compilation of photomicrographs of the tissues during differentiation on a.** Day 33 (after 10 days of  $\text{Ca}^{2+}$  0.05 mM treatment) **b.** Day 34 (after 8 min treatment with Accutase in preparation for the second passage) **c.** Day 34 (right after the second passage) and **d.** Day 41 (after 7 days of  $\text{Ca}^{2+}$  0.15 mM treatment).

As cell density reached an adequate level for passaging on Day 33, I prepared a new well by coating it overnight so I could perform the second passage. The next day, I incubated the cells with Accutase for 8 min until the first cells started to detach from the plate. I then scraped the other cells off the plate and transferred them to the new coated well. I cultivated the cells with medium enriched with 0.15 mM of  $\text{Ca}^{2+}$  and observed that the cells stretched into polygonal forms, just as keratinocytes do in superficial skin layers.

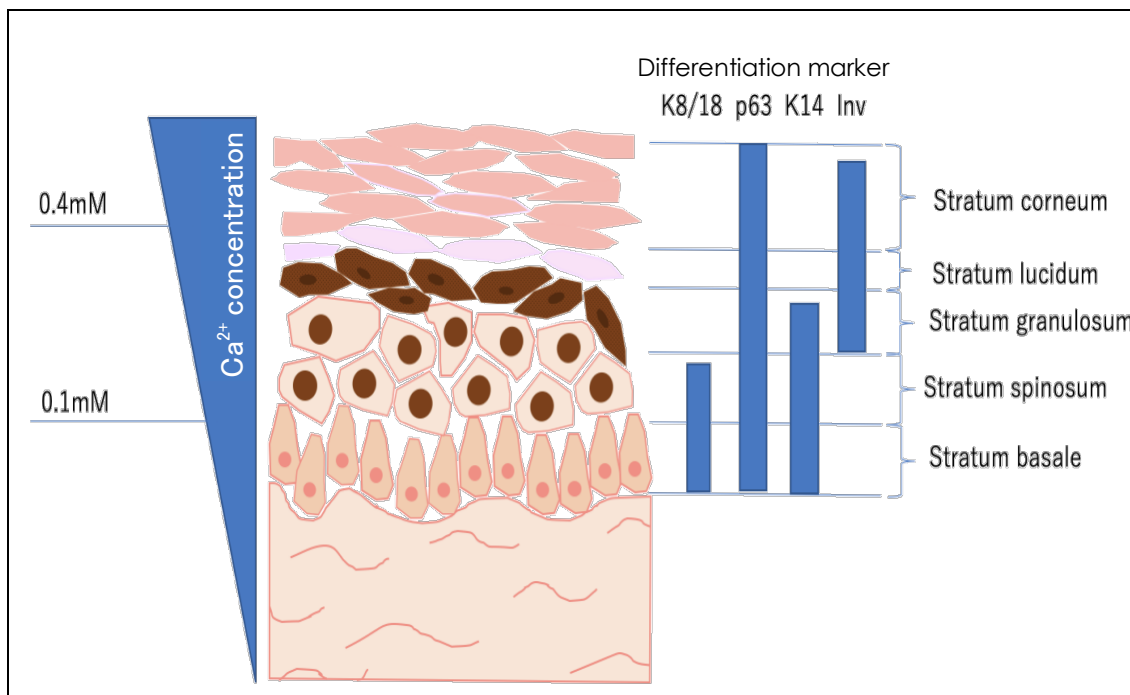


**Figure 13. Schematic drawing of human epidermis.** A constantly elevating gradient of calcium concentration occurs from the stratum basale to the stratum corneum, with compilation of specific proteins matched to the layers in which they are typically expressed.

K8/18 = Keratin 8/18, K14 = Keratin 14, Inv = Involucrin

I compared three samples for 28 days. Each sample received 0.05 mM  $Ca^{2+}$  treatment for the first seven days, which was similar to the concentration in the stratum basale (0.05 mM). As a control, I left one of the three samples at this level for the entire four weeks. For the first treatment group, I increased the  $Ca^{2+}$  to 0.3 mM on Day 8 and maintained this level until Day 28. The last sample was successively elevated to 0.3 mM, starting with 0.1 mM on Day 8, then 0.2 mM on Day 14 and finally 0.3 mM on Day 21. All the samples' mediums were renewed every two days by maintaining the conditions implied, before staining the nuclear DNA (DAPI) and K14 and involucrin on Day 28 (Figure 14). The staining results are shown in Figure 26.

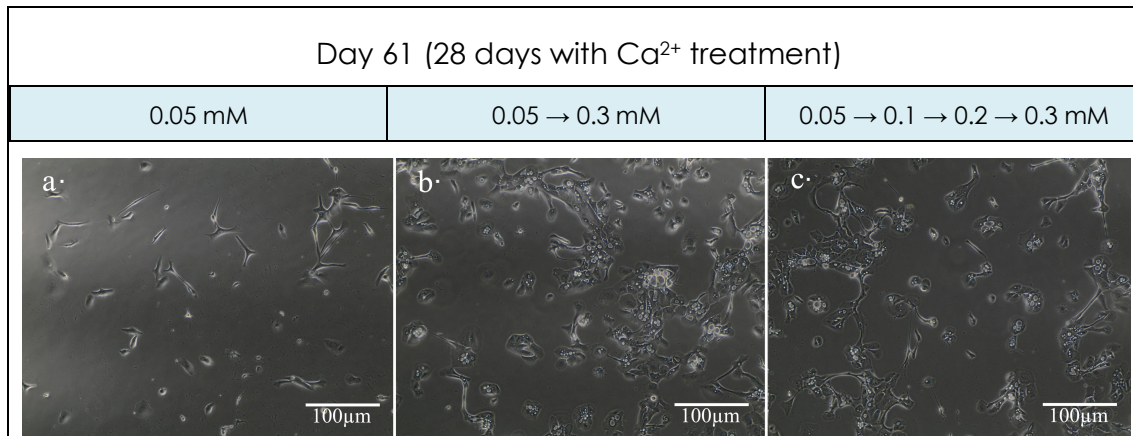
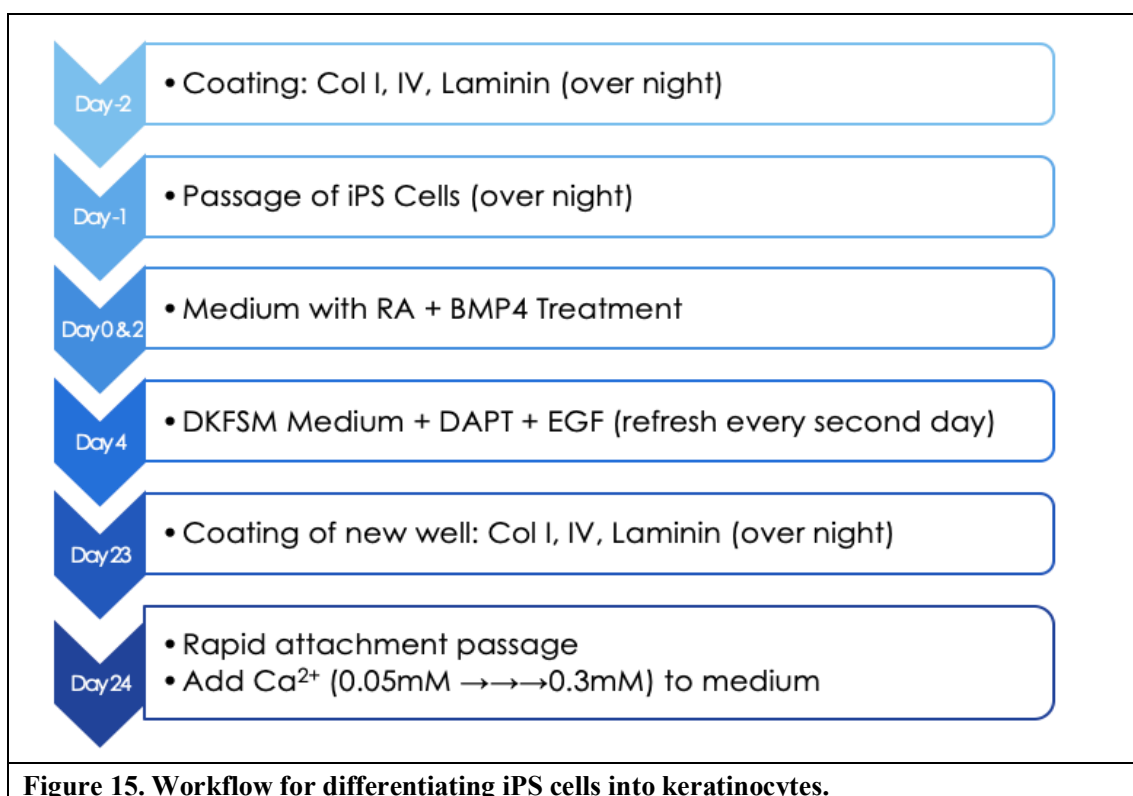


**Figure 14. Compilation of photomicrographs of tissues treated with different concentrations of Ca<sup>2+</sup> (Day 28 of Ca<sup>2+</sup> treatment, Day 61 since start of differentiation).**

**a.** The cells constantly treated with 0.05 mM of calcium retained comma-like shapes and continued to stretch as if seeking contact with other cells. In comparison to the other two plates, fewer cells detached from the plate and showed slow but steady proliferation. **b. c.** In the other two plates, an arrest of proliferation seemed to occur along with a higher grade of differentiation. I observed intracellular “bubbles” that may imply further differentiation; however, cellular stress must also be considered.

To aid comprehension of the various steps in the protocol, I summarized my observations during the exploration of the most effective differentiation process. These are shown in the basic workflow in Figure 15.



During the whole differentiation process, I repeatedly checked the expression rate of several keratinocyte-specific markers (p63, Keratin 8/18, Keratin 14, Involucrin). Staining was performed according to the product protocols, mainly using 4% paraformaldehyde phosphate for fixation, and 100% methanol or 0.1% Triton (dissolved in PBS) for cell-membrane degeneration. The dilution rates are shown in Table 10.

**Table 10.** Primary and second antibodies used

Primary Antibody	Dilution Rate		Responding animal
Anti-DAPI	1:1,000		/
Anti-Keratin 8/18	1:100		Mouse
Anti-Keratin 14	1:100		Rabbit
Anti-p63	1:300		Rabbit
Anti-Involucrin	1:200		Mouse
Second Antibody	Filter/Color	Dilution Rate	Responding animal
IgG1 ( $\gamma$ 1), CF <sup>TM</sup> 647 antibody produced in goat (for Keratin 8/18-AB)	Cy5 = magenta	1:1,000	Mouse
IgG1 ( $\gamma$ 1), CF <sup>TM</sup> 488A antibody produced in goat (for p63-AB)	GFP = green	1:1,000	Mouse
IgG (H+L), CF <sup>TM</sup> 488A antibody produced in chicken (for Keratin 14-AB)	GFP = green	1:1,000	Rabbit
IgG (H+L), CF <sup>TM</sup> 750 antibody produced in goat (for Involucrin-AB)	FR = far/deep red (Filter used: TexasRed: 625/75nm)	1:1,000	Rabbit

## 2.4. Comparison of cell lines WTC, C5, ERCC3, ERCC6, EIIS and UVSSA

### 2.4.1. Basic comparison on iPS cell level

#### 2.4.1.1. Material

<b>Material</b>	<b>Source</b>
Coating Matrix Kit, Buffer and Matrix, mainly type 1 Collagen	ThermoFisher Scientific
Collagen, type 4, Collagen Type IV from human cell culture	Sigma-Aldrich (Merck)
Laminin, iMatrix 511 silk	nippi
Retinoic acid	Sigma-Aldrich (Merck)
Bone morphogenetic protein 4 (BMP4)	Peprotech
StemFit AK02N	Takara
Defined Keratinocyte-Serum Free Medium, DKFSM	ThermoFisher Scientific
DAPT (N-[N-(3,5-difluorophenacetyl)-1-alanyl]-S-phenylglycine t-butyl ester)	Sigma-Aldrich (Merck)
Accutase	Innovative Cell Technologies Inc.
Phosphate Buffered Saline	Wako
Epidermal Growth factor	Gibco
Rock-Inhibitor, Y-27632	Focus Bio Molecules
CHIR, 10mM	Wako
<b>Equipment</b>	<b>Source</b>
LAF (Lamina Airflow) bench	Sanyo
CO2 Incubator MCO-170AIC	Panasonic
Pipet-Aid XP	Drummond
Pipetman	Gibson
BioLite 12well Multidish	Thermofisher Scientific
LUNA <sup>®</sup> Automated Cell Counter	Logos
T13001 Trypan Blue Stain, 0.4%	Logos
LUNA <sup>®</sup> Cell Counting Slides,	Logos

#### 2.4.1.2. Methods

After implementing my protocol for iPS cell-to-keratinocyte differentiation and producing my disease model cells with CRISPRi successfully, I compared the following cell lines under varying conditions: WTC (iPS cells derived from a healthy proband without dCas9 activity), C5 (same as WTC but with dCas9 activity), ERCC3 and ERCC6 (CRISPRi-induced knockdown, dCas9 activity), and EIIS (derived from a patient with genetically determined CS, subtype *ERCC6* point mutation). Before starting with the analysis of differentiation, I aimed to document basic differences at the stage of undifferentiated iPS cells. Therefore, I prepared a 12-well plate and plated each of the cell lines on two wells (about 14 000 cells per well). In one well, I added doxycycline to the medium, and to the other I did not. I then observed the cell form, colony form, growth rate and viability, using the LUNA<sup>®</sup> Automated Cell Counter following the manual<sup>70</sup>.

As the main comparison experiment, I differentiated my four cell lines to keratinocytes under constant observation. I also performed a cell count on Day 24 when performing the rapid attachment. After an additional seven days with treatment of 0.05 mM calcium, epidermal growth factor and Y-27632, I passaged the cells normally to two different wells: one for staining (K14, p63) and the other for further experiments using UV light and H<sub>2</sub>O<sub>2</sub> (as mentioned above).

## 2.4.2. Comparison on iPS cell level and differentiated level using UV light and H<sub>2</sub>O<sub>2</sub>

### 2.4.2.1. Material

Material	Source
Penicillin-Streptomycin (10,000 U/mL)	ThermoFisher Scientific
Crystal Violet	Wako
Reactive Oxygen Species (ROS) Detection Reagents®	Invitrogen
Primary Antibodies	
Q92896 Mouse anti-Human Golgi Marker Primary Antibody	RayBiotech
Anti-Transferrin Receptor antibody (ab1086)	abcam
Anti-EEA1 antibody - Early Endosome Marker (ab2900)	abcam
Second Antibodies	
SAB4600030 Anti-Rabbit IgG (H+L), CF™ 488A antibody produced in chicken (for keratin 14-AB, Transferrin und Early Endosome)	Sigma
SAB4600325 Anti-Mouse IgG1 (γ1), CF™594 antibody produced in goat (for Cis-Golgi)	Sigma
Equipment	Source
All-in-One Fluorescence Microscope Keyence XZ-710 (Lenses: CFI PlanFluor DL x4 NA 0.13 PhL field (um) 3623x2728, CFI PlanFluor DL x10 NA 0.30 PhL field (um) 1449x1091, CFI PlanFluor DL x20 NA 0.45 PhL)	Keyence
OP-87762 BZX Filter DAPI Excitation wavelength 360/40, Emission wavelength 460/50	Keyence

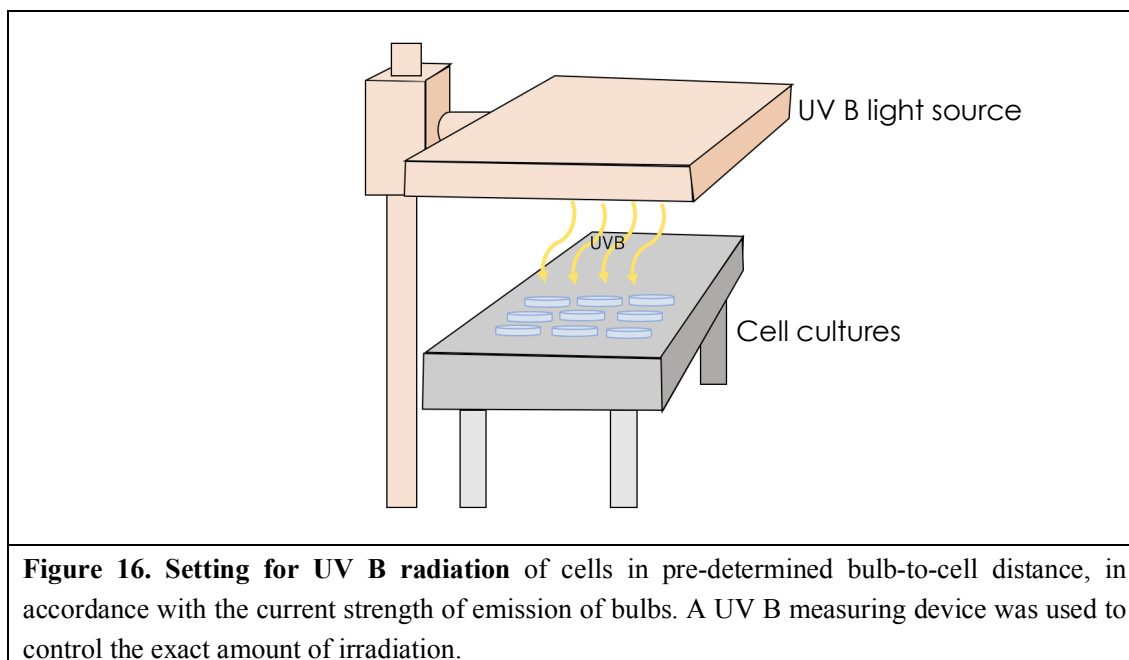
OP-87764 BZX Filter TRITC, Excitation wavelength 545/25, Emission wavelength 605/70	Keyence
OP-87765 BZX Filter TexasRed, 560/40, 630/75	Keyence
OP-87766 BZX Filter Cy5 Excitation wavelength 620/60, Emission wavelength 700/75	Keyence
UV A and B measuring device (SOL – 000539 - 01	MK Scientific, Inc.

#### 2.4.2.2. Methods

After I examined the cell lines C5, ERCC3, ERCC6, UVSSA and EIIS at the iPS cell level systematically, I tested their reaction to different kinds of stress. Patients with XP are susceptible to UV light exposure, so I devised a setting to irradiate the cells with UV light. UV light itself is subdivided in UV types A, B and C. Although about 99% of UV C and 95% of UV B is said to be absorbed by the atmosphere<sup>71</sup> and does not reach the earth's surface, most prior research has used UV C. Because UV C has the shortest wavelength and thus possesses the highest level of energy, it needs a shorter period to achieve the same level of stress application as that induced by using UV B or UV A. However, it is not only the quantity in Joule that separates the three types of UV light; the qualitative effect on the cells also differs. Applying the same amount of Joule by longer radiation with UV B compared to an equivalent radiation with UV C causes different effects inside the irradiated cell. UV C mainly leads to severe DNA damage and often results in cell apoptosis, whereas UV B activates the cell to inflammation<sup>72</sup> and changes the cell's paradigm from growth to DNA protection and damage repair. My results confirmed these patterns.

Looking through many publications, I decided to reference the protocol of Gentile et al.<sup>73</sup>, which in my view was the most properly standardized and suitable setting to test on my cells. I prepared three 12-well plates with C5, ERCC3 and ERCC6 (one doxycycline-treated and one untreated) and EIIS. The cells were allowed to attach overnight. I kept one plate as a negative control without irradiation and the remaining two were exposed to 1 mJ/cm<sup>2</sup> and 5 mJ/cm<sup>2</sup> respectively, resulting in complete cell death on the irradiated plates the next day. As 1 mJ/cm<sup>2</sup> was the lowest setting of our UV C machine, I worked together with the department of dermatology at the Osaka Medical College, which possesses a machine that emits UV A and B. To standardize the experimental setting, I stated a fixed distance between the UV lamps of 48 cm. This would expose the plates on the work surface to 2.25 mJ/cm<sup>2</sup>/sec, and the machine confirmed this measurement.

After plating each cell line on multiple singular 35-mm plates, I aspirated the medium, washed them once with PBS, and aspirated it again. I then exposed the blank cells to UV B light for different periods (2 sec, 4 sec, 5 sec, 11.5 sec and 23 sec). I then added new medium, enriched with penicillin-streptomycin (10 000 U/mL), before incubating the cells again at 38 °C (Figure 16).



After the exposure, I added 1.5 mL of StemFit enriched with penicillin-streptomycin (100  $\mu\text{g}/\text{mL}$ ) to prevent contamination as the procedure was not performed in a sterilized environment. As the examination method, I used staining with the reagent crystal violet. I first aimed to determine the doses of radiation the cells could endure without being extinguished within a week.

On Day 7 after irradiation and with a medium exchange every two days, I aspirated the StemFit medium and fixed the cells on the plate with 4% paraformaldehyde for 10 min at room temperature. In the second step, I washed all the plates twice with PBS before adding a solution of 25% methanol containing 0.2% crystal violet (e.g. 0.02 g crystal violet, 2.5 mL of 100% methanol and 7.5 mL purified water). After 15 min, the cells were sufficiently stained so I could wash off excess crystal violet solution with purified water. I let the plates dry for several hours before photographically documenting them.

After analyzing the results, we fixed the radiation dose at 2 sec (4.5 mJ/cm<sup>2</sup>) and 4 sec (9.0 mJ/cm<sup>2</sup>). I examined the cells with the ROS Detection Reagents<sup>®</sup> Kit by Invitrogen, 60 min after irradiation and one day after irradiation.

As far as possible, I exposed the differentiated cell lines to UV light and observed their reactions. Differentiated keratinocytes are expected to be more robust than iPS cells, so I elevated the irradiation levels to 25.0 mJ/cm<sup>2</sup>, 50.0 mJ/cm<sup>2</sup> and 75.0 mJ/cm<sup>2</sup>. The control was not irradiated.

In addition to DNA damage caused by UV light, oxidative stress is thought to be a significant factor in the pathology of CS especially<sup>74</sup>. Thus, I developed an experiment to expose the cells to different concentrations of hydrogen peroxide (H<sub>2</sub>O<sub>2</sub>), which is known as an inducer of ROS<sup>75</sup>. It is often used as a standardized ROS inducer to create positive controls in ROS examination kits.

To calculate the optimal concentrations, I referred to the work of Li et al.<sup>76</sup>, in which iPS cells were exposed to 25.0 μM, 50.0 μM, 100.0 μM and 200.0 μM for 24 h, 48 h and 72 h each and the cell viability was then checked. I was not interested in inducing apoptosis, as did Yangxing et al., and certain types of ROS are said to disappear as quickly as they are induced. I therefore decided on a period of 1 h from H<sub>2</sub>O<sub>2</sub> exposure to ROS examination. I first tried 0 μM (negative control), 50 μM, 100 μM and 500 μM; the 500-μM dose extinguished all cells, so I then focused on 50 μM and 200 μM for 1 h. Examination was performed with an All-in-One Fluorescence Microscope XZ-710 (Keyence) and GFP filter (460/50 nm).

To find out if a cell compartment was correlated to the ROS I observed, I stained the cells with different markers of cell compartments that seemed likely to match with the

observed structures. Regarding the staining method, I referred to the protocols provided with the antibody makers. The dilution rates are shown in Table 11.

**Table 11.** Primary and secondary antibodies used.

Primary Antibody	Dilution rate		Responding animal
Anti-Cis-Golgi	1:1,000		Mouse
Anti-Transferrin Receptor	1:1,000		Mouse
Anti-Early Endosome	1:1,000		Rabbit
Second Antibody	Filter/Color	Dilution rate	Responding animal
IgG1 ( $\gamma$ 1), CF <sup>TM</sup> 594 antibody produced in goat (for Cis-Golgi)	TRITC = red	1:1,000	Mouse
IgG (H+L), CF <sup>TM</sup> 488A antibody produced in chicken (for Transferrin Receptor-AB und Early Endosome-AB)	GFP = green	1:1,000	Rabbit

### **3. Results**

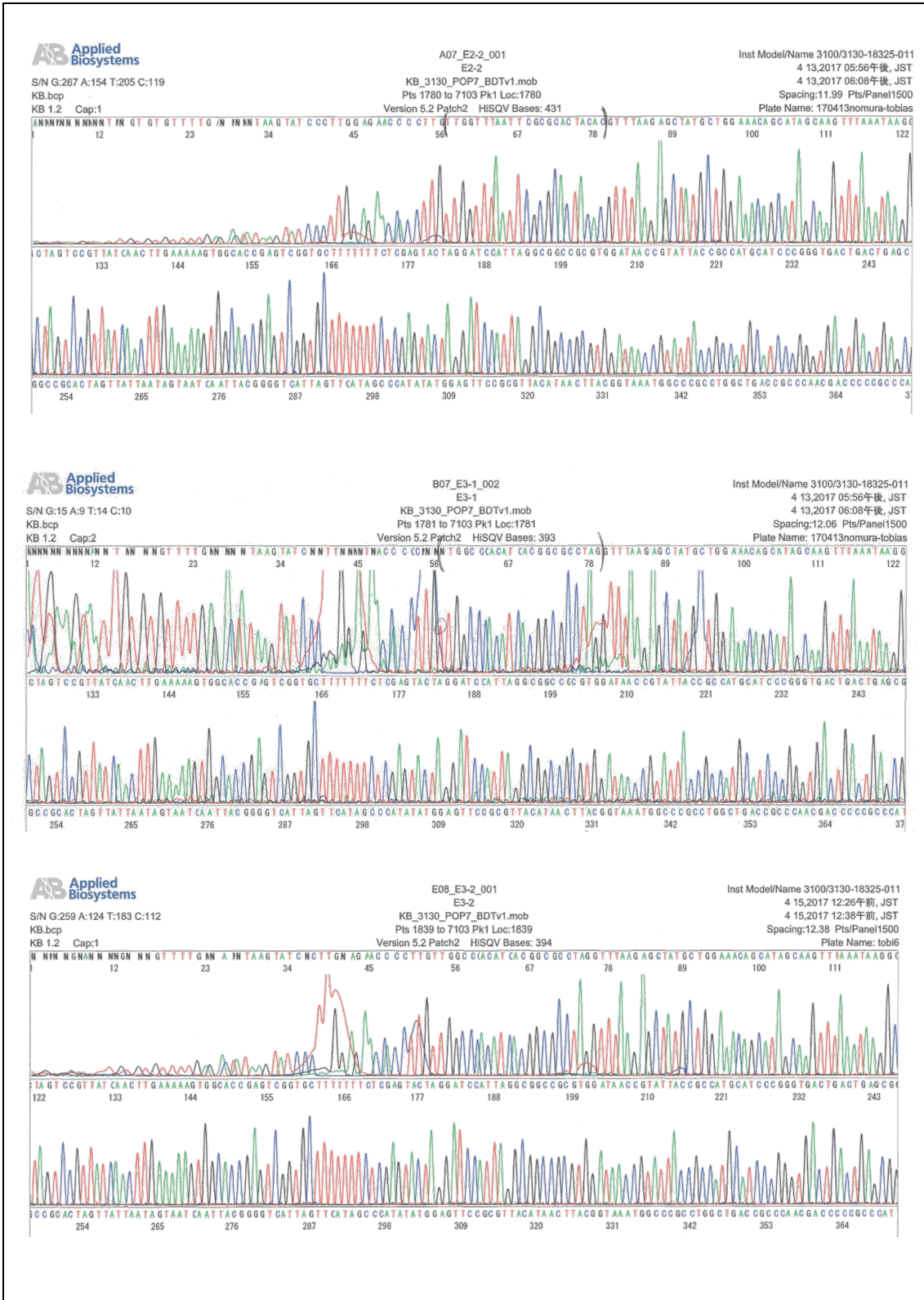
#### **3.1. Inducing pluripotency in somatic cells from a CS patient**

To induce pluripotency, we used the well-established protocols to derive iPS cells. We noted the characteristic form of the derived cells (Figure 6) and their biochemical performance, such as susceptibility to external stress like changes in temperature or contamination, and their typically high proliferation rates. The success of induction of pluripotency was further examined and confirmed by other lab members (data not included in this thesis).

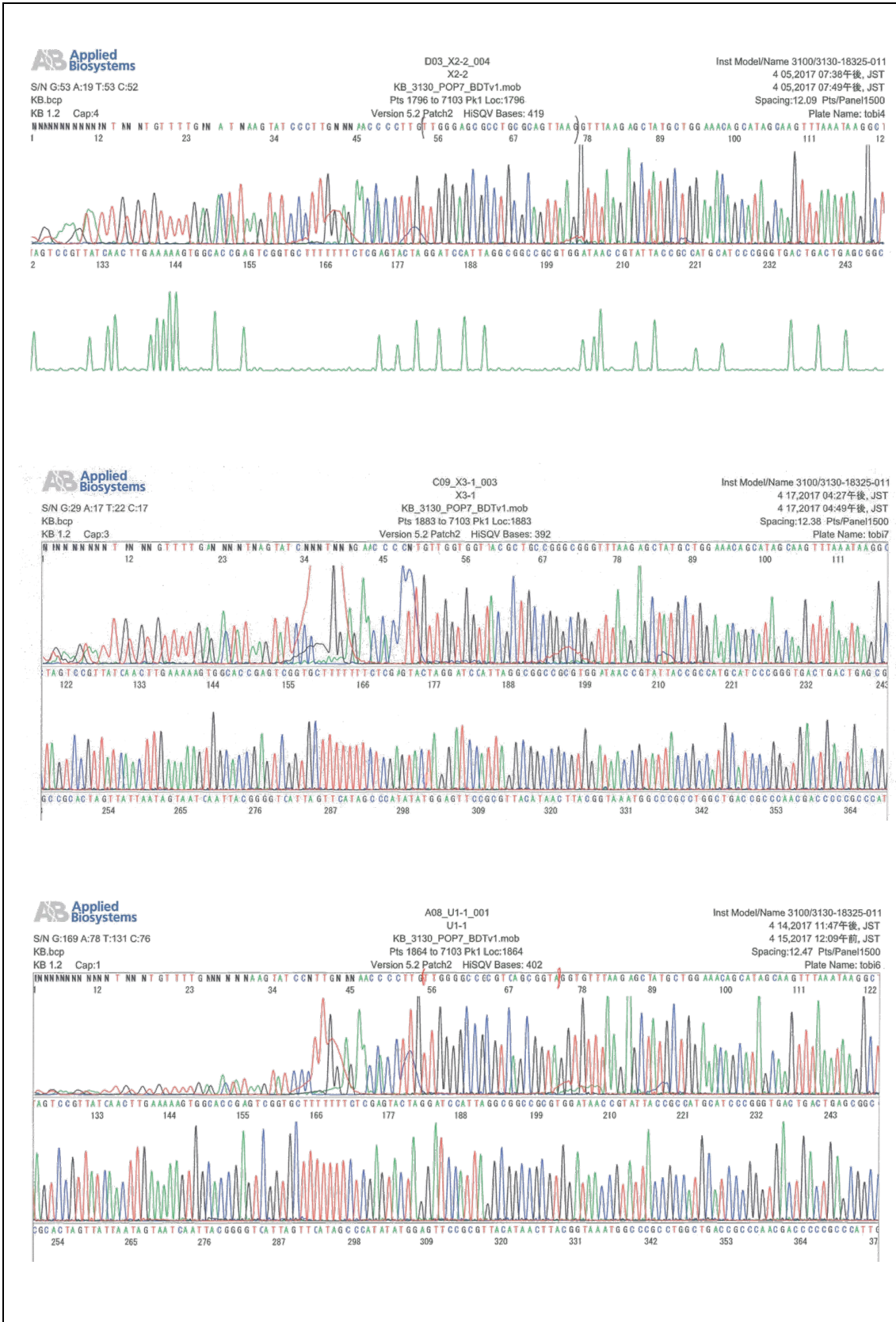
#### **3.2. Specific genomic knockdown using CRISPRi technology**

Using the DNA Sequencer 3130, I confirmed that the gRNA oligoprimer I had designed was successfully inserted into the genome at the targeted place. There were no spontaneous mutations (Figure 17).









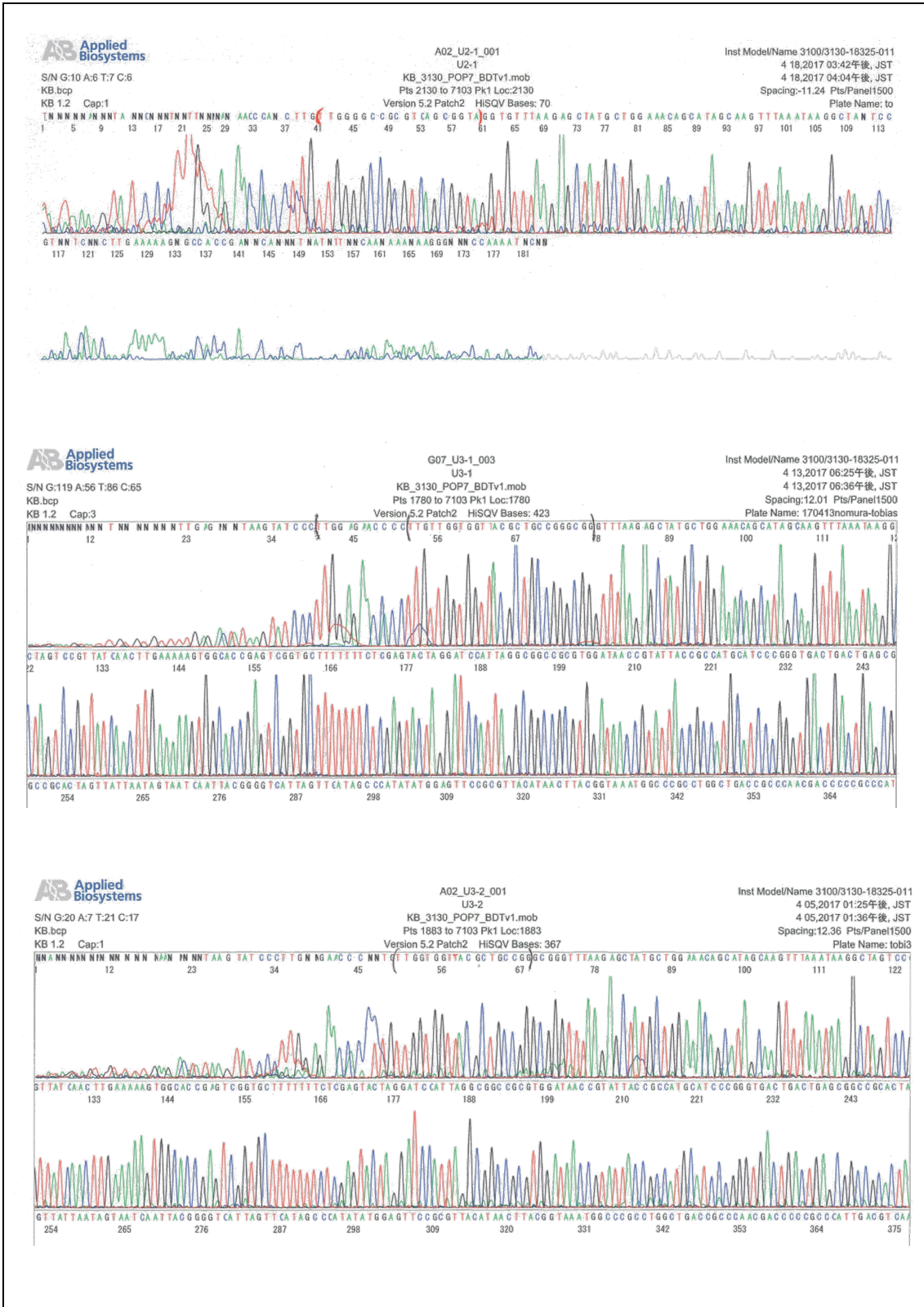


**Figure 17. DNA sequencing of genomic sites to check on the correct, mutation-free integration of gRNA.** E1-E3 = ERCC3, X1-3 = XPA, U1-3 = UVSSA. Two samples for each gRNA. X3-2, U1-2, U2-2 samples were not pure enough to be reliably analyzed. Sequencing data of ERCC6 is missing.

I then transfected the plasmid mix into the cells and cultured them on 10-cm plates and 6-well plates, with and without the application of doxycycline to activate the effect of dCas9. After this I performed a first analysis of the mixed state of cells and determined the following knockdown rates (Figure 18).

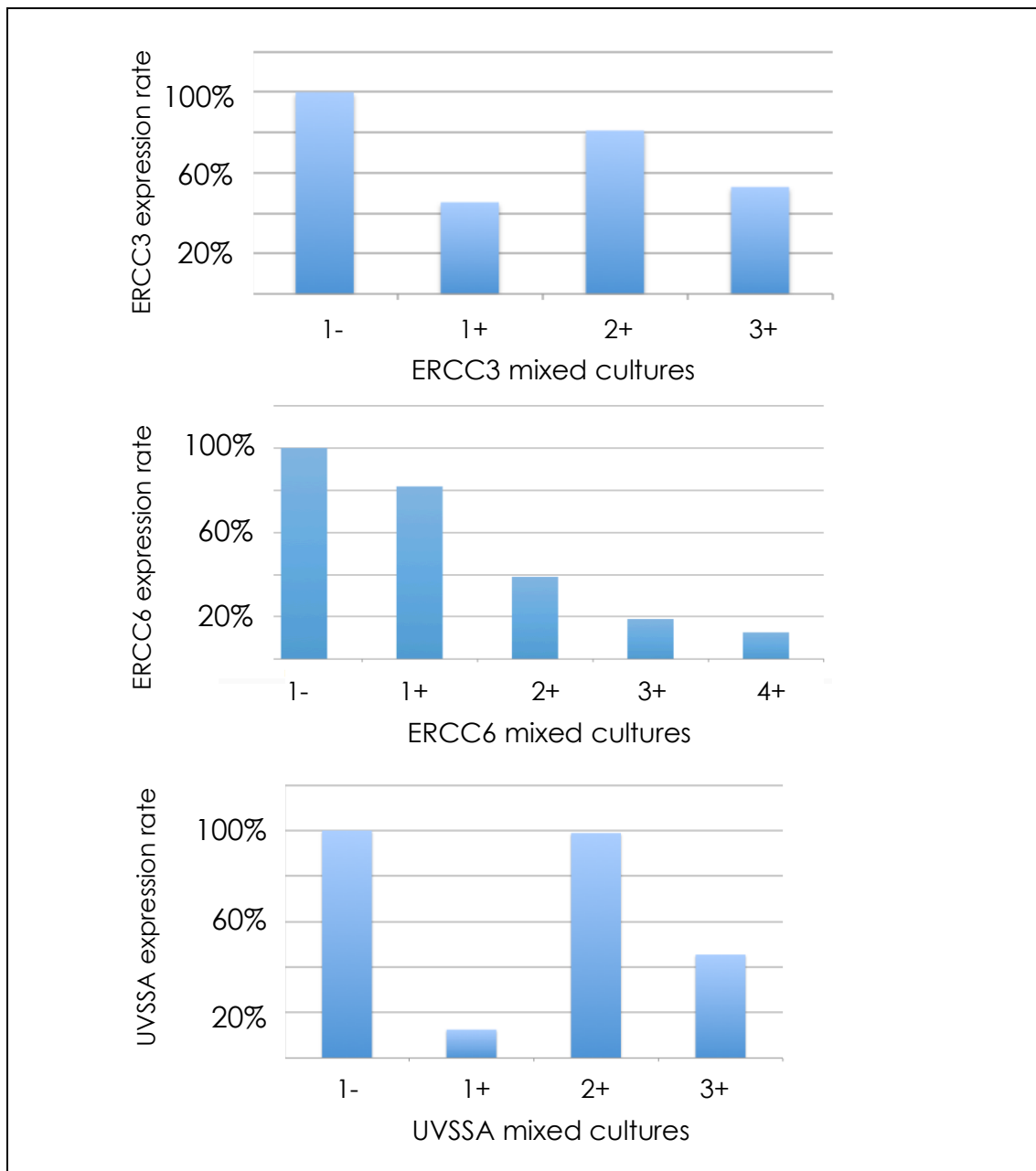


**Figure 18. Knockdown rates of mixed cultures after gRNA integration.** As knockdown is induced by doxycycline treatment, the rates result from the RNA expression of untreated cells (1-) in relation to treated cells (1+, 2+, 3+). Clones used for further examination were ERCC3 1, 3; ERCC6 3,5; and UVSSA 1.

Based on these results, five single clones from each cell population with the most effective knockdown were selected: ERCC3-E1 and E3, ERCC6-E3 and E5, and UVSSA-U1 (Figure 19). These were chosen from the corresponding 10-cm plates and I checked them after further culturing. (We noted that E1-3+, E3-1+, and E3-4+ showed relatively slow cell growth, so I analyzed the other colonies first. As shown in Figure 19, I gained single cell clones that were knocked down effectively enough that I decided not to analyze the remaining colonies.)

With this method I was able to isolate single clone cells with knockdown rates between 89% and 99%. For ERCC3, I used the E3-2 (99%) clone; for ERCC6, the E5-4 (99%) clone; and for UVSSA the U1-6 (89%) clone. I accepted the U1-6 clone with a resting expression of 11% because the threshold cycle during RT PCR (used to check on the expression rate) had an average of 33 cycles (max.: 40 cycles). This implies the expression rate itself is close to undetectable levels (threshold cycles above 35 are said to be unusable).

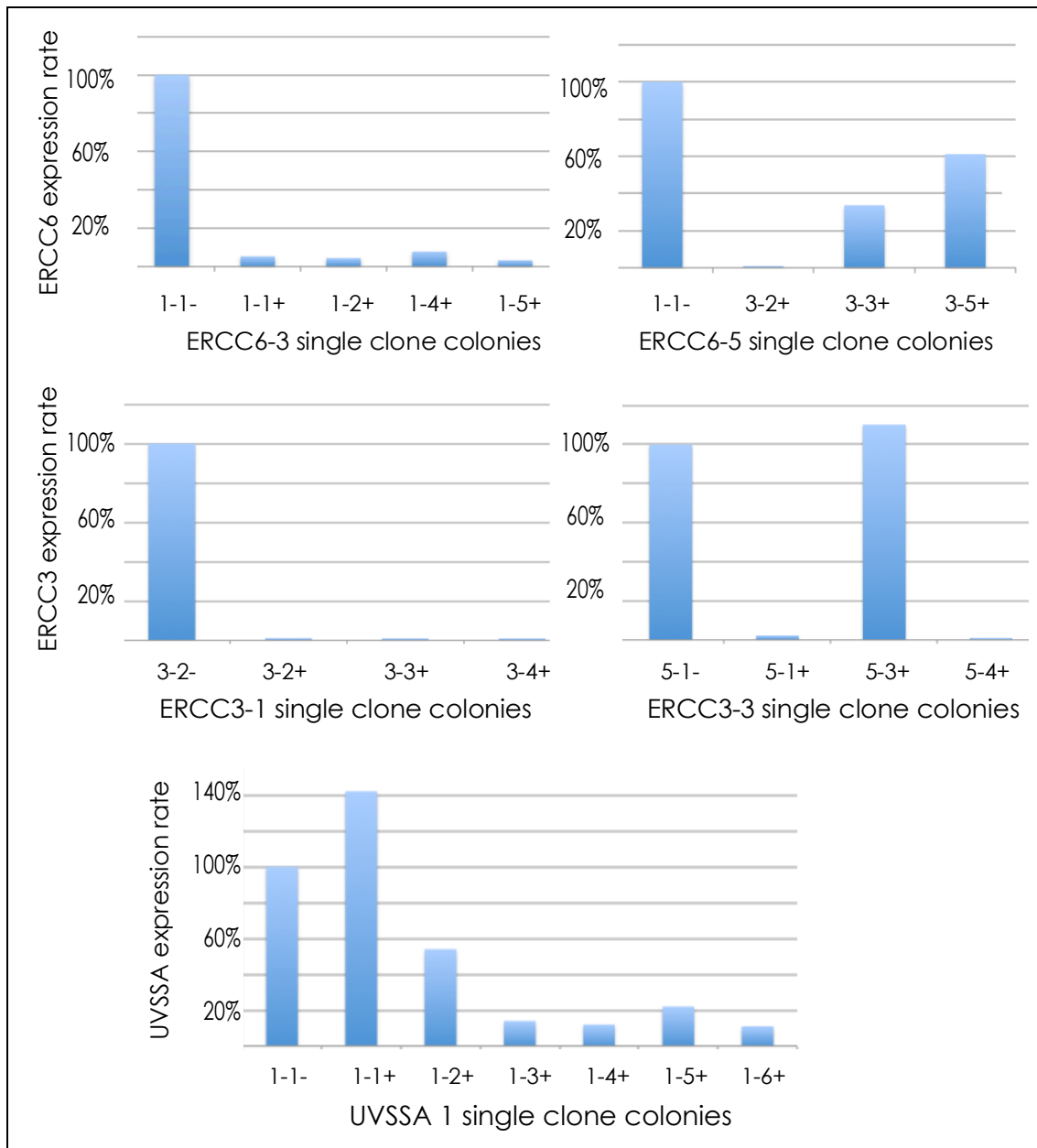


**Figure 19. Knockdown rates of single cultures after gRNA integration** and selection on mixed colony level in relation to cells not treated with doxycycline (-). Clones preserved in nitrogen tank were ERCC3 1-2, 1-5, 3-2; ERCC6 3-3, 3-4, 5-4; and UVSSA 1-4, 1-6. Clones used for experiments in this study were ERCC 3-2; ERCC6 5-4; and UVSSA 1-6.

After testing the degree of reduced gene transcription by rtPCR on the RNA level, I also confirmed the knockdown at the protein level. I performed western blots on the *ERCC3/ERCC6* cell lines (UVSSA not performed yet) examining protein expression,

which showed that only slight levels remained (Figure 20) for ERCC6 and ERCC3.

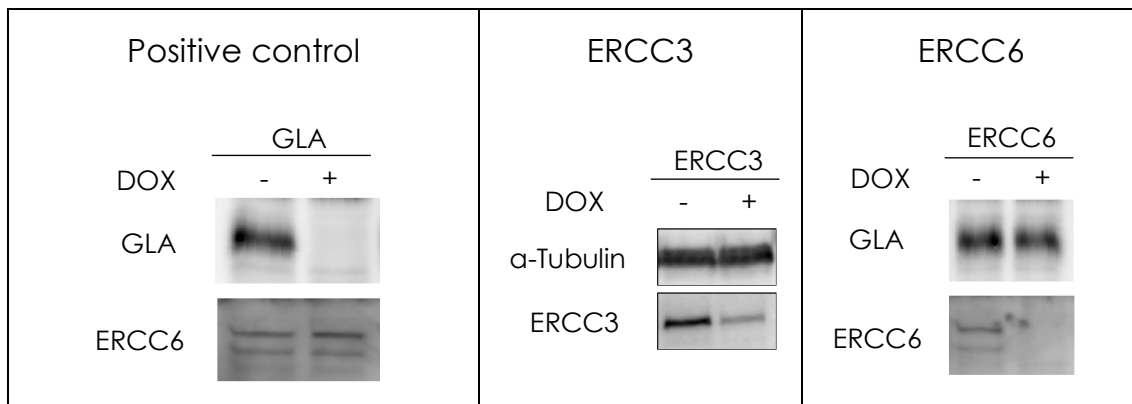


**Figure 20. Western blot on gene expression of knocked-down genes into protein.** A cell line with secured doxycycline-inducible GLA knockdown was used as positive control to check doxycycline was effective; as ERCC6 was not knocked down in this cell line, it was equally expressed with and without doxycycline treatment. ERCC3 and ERCC6 knockdown cells are shown with dox-untreated negative control and alpha tubulin, respectively GLA, as control for regular expression. Unfortunately, I was not able to perform a western blot on UVSSA knockdown cells yet. DOX = doxycycline, GLA = galactosidase

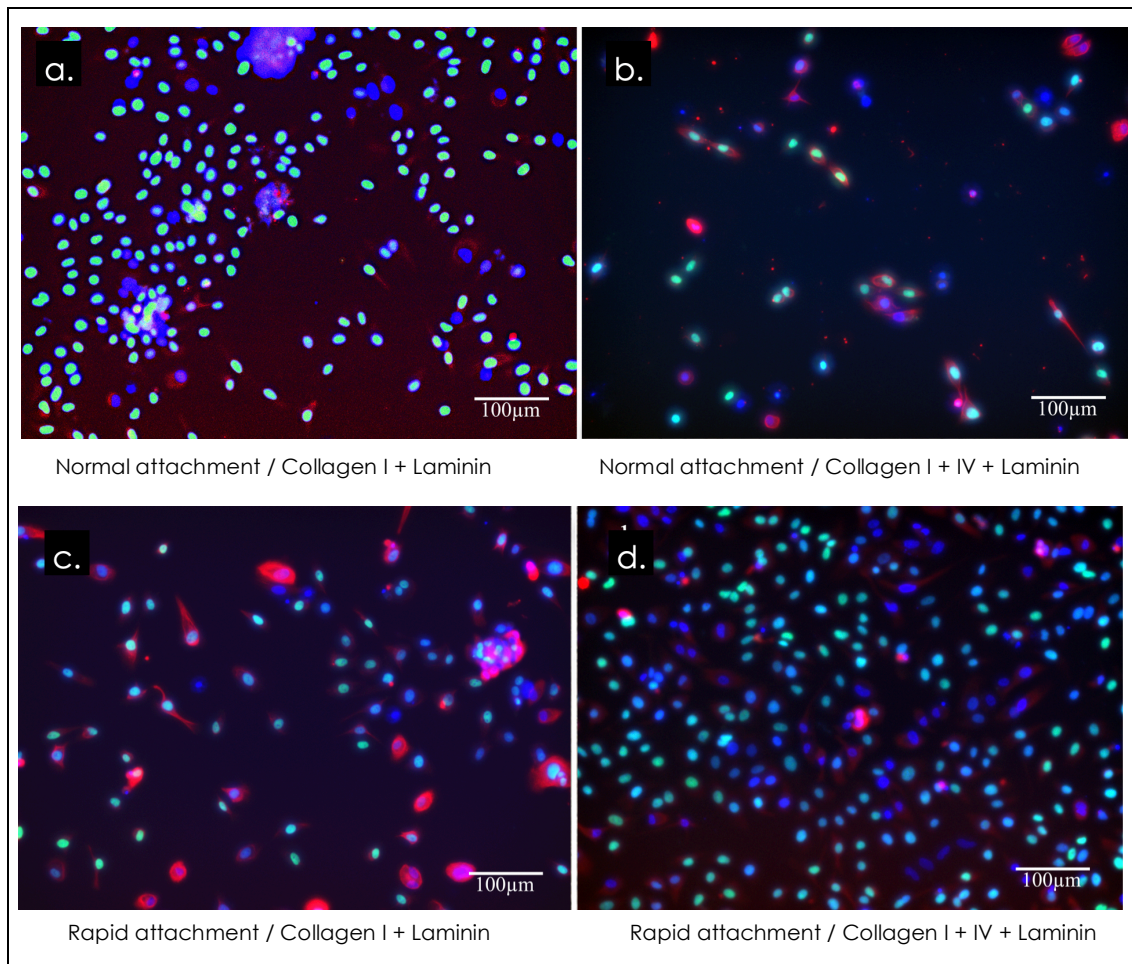
### 3.3. Implementation of iPS cell-to-keratinocyte protocol

Mainly referring to the protocol of Kogut et al.<sup>65</sup>, further promising elements from other approaches were screened and some of them implemented to improve the efficiency and shorten the time needed to derive keratinocytes – especially the adoption of the  $\gamma$ -secretase inhibitor DAPT and EGF resulted in a significant improvement of the protocol. As a final goal I stated the derivation of K1/14 positive keratinocytes. This type has a stem-cell character as found in the basal layer of the skin, providing hypothetically endless growth.

The first modification I tested using the Kogut et al. protocol, was the optimal coating of the wells in which I plated the cells. Kogut et al. suggested a simple coating with collagen I in the first phase of differentiation, and adding collagen IV after the first passage. I added collagen IV from the beginning, reasoning that in the basal membrane of the skin

collagen IV is present from the start of differentiation. For the same reason, I added laminin, which is also naturally present in the basal membrane. Indeed, the combination of collagen I + IV + laminin seemed to result in the best attachment and offered ideal conditions for the cells' differentiation (Figure 21).

Another element of the protocol by Kogut et al. I examined is the rapid attachment method. I confirmed that the percentage of K14 positive cells was elevated by this method, which I then implemented in my protocol (Figure 21).



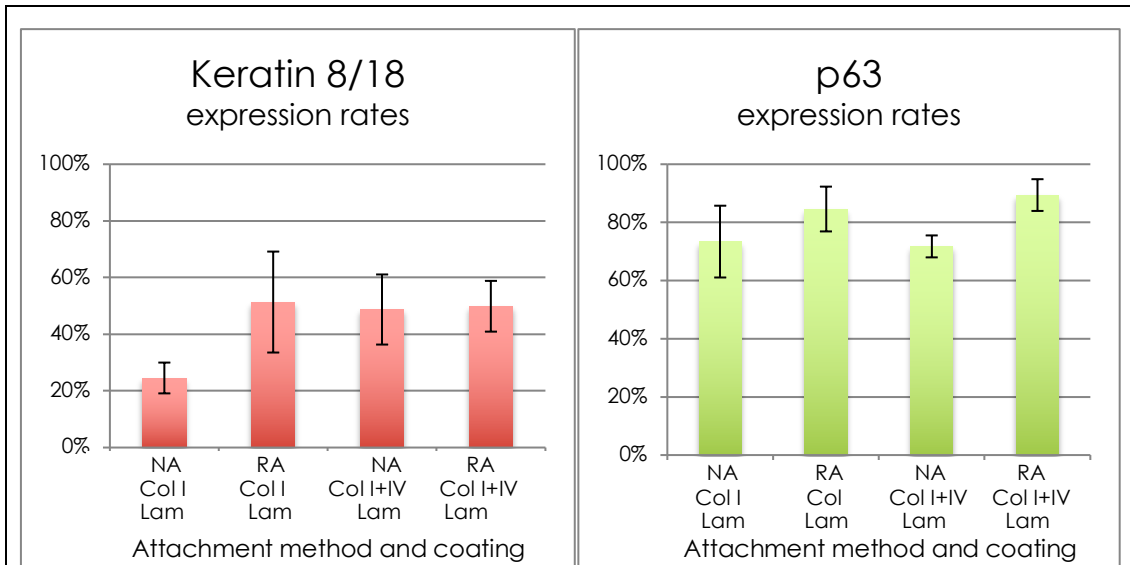


**Figure 21. Staining of characteristic proteins in four plates.** (Keratin 8/18 for early state of differentiation, p63 for advanced state of differentiation; blue = DAPI, red = keratin 8/18, green = p63.) Plates differed in coating and passaging method, with statistical analysis shown below. To compare the number of cells expressing the characteristic proteins with the overall number of cells, the nucleoli were stained by DAPI.

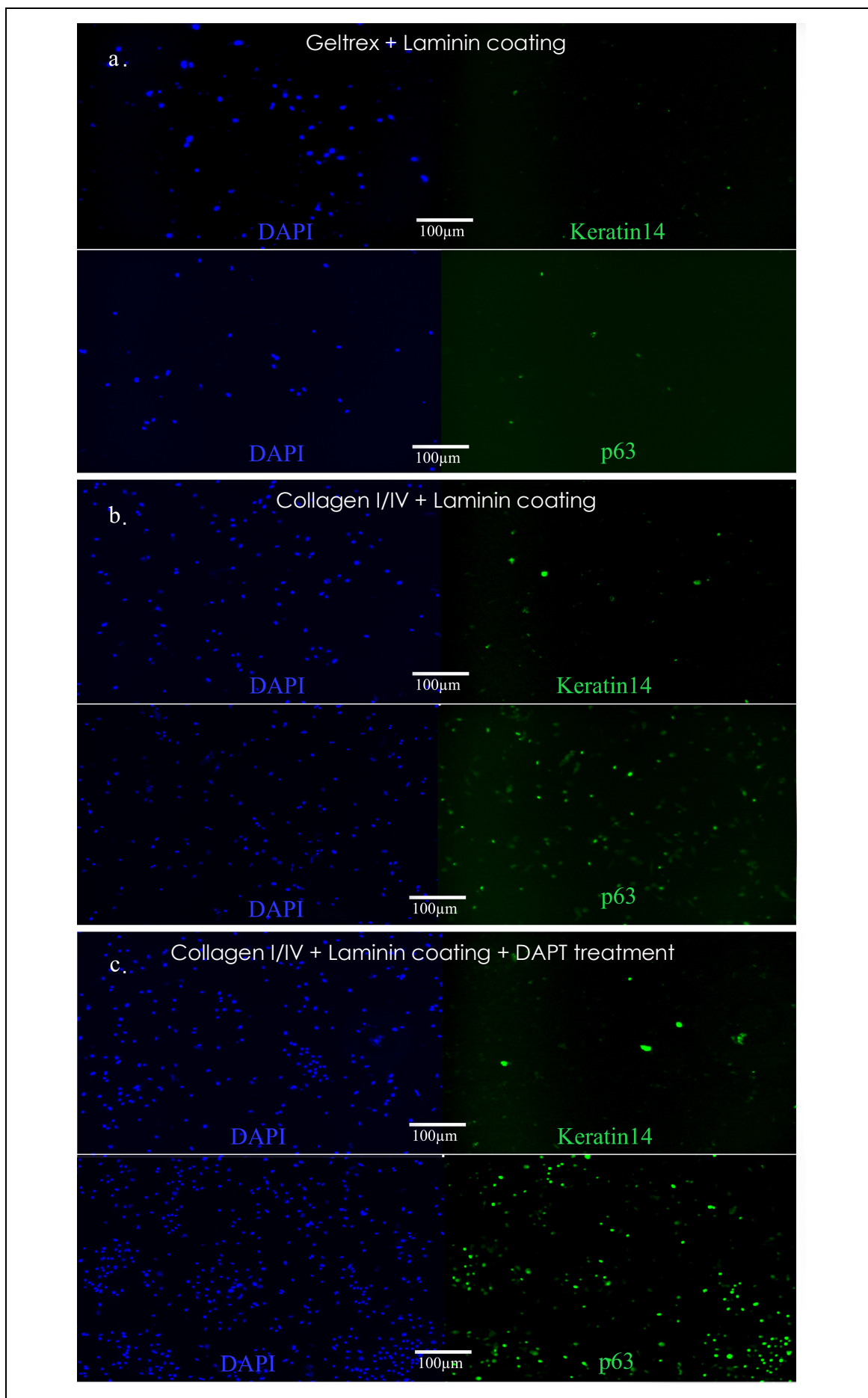
**a. b.** Normal attachment (NA) method. **c. d.** Rapid attachment (RA) method. **a. c.** Collagen I (Col I) coating **b. d.** Collagen I + IV (Col I + IV) in addition to laminin (Lam) coating on all plates.

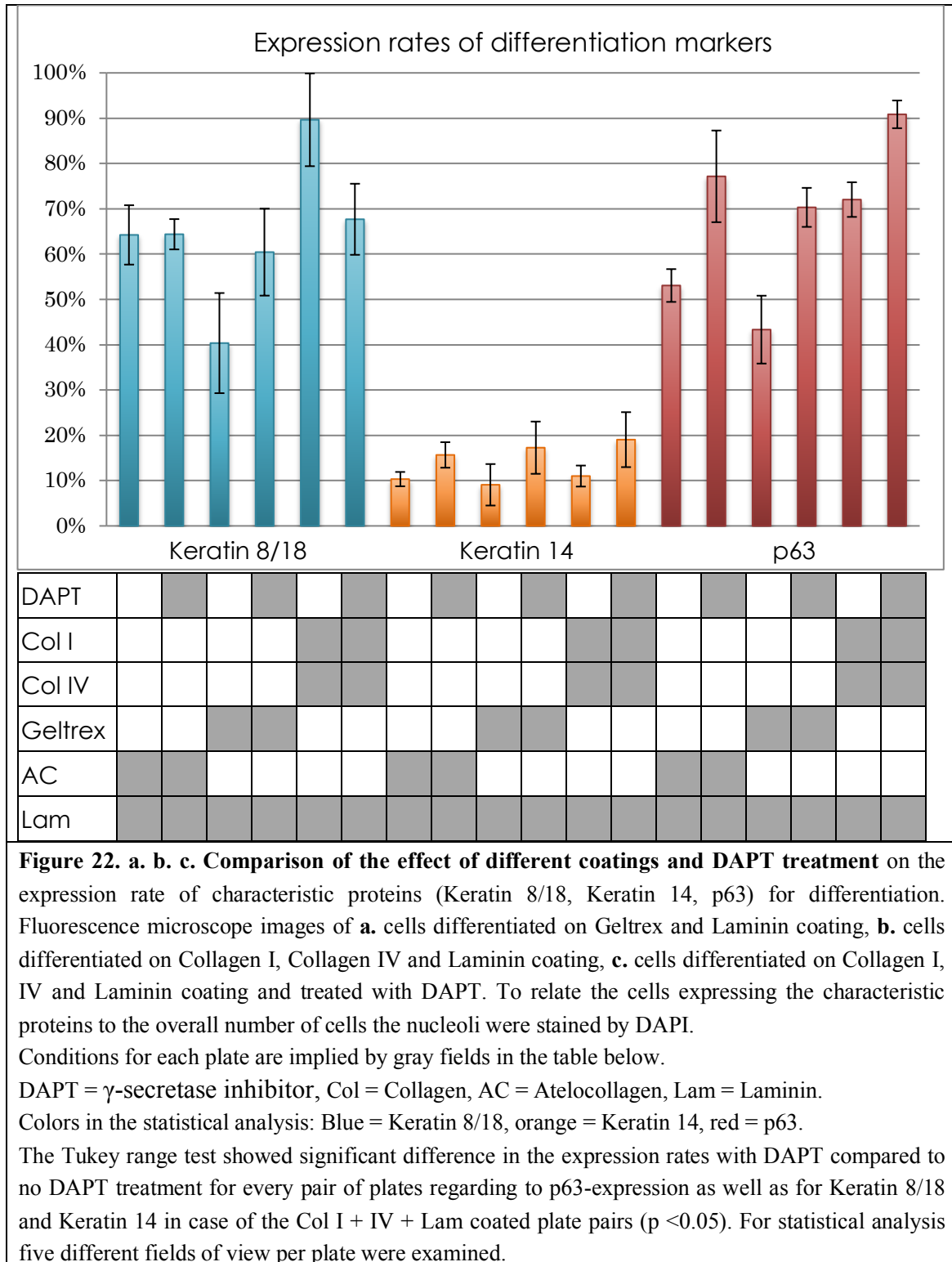
The t-test analysis showed significant differences for keratin 8/18 in the Col-I coated plates, and for p63 regarding comparison of NA and RA in Col I + IV-coated plates. For statistical analysis three different fields of view per plate were examined.

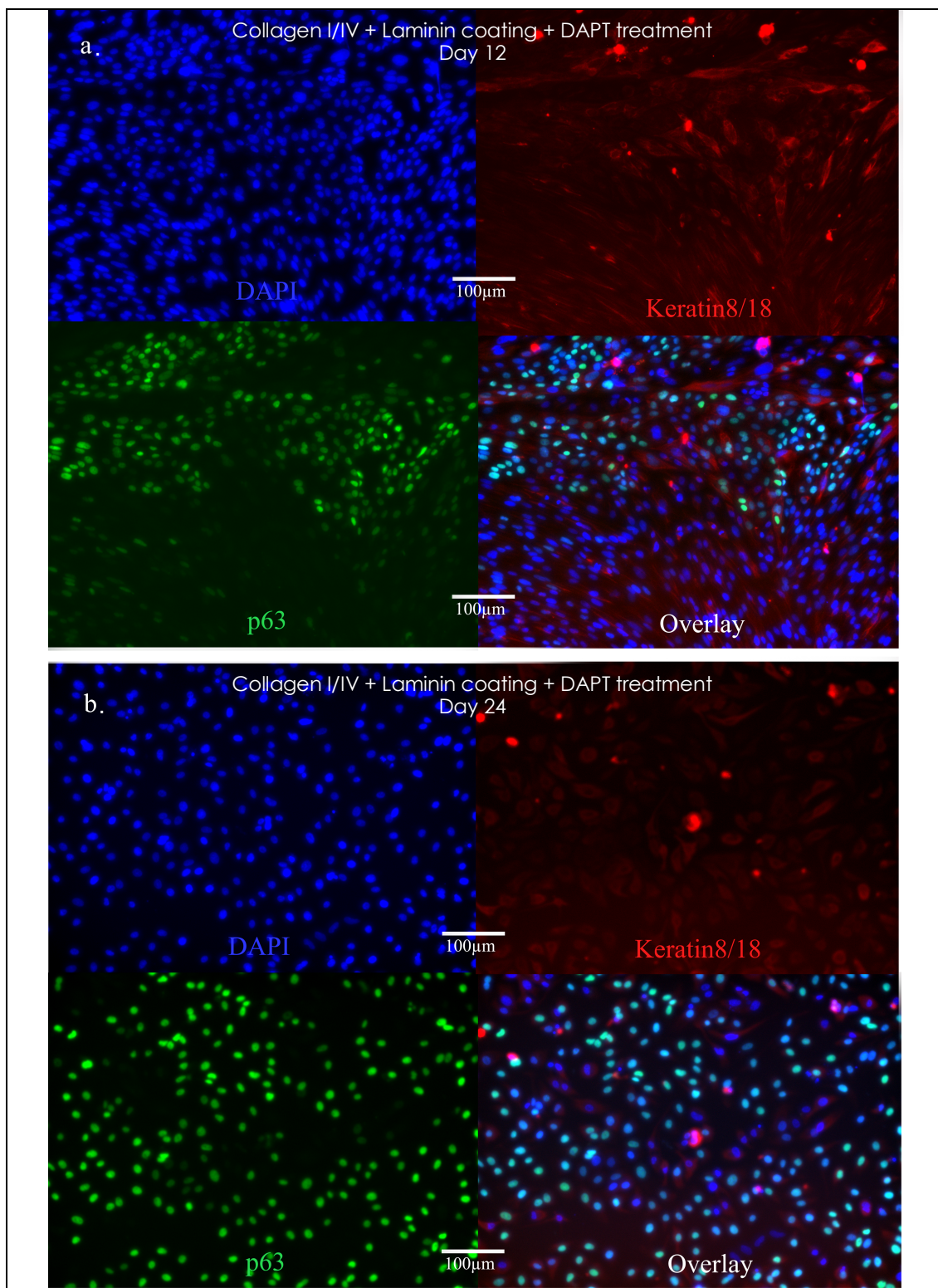
In further examinations I compared the above combination to Geltrex, which was originally recommended in Kogut's protocol. I also compared it to Atelocollagen. Both resulted in poor attachment and a relatively slow differentiation process. I assumed that the iPS cells were accustomed to laminin coating as they had always been plated on laminin-coated plates before my experiments. I thus added laminin to the Geltrex-kit and to the Cellgen-kit in a third attempt, which improved the attachment rate. However, I used the collagen I + IV + laminin combination successfully three times. It is recommended in Kogut's protocol to use a collagen I + IV coating after the rapid attachment passage method on Day 24 of differentiation, and I continued to use this combination to keep the protocol simple and to minimize the number of chemicals used (Figure 22). This coating

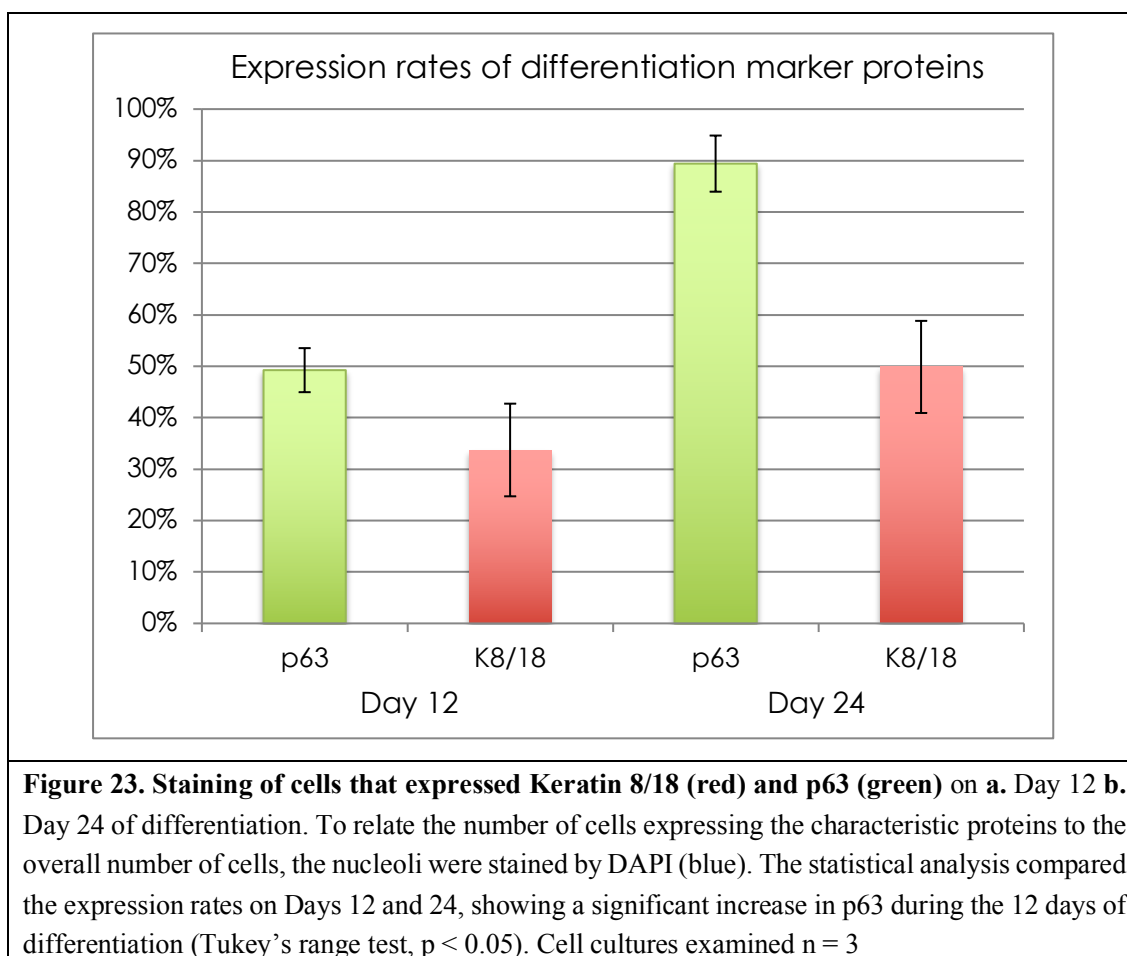
is also the closest to the natural setting, as the basal membrane of human skin is mostly composed of collagen I and IV and laminin, which provided further scientific justification for my decision.

A study on keratinocyte differentiation by Tadeu et al.<sup>77</sup> documented the elevation of p63 expression during the differentiation process through adding the  $\gamma$ -secretase inhibitor DAPT. p63 is a central marker-protein for gaining keratinocyte-character, also used e.g. in clinical pathology to characterize skin cancer. Therefore, I also made a DAPT vs. No-DAPT approach parallel to the coating comparison experiment shown in Figure 21. I reproduced similar results to those of Tadeu et al. and furthermore showed that the collagen I + IV + laminin combination led to the highest rate of K14 expression all over the cytoplasm (Figure 22). For p63, I verified a steady increase during the differentiation period (Figure 23).









Next, I examined the suggestion of Kajiwara et al.<sup>68</sup> to add EGF from the first day after the BMP4 + RA treatment using my WTC cell line to compare DKFSM + DAPT + EGF and DKFSM + DAPT treatment. The results in Figure 24 show that EGF accelerated the expression of the keratinocyte-specific protein K14 significantly.

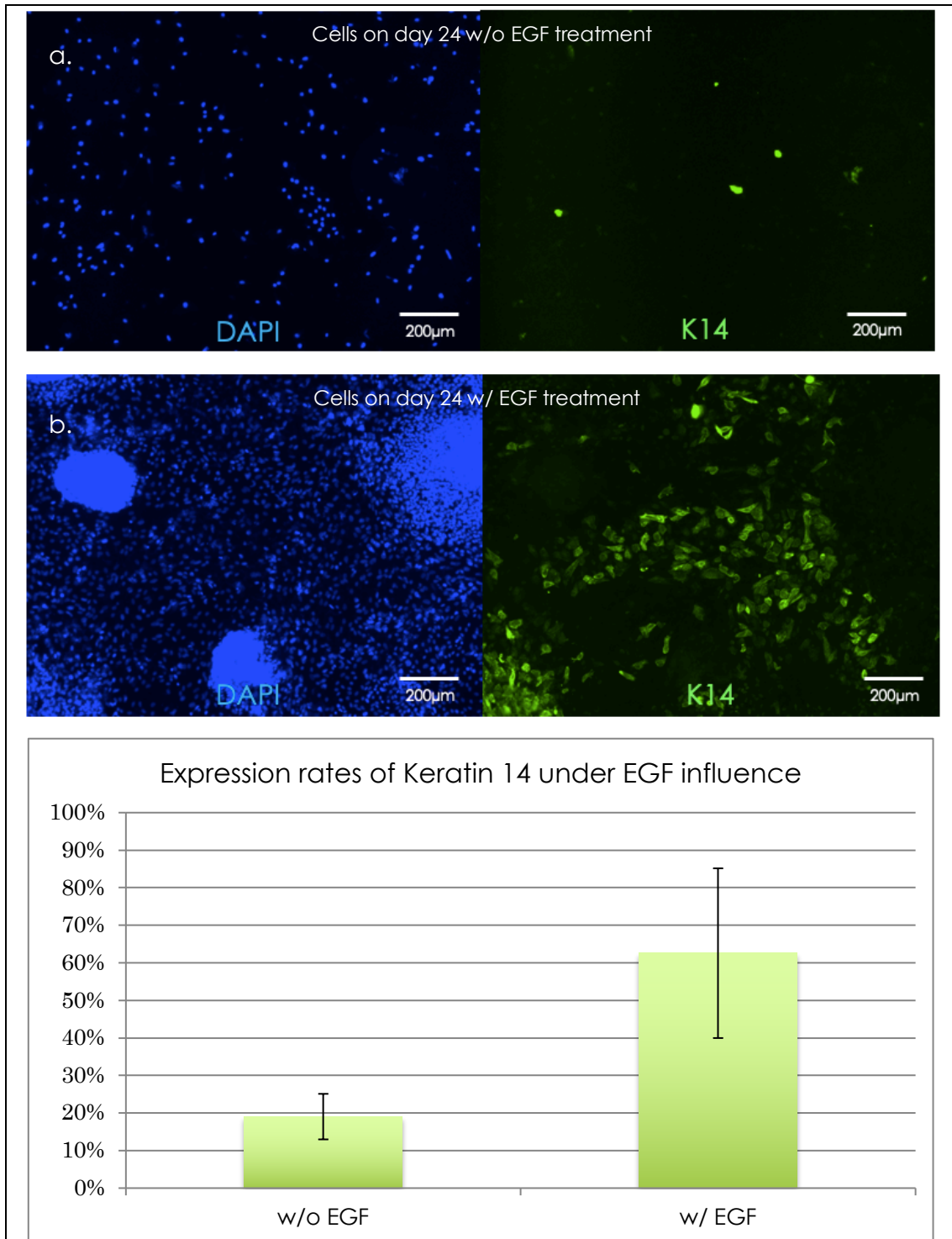


**Figure 24. Effect of EGF on Keratin 14 (green) expression.** This staining shows a significant effect of EGF treatment on K14 expression comparing cells **a.** not treated vs. **b.** treated with EGF for 20 days, starting on Day 4 of differentiation. To relate the cells expressing the characteristic proteins to the overall number of cells, the nucleoli were stained by DAPI (blue). (T-test result for K14 expression-rate comparison:  $p = 0.032$ ). Plates examined:  $n = 3$ .

The comparison of DAPI and K14 staining seem to imply that areas with a low confluence of cells displayed higher expression of K14. This finding suggests that limiting the cell number passaged in the first plate, and passaging them evenly over the plate, were important factors to improve the efficiency of keratinocyte-differentiation.

After performing the rapid attachment, my experiments showed that treatment with EGF + Y-27632 + CHIR and 0.05 mM of  $\text{Ca}^{2+}$  dissolved in the medium yielded the best cell proliferation rate. The cells were passaged every 14 days on average.

CHIR is used to boost cell activity<sup>78</sup> so we added it as an attempt to improve the growth rate after the second passage leading to promising results. However, as CHIR is also used in other differentiation protocols (mainly for deriving cardiomyocytes from iPS cells), it was necessary to assess its effect on the expression rate of the two keratinocyte-specific markers, p63 and K14. I thus compared it to my previous attempts. The results showed that the expression rate did not worsen even though the proliferation rate increased (Figure 25).

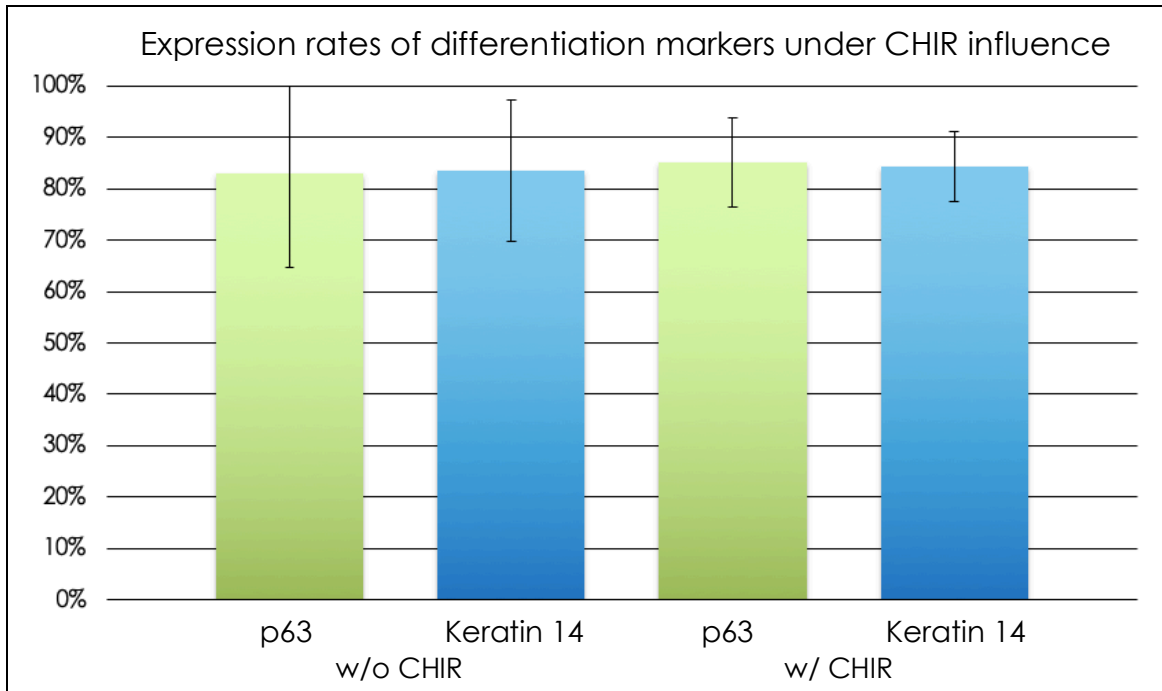
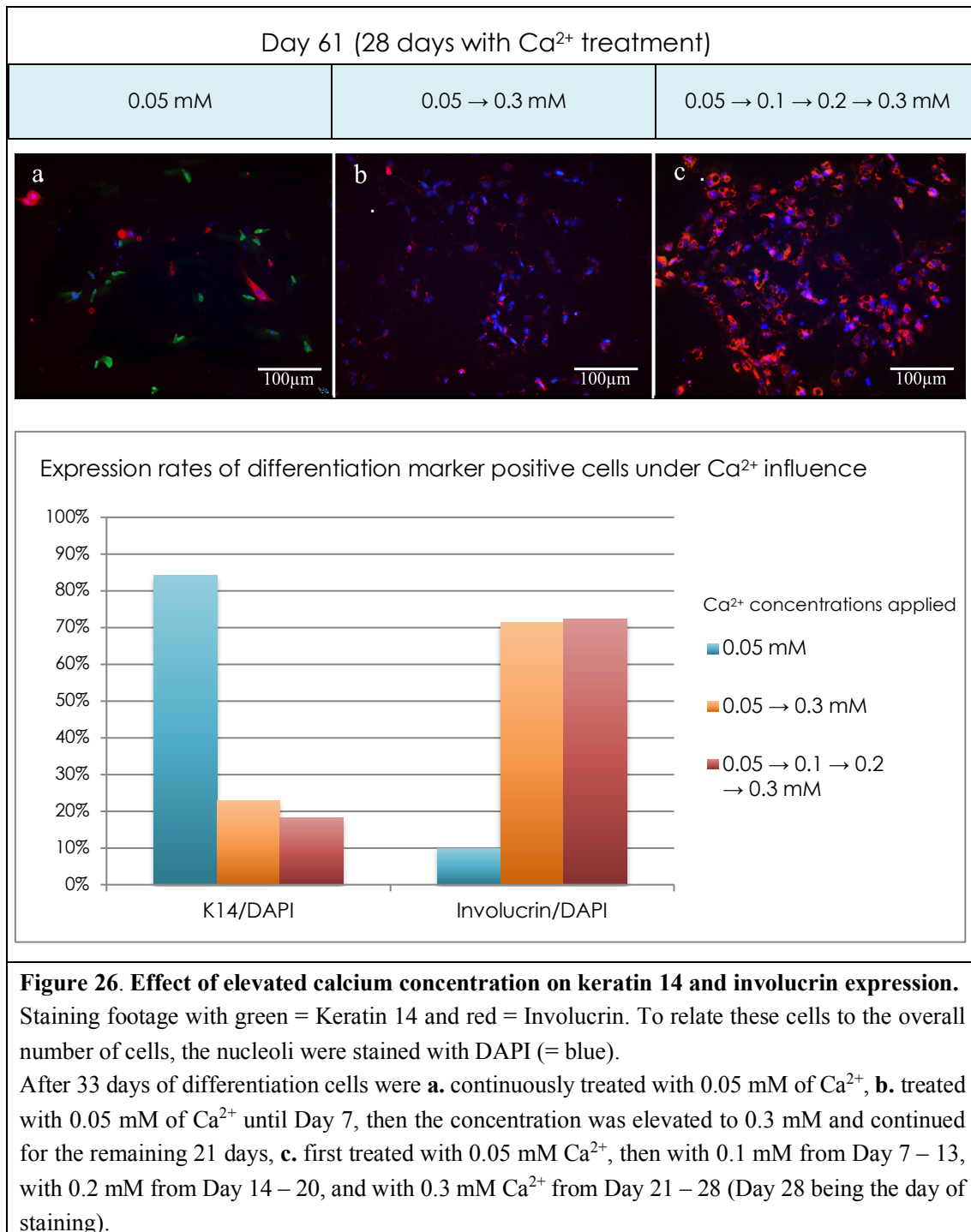
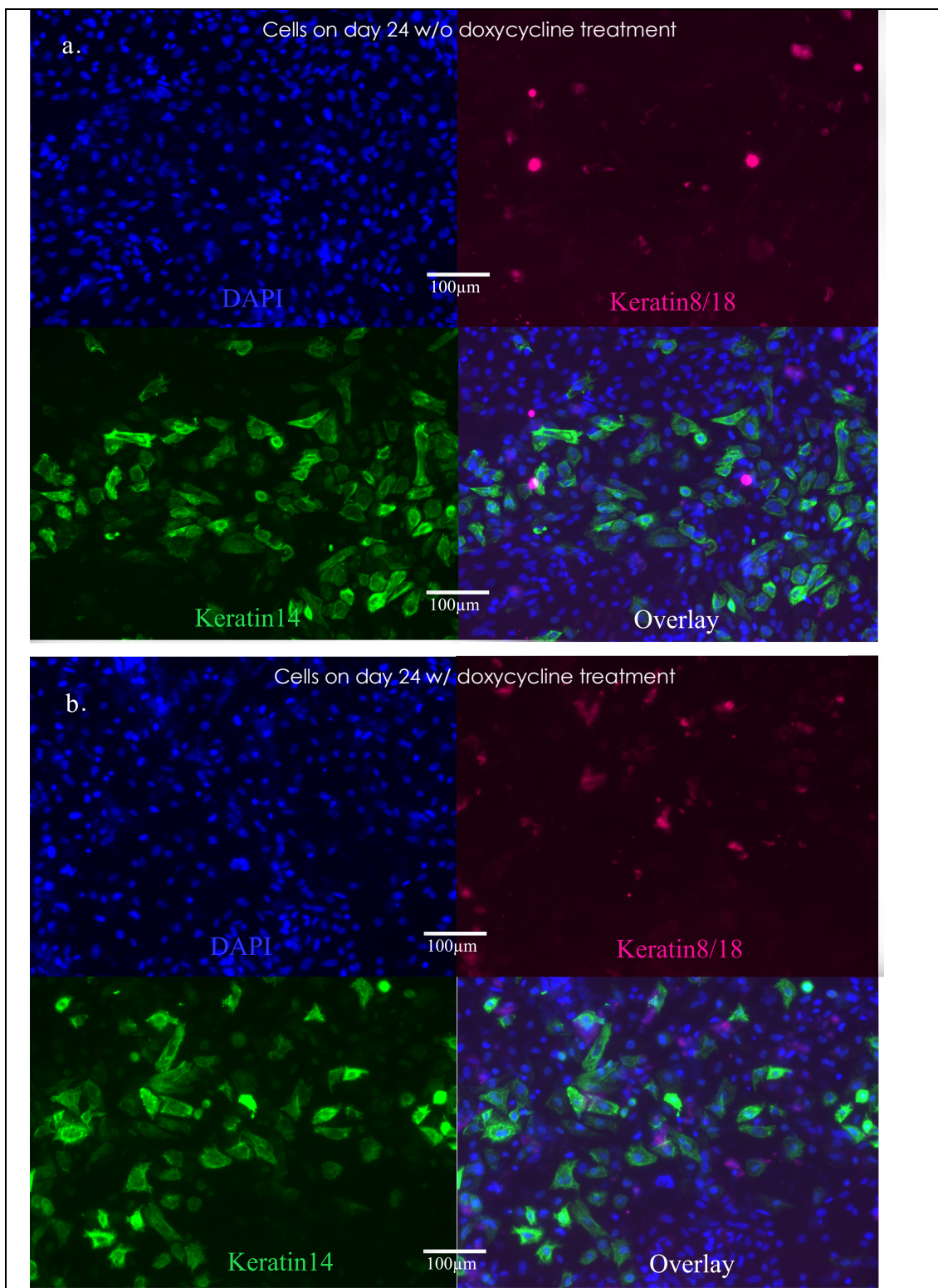


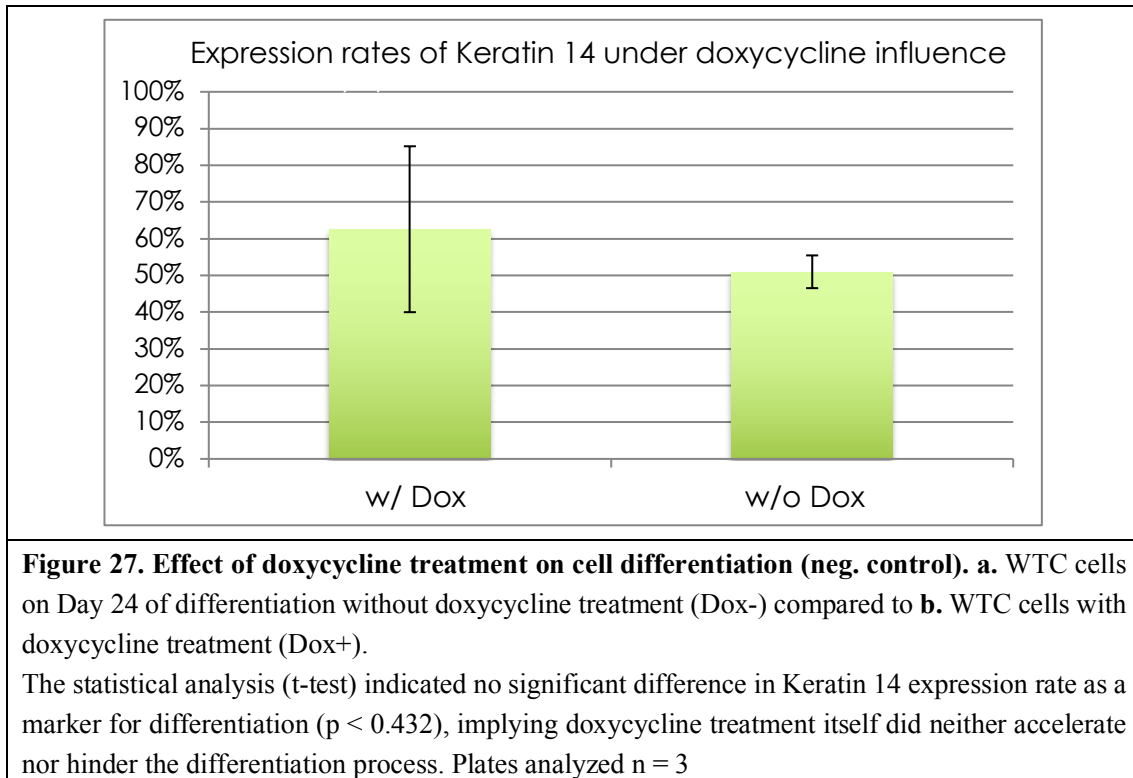
**Figure 25. Effect of CHIR treatment on p63 and K14 expression.** No significant difference in the expression rate was evident (analyzed by Tukey's range test), indicating that CHIR did not hinder the differentiation process. To relate the cells expressing the characteristic proteins to the overall number of cells, the nucleoli were stained by DAPI. Plates examined  $n = 3$

With this improved protocol, I proceeded to the final step of differentiation by imitating the microenvironment of superficial skin layers and elevating the concentration of calcium to which the cells were exposed. As described, I compared three samples. One was a control with  $\text{Ca}^{2+}$  levels similar to the basal layer of the epidermis (0.05 mM); one was elevated from 0.05 mM to 0.3 mM from Day 7 on; and for the third, the concentration was elevated more naturally and gradually, from 0.05 to 0.1 mM on Day 7, 0.2 mM on Day 14 and 0.3 on Day 21. Staining for K14 and stratum granulare and corneum characteristic protein involucrin showed that the gradual elevation of  $\text{Ca}^{2+}$  surrounding the cells was the most effective method. This implies that a close-to-nature setting is to be preferred (Figure 26). For comparableness while implementing these different treatments of calcium concentrations, I still performed an equal number of medium changes in the same timing in all three settings during the whole differentiation.

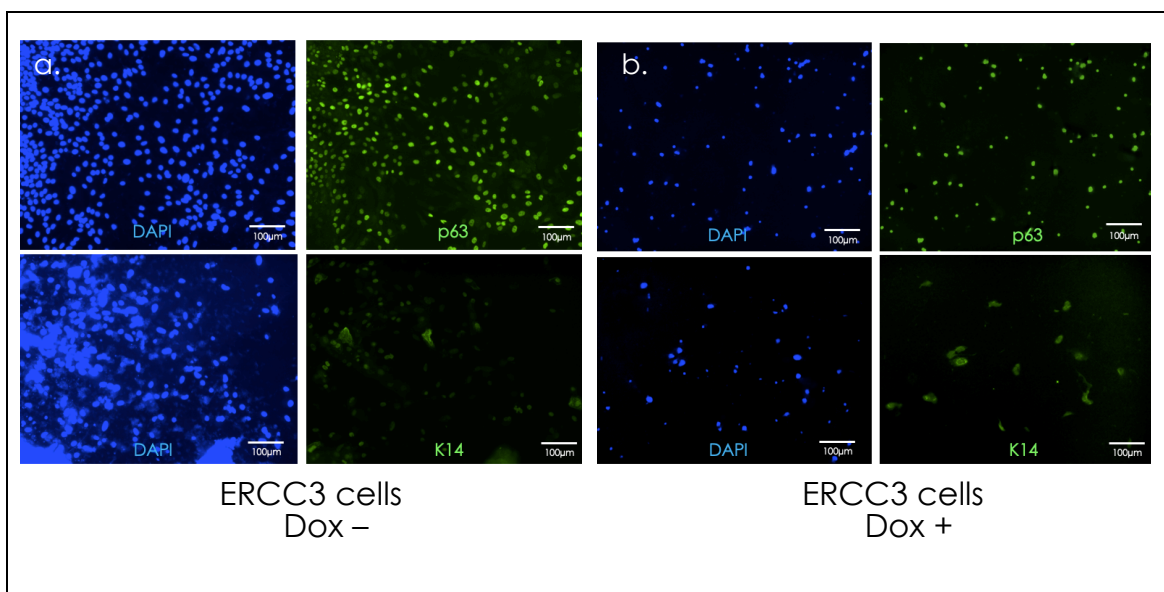


To transfer my protocol for healthy iPS cells to my knockdown cells, I had to show that treatment with doxycycline did not affect the differentiation process I had illustrated with the healthy cell line WTC (Figure 27). The doxycycline is needed to activate dCas9 that suppresses the expression of the targeted gene-loci (*ERCC3 ERCC6, UVSSA*).





In the next step, I proved that the cell line C5 I used for designing my ERCC3, ERCC6, and EIIS cells by CRISPRi knockdown, is also suitable for differentiation via the protocol developed in my research. Although compared with my previous experiments with WTC cells the K14 expression rates appeared to be lower in C5, ERCC3, ERCC6, and EIIS cells, they generally seem to differentiate without any further problems. This is exemplified in the figure below by the cell line ERCC3 representing all other cell lines derived from C5 (Figure 28).



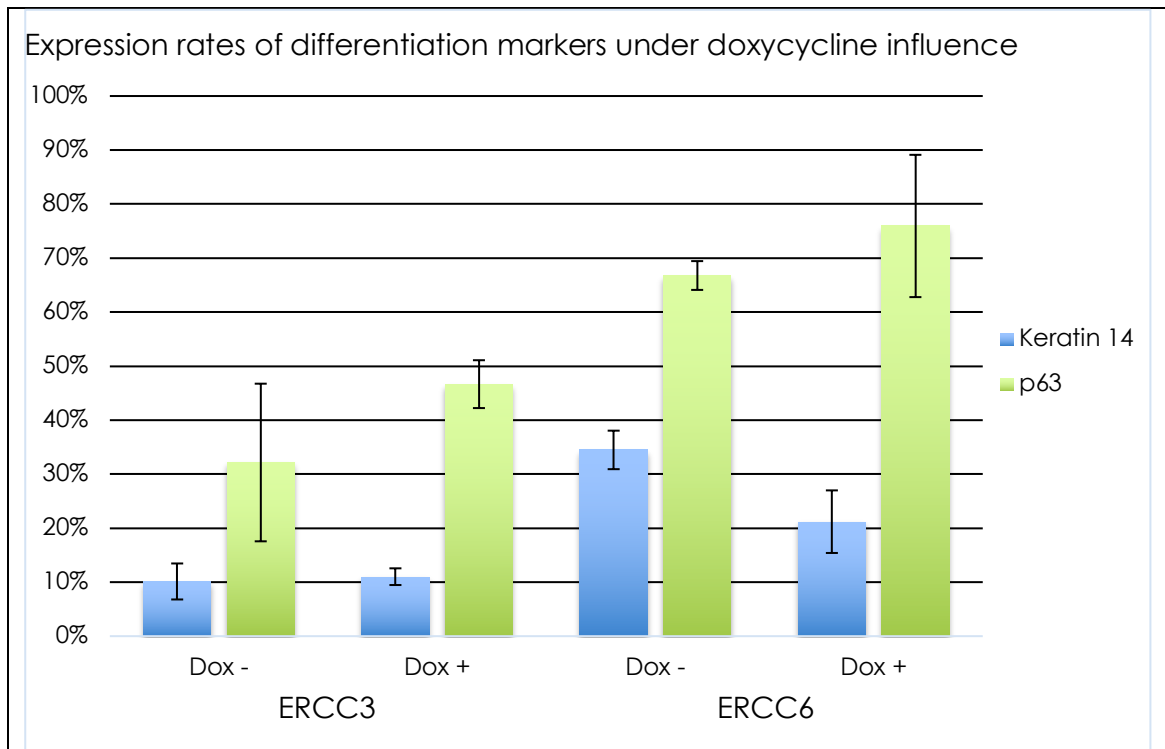


**Figure 28. Effect of doxycycline treatment on iPS cell to keratinocyte differentiation. a.** Exemplified staining of ERCC3 without doxycycline treatment (Dox-) on Day 24 of differentiation; **b.** ERCC3 with doxycycline treatment (Dox+) on Day 24. Statistics for the expression rate of K14 (blue) and p63 (green) as markers of differentiation showed no significant differences in expression rates (Tukey's range test) except the comparison on Keratin 14 in ERCC6 Dox- vs Dox+. The results imply that doxycycline did not strongly affect the differentiation process in my knockdown cell lines, though the cell count seemed reduced (see next section: 3.4.1.). For statistical analysis three different fields of view per plate were examined.

### 3.4. Comparison of cell lines WTC, C5, ERCC3, ERCC6, EIIS, and UVSSA

#### 3.4.1 Basic comparison on iPS cell level

The experiments started with about 14 000 cells initially plated in each well. The proliferation during one week of observation differed for each cell line and between the doxycycline-treated (knockdown) cells and their untreated counterparts. The healthy cell line C5 with induced dCas9 activity was used as a control to examine a possible effect of dCas9 that might cause a difference in proliferation. As expected there was no detectable difference in the doxycycline-treated and untreated cells. Therefore, every effect shown in the ERCC3, ERCC6 and UVSSA knockdown cells is caused by the knockdown itself.

The dCas9 induction showed a significant drop in the proliferation rate for ERCC3 and ERCC6. In accordance with the phenotype and less severe clinical presentation of UVSS, the UVSSA knockdown cells did not display a significantly lower ability to proliferate due to the knockdown.

The similarity between EIIS (derived from a patient with a point mutation in *ERCC6*) and my ERCC6 Dox+ cells may imply the functionality of my created model cells. Figure 29 summarizes the cell counts on Day 7, calculated as an average of at least eight plates for each cell line.

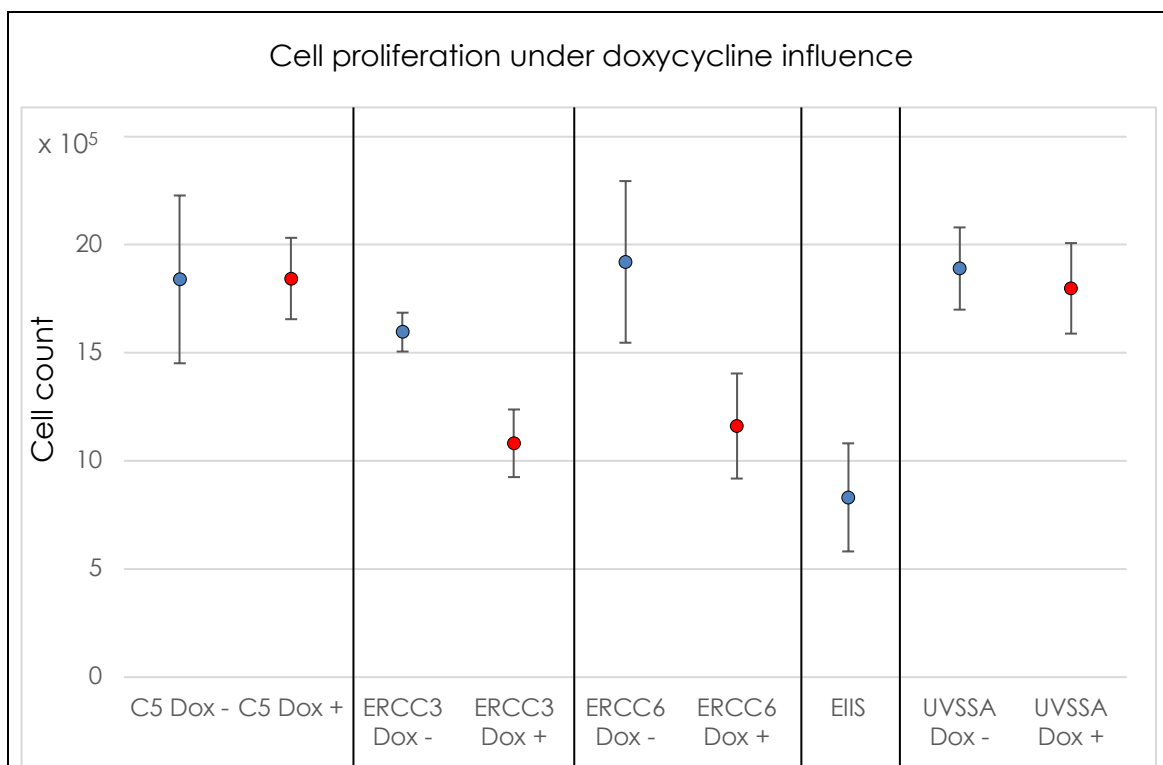
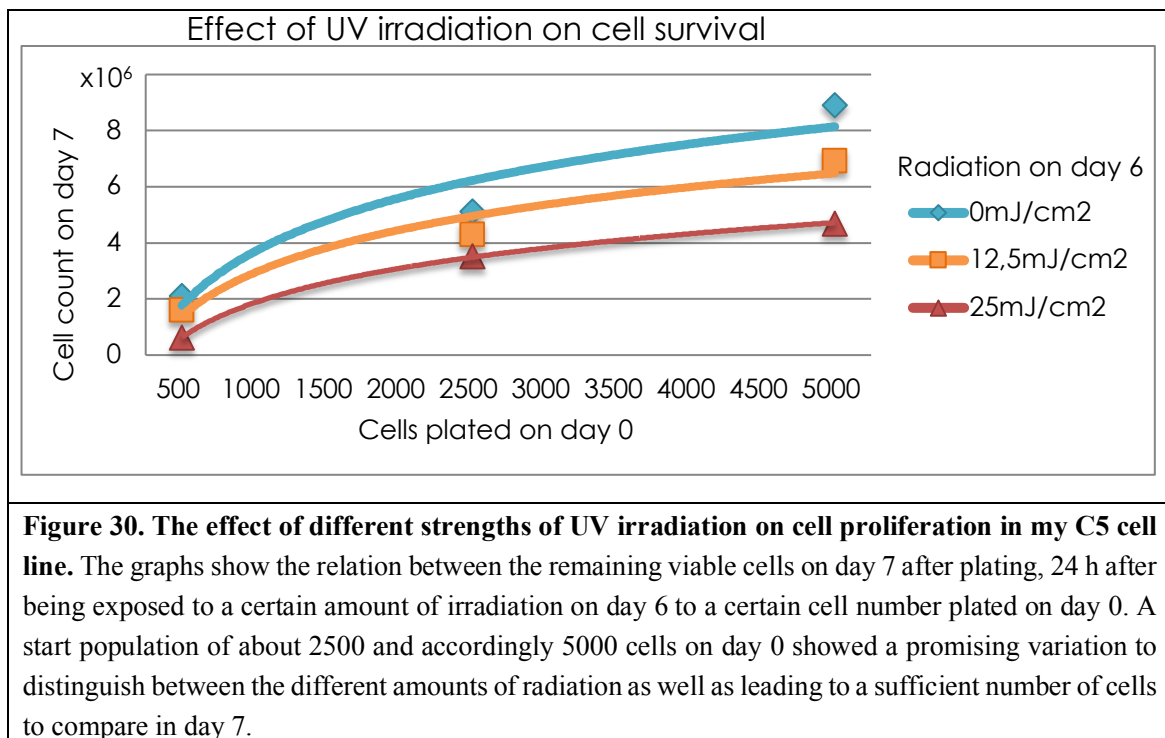


**Figure 29. Cell count on Day 7 after plating roughly 14,000 cells in each well.** Each cell count is the average of at least eight plates. The healthy cell line C5 with inducible dCas9 activity was used as a control to exclude an effect of dCas9 itself which could be proven as expected. The knockdown cell lines showed a significant drop in their proliferation rate due to dCas9 induction (induction via Doxycycline: Dox+, red dot; Dox-, blue dot). A similarity between EIIS (derived from patient with point mutation in *ERCC6*) and my ERCC6 Dox+ cells may imply the functionality of my created model cells.

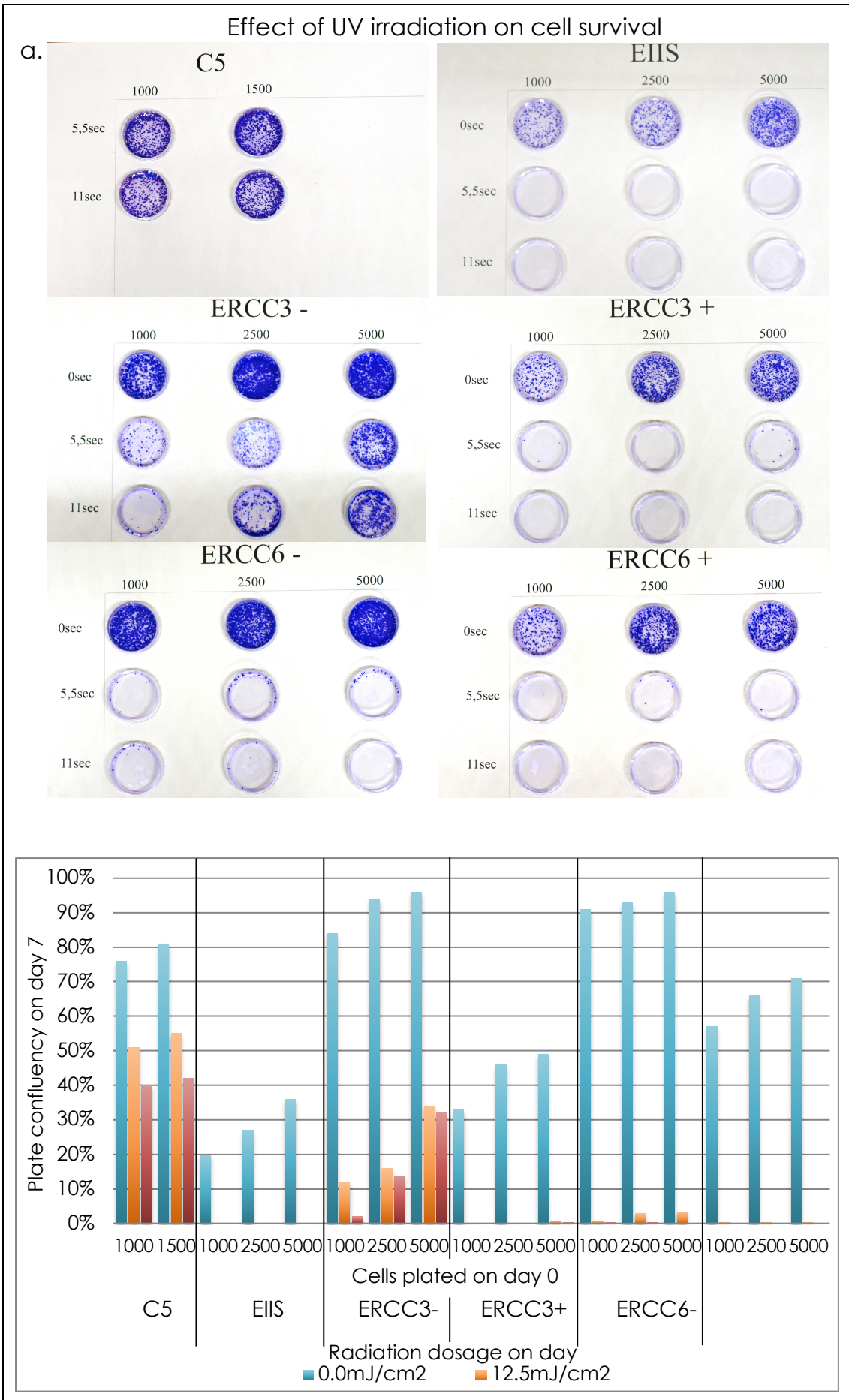
### 3.4.2 Comparison on iPS cell level and differentiated level using UV light and H<sub>2</sub>O<sub>2</sub>

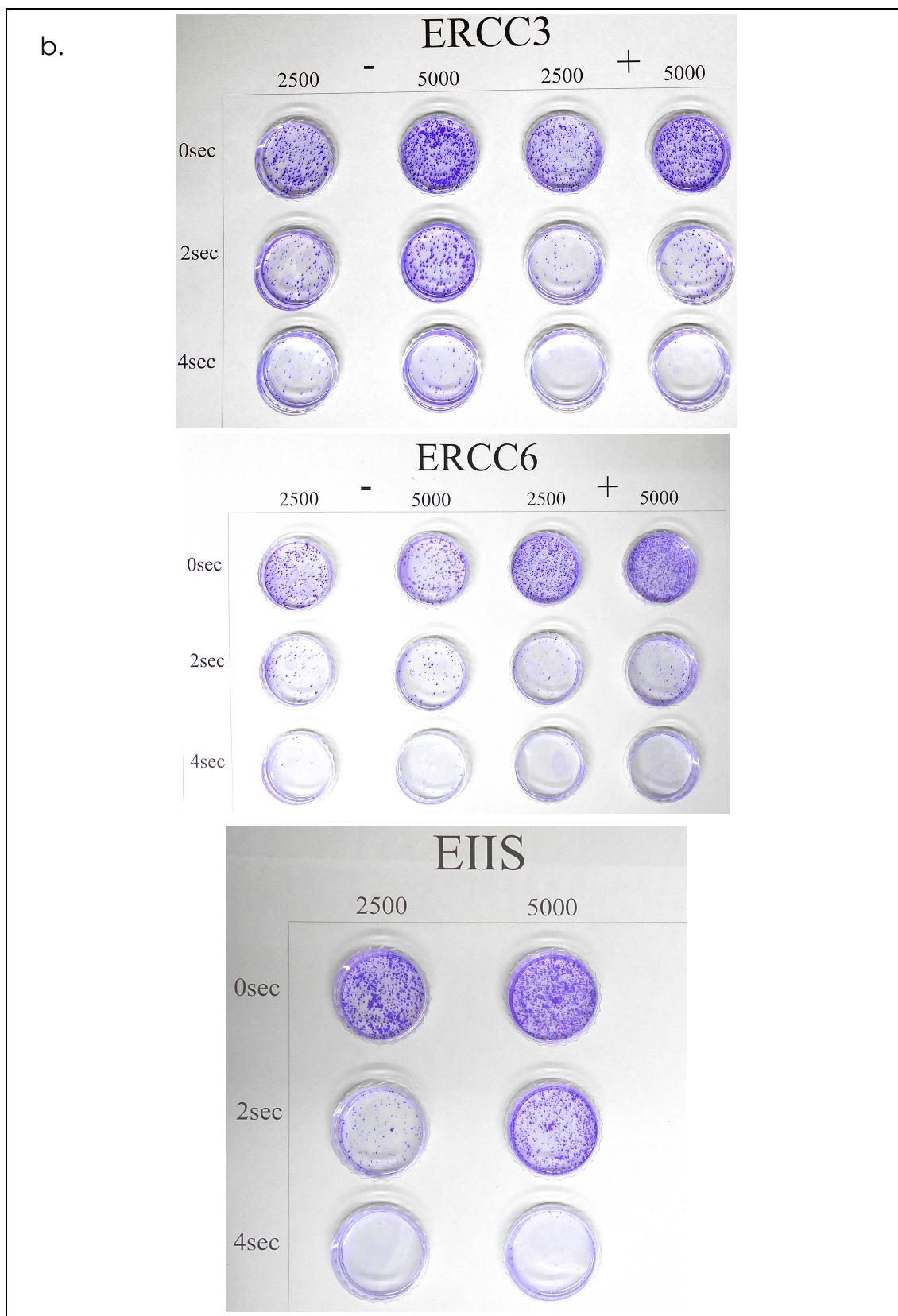
First, I determined a suitable amount of radiation that would provide data for my model cells at the undifferentiated and differentiated levels. There is little data on UV irradiation of undifferentiated iPS cells, so screened for the lowest rate of UV C irradiation, which lead to total extinguishment of all cells plated. I then used UV B at a low dose. For the C5 cell line, suitable survival rates were achieved in a setting of 0 – 12.5 – 25 mJ/cm<sup>2</sup> as doses of irradiation on day 6, analyzed on day 7 (Figures 30 and 31 a).



I then used the same amount of energy on my disease model cell lines, resulting in an extinction rate of between 70% and 99%. Interestingly, the cell lines ERCC3 and ERCC6, derived from C5, had higher extinction rates than C5, even without inducing the gene knockdown with doxycycline (Figure 31). These results led to the decision to test even

lower doses of radiation, and I next experimented with 4.5 mJ/cm<sup>2</sup> and 9.0 mJ/cm<sup>2</sup> applied for 2 sec and 4 sec.





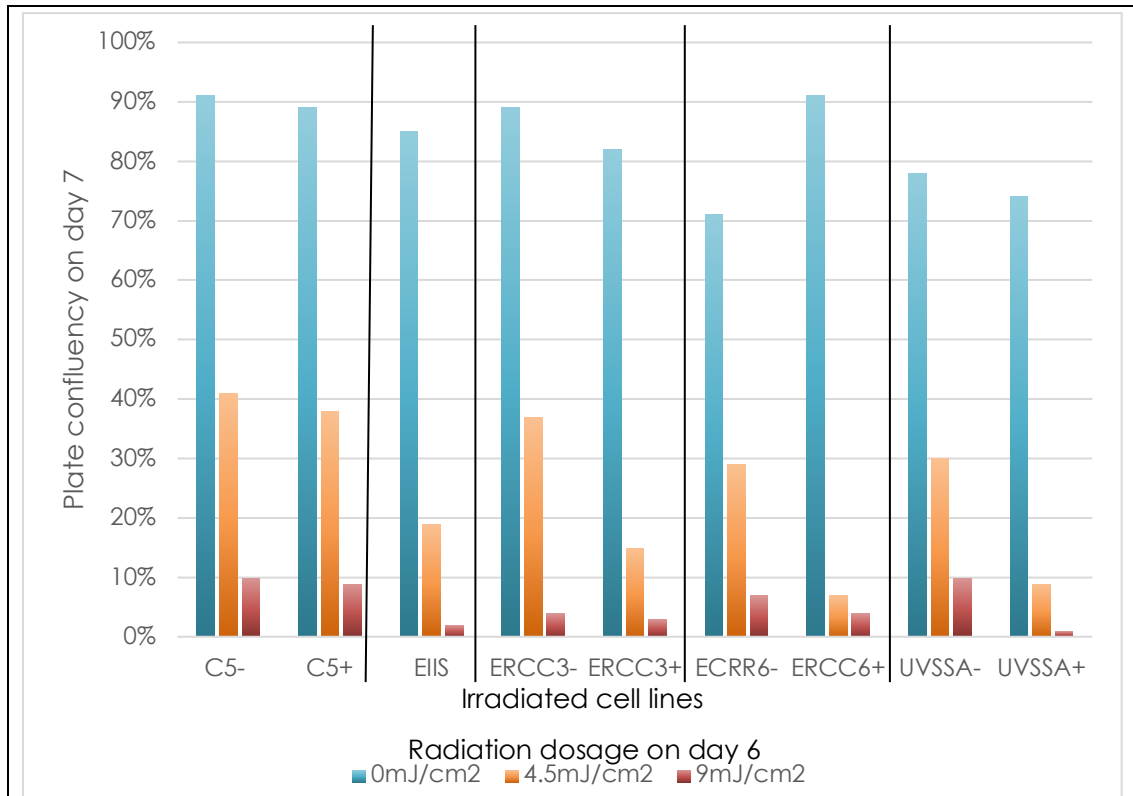


**Figure 31. Screening for an adequate number of cells on one plate for UV B light irradiation experiments. a.** The upper photographs show my plates on Day 7 after UV B irradiation at 0 – 5.5 – 9 sec (equaling 0 – 12.5 – 25 mJ/cm<sup>2</sup>) and then stained with crystal violet to indicate the plates' confluency. Below the photographs is an analysis of the plates, relating the stained area to the overall plate size. As too many cells died under the conditions shown in **a.**, I repeated the experiment with different radiation, shown in **b.**, namely UV B irradiation at 0 – 2 – 4 sec (equaling 0 – 4.5 – 9 mJ/cm<sup>2</sup>). The – or + indicated the absence or presence of Doxycycline. Plates were analyzed with ImageJ<sup>79</sup>.

Enough cells survived to be examined, and 2 sec and 4 sec provided practical times to use; therefore, I adhered to the tested setting. Next, I determined a suitable setting for differentiated cells, and screened with 0 – 25 – 50 – 75 mJ/cm<sup>2</sup> as keratinocytes are thought to be more robust than iPS cells. Furthermore, I examined the impact of CHIR on UV resistance. There is a tendency of improved survival rates, but statistical analysis showed a significant difference only in the pair of wells irradiated with 50 mJ/cm<sup>2</sup> and 75 mJ/cm<sup>2</sup> (Figure 32).

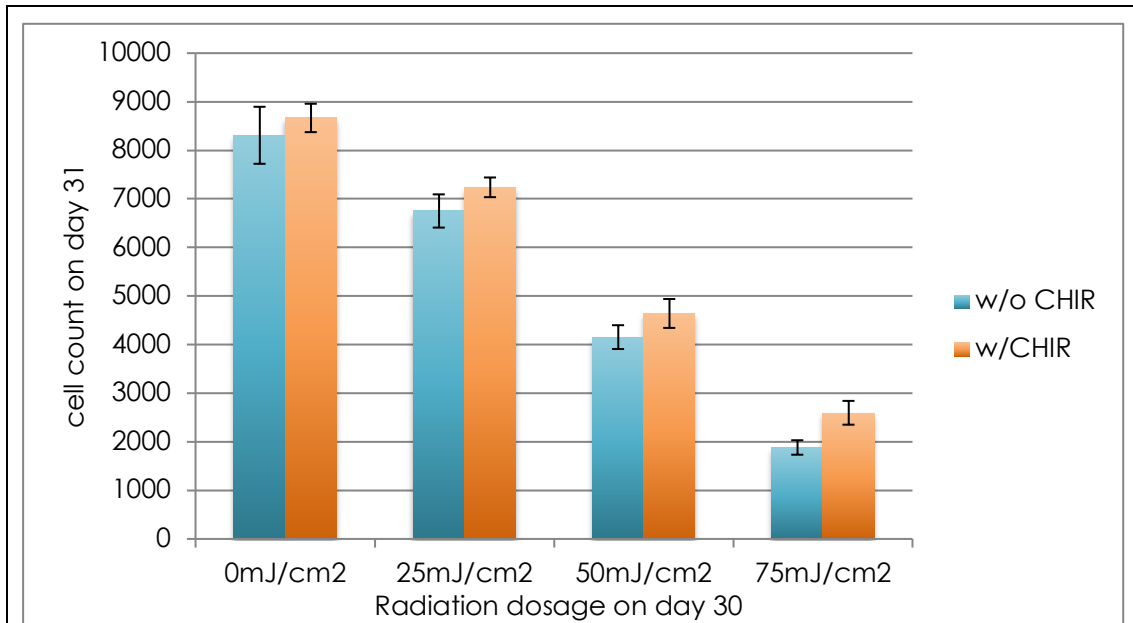


**Figure 32. Cell counts of iPS cells (C5 cell line) on day 30 of differentiation into keratinocytes, 24 h after UV B light irradiation at different doses.** For each dose, I compared two wells, one treated and one not treated with CHIR. The results showed consistently higher cell counts for CHIR-treated cells, although significance was only shown for doses of 50 mJ/cm<sup>2</sup> and 75mJ/cm<sup>2</sup> ( $p < 0.05$ ). Number of plates examined  $n = 3$ .

With these conditions set for my following experiments, I tested the damaged cells for reactive oxygen species (ROS), specifically H<sub>2</sub>DCFDA. Similar ROS rates were shown for C5 and untreated ERCC3 and ERCC6 (Dox-), while I found overall higher rates in the knocked-down cell line ERCC3 and ERCC6 (Dox+). The highest ROS count was noted in the EIIS cell line. After one day, ROS expression dropped at a similar rate in all cell lines. The same tendencies were observed in differentiated C5 and differentiated EIIS cells (Figure 33).

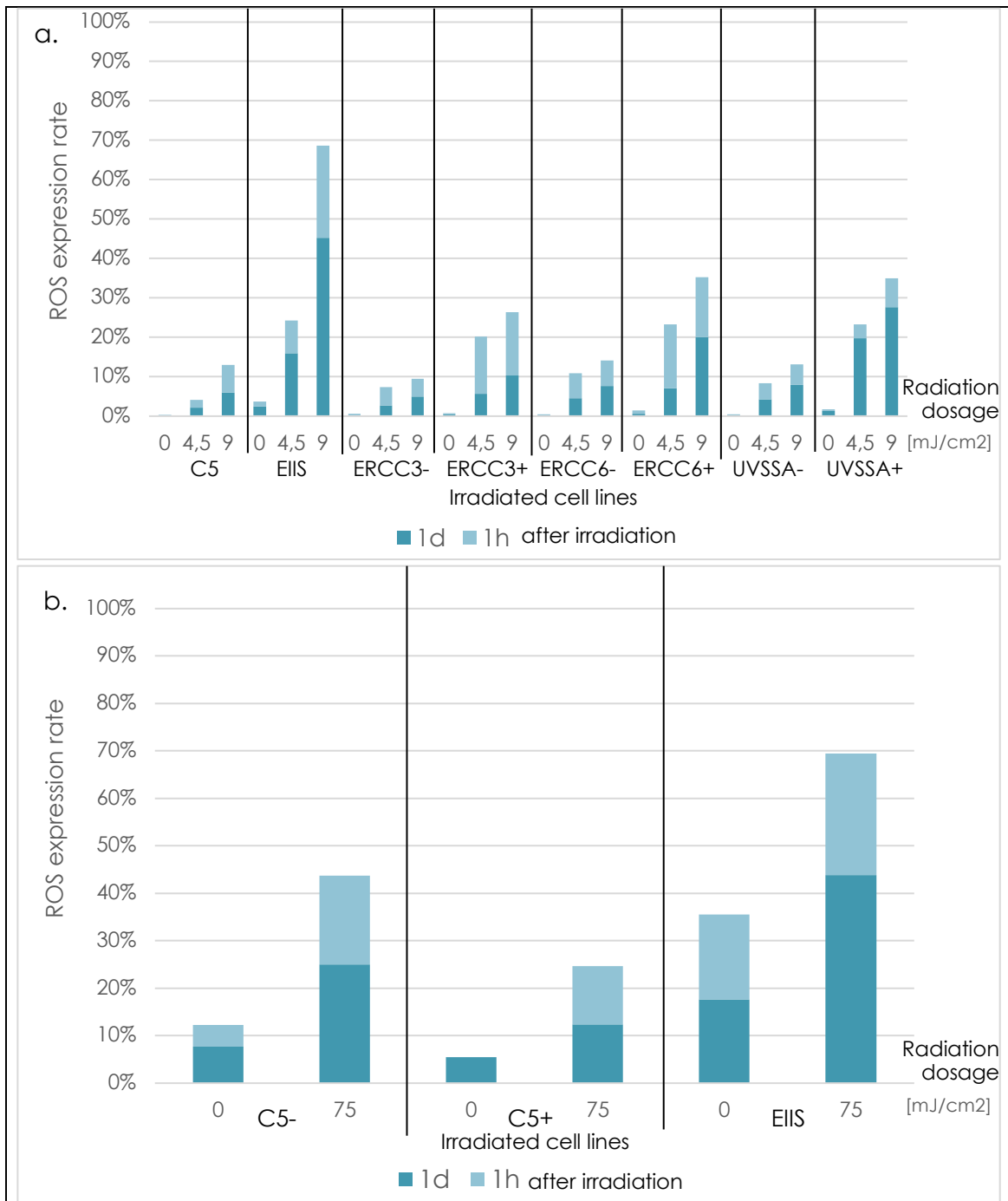


**Figure 33. ROS expression after UV B light irradiation.** The statistic shows cells expressing reactive oxygen species (ROS; immunofluorescence staining of H<sub>2</sub>DCFDA) in relation to the full cell count (DAPI staining). The light blue portions of the bars indicate the ROS expression 1 h after irradiation, which then dropped in all wells during the next 24 h. The final percentage is indicated by the dark blue bars.

**a.** In this experiment I radiated undifferentiated iPS cells with doses of 4.5 and 9 mJ/cm<sup>2</sup>. I separated one well for each cell line as a negative control, which was not radiated.

**b.** The cells compared were iPS cells, cells on Day 30 of differentiation, and keratinocytes. Four wells with C5 cells were prepared; two were treated with doxycycline and the other two untreated so that I could exclude doxycycline-induced ROS expression. Of each of pair of cells, only one was radiated with a UV B dose of 75 mJ/cm<sup>2</sup>.

An example of the data, which was analyzed statistically, taken with the Keyence fluorescence microscope is shown in Figure 34 as a 20x magnified picture. I counted cells as “positive” if they had defined bright green spots in them, and excluded cells that were stained all over their cell body. This avoided counting cells on which the fluorescence marker had just randomly attached.

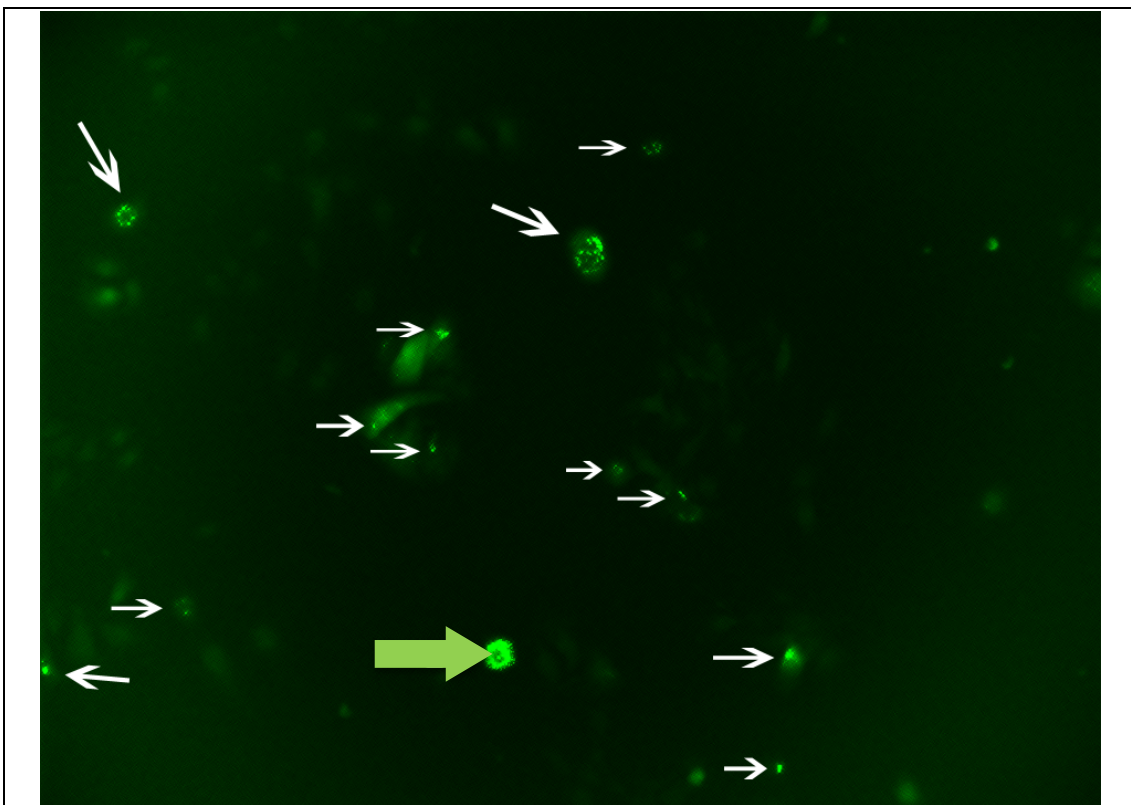


**Figure 34. Fluorescence microscope images of H<sub>2</sub>DCFDA-staining in C5 cells after UV B light irradiation.** The white arrows indicate cells counted as “ROS-positive”. Green arrows indicate cells that could not be determined as positive (C5 cell line, Day 30 of differentiation, 1 h after UV B irradiation at 75 mJ/cm<sup>2</sup>).

Furthermore, I observed that damage due to irradiation led to radically inhibited growth rates for both C5 and EIIS. In the negative control, cells became confluent and formed colonies, whereas the irradiated cells remained mainly singularized or formed clusters of two or three cells at most (Figure 35).

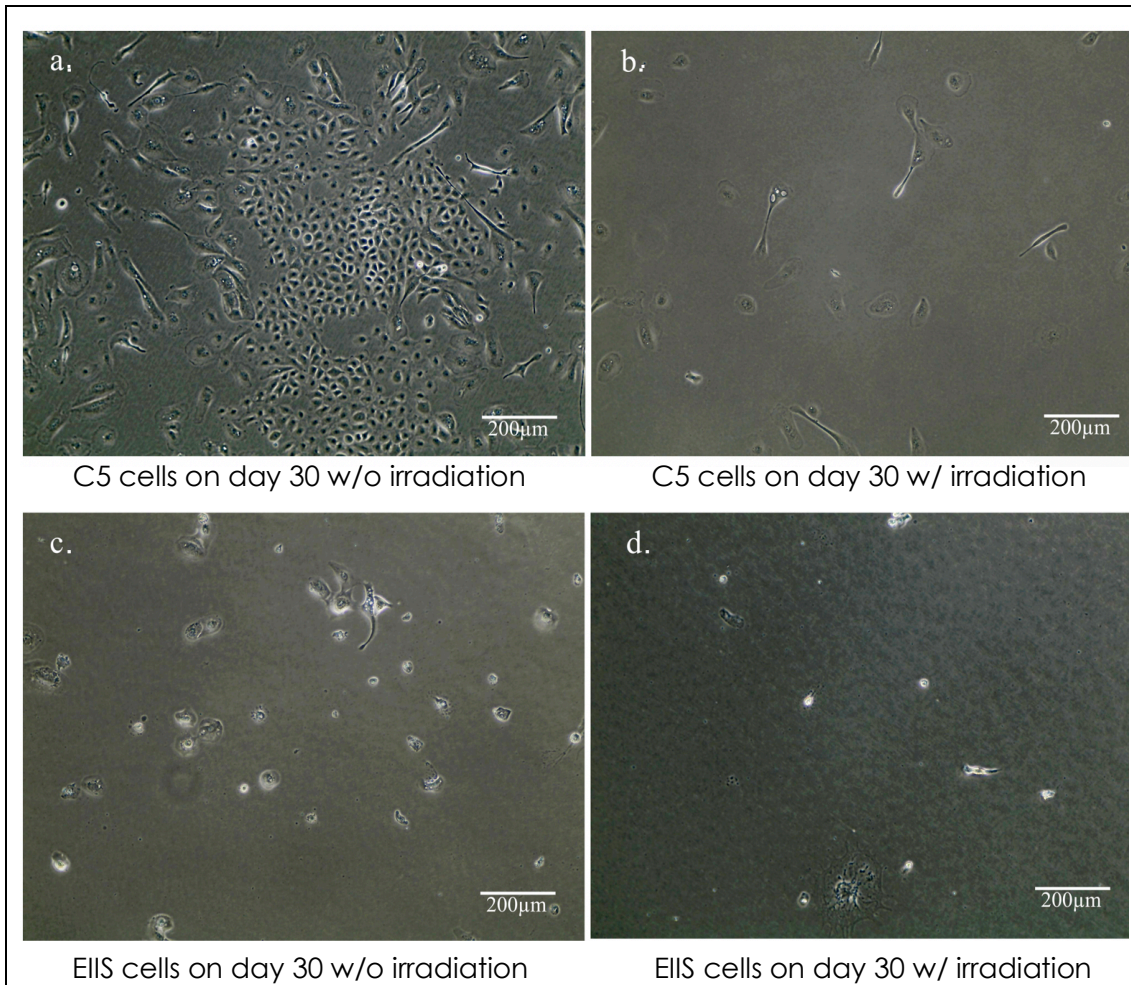


**Figure 35. Photomicrographs of C5 and EIIS cells after UV B light irradiation and negative controls: a. & b.** C5 cells on Day 30 of differentiation, **c. & d.** EIIS cells on Day 30 of differentiation. **a. & c.** Non-irradiated (negative control) cells. **b. & d.** Cells irradiated with  $75\text{mJ}/\text{cm}^2$  of UV B light.

In a second experiment, I induced stress in the cells using hydrogen peroxide at various concentrations. This yielded similar results as the UV experiments (Figure 36).

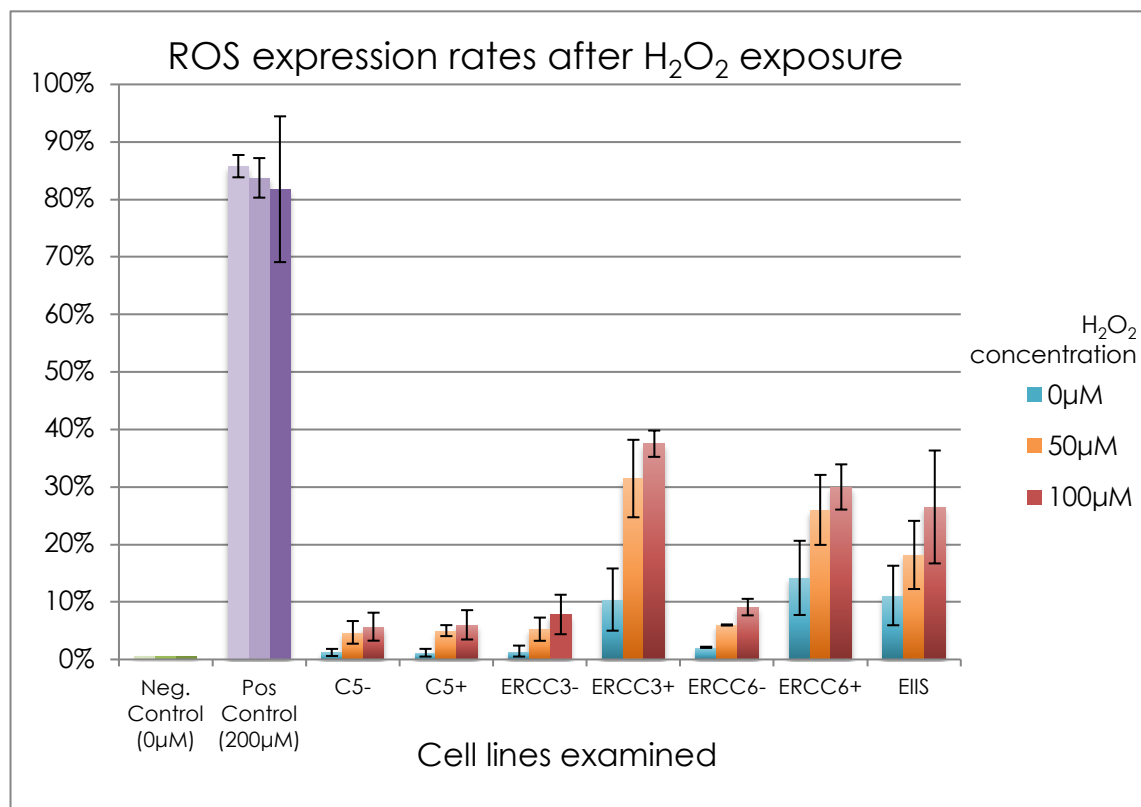
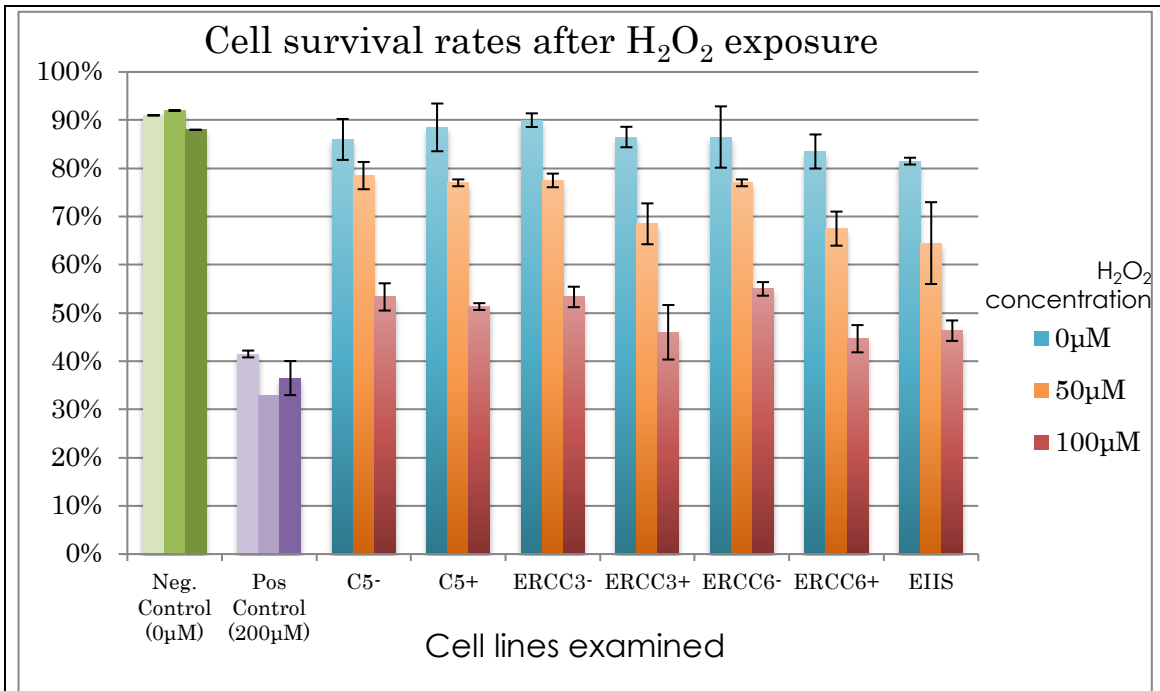
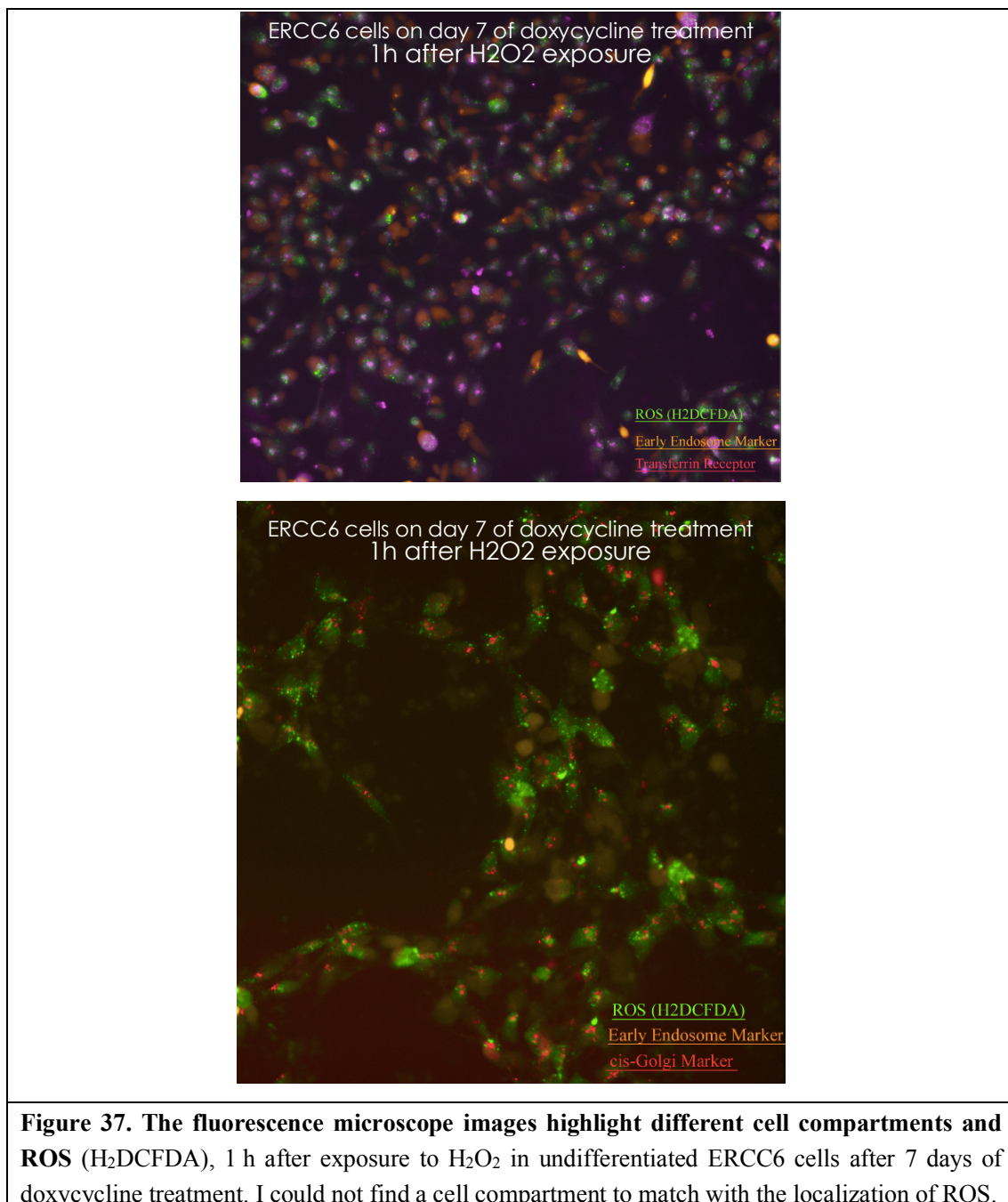


**Figure 36. Effect of H<sub>2</sub>O<sub>2</sub> exposure on each cell line** **a.** Viability of each cell line (undifferentiated iPS cell stage) after H<sub>2</sub>O<sub>2</sub> exposure at various concentrations on Day 7 after plating. Measurement were made using LUNA<sup>®</sup> Automated Cell Counter. **b.** Cells expressing ROS (immunofluorescence staining of H<sub>2</sub>DCFDA) in relation to full cell count (DAPI staining) 24 h after exposure to different concentrations of H<sub>2</sub>O<sub>2</sub>. A negative control (green) of three unexposed wells and a positive control (violet) of three wells exposed to a high dose (200 μM) of H<sub>2</sub>O<sub>2</sub> were included in each experiment. The examinations included n = 3 wells each.

To assess whereabouts in the cells the ROS appeared, I stained several components of the same cells I had examined for ROS, and merged the pictures. I stained the Golgi apparatus and endosomes, but could not find any clear overlays in the staining patterns; this suggests H<sub>2</sub>DCFDA species might be organelle-independent products in a pathway induced by certain damage to the cell (Figure 37).



## **4. Discussion**

### **4.1. Implementation of an iPS cell-to-Keratinocyte differentiation protocol**

In the scale of scientific history, research based on iPS cells is still a young field. Therefore, many new experiments are conceived and must be proven as scientifically adequate, and they must endure the long procedure to be established as standard methods for the future. One such tool is the differentiation of iPS cells into a distinct tissue. The first part of my research was focused on one of these protocols, namely the efficient differentiation of keratinocytes, under conditions simple enough to be possible in most laboratories around the globe and applicable to any human iPS cell lines. With the latter, I had problems when referring to the reputable protocol of Kogut et al.<sup>65</sup>. I tried to reproduce their results and efficiency of differentiation using my WTC and C5 cells. I could not achieve comparably high levels of keratinocyte-specific protein expression (keratin 8/18, keratin 14, p63, involucrin), although I reproduced and confirmed their claim that the “rapid attachment” method (described in 2.3) is superior to an overnight attachment (Figure 21) as keratin 14 did elevate significantly. As keratin 8/18 is a protein of early differentiation in keratinocytes<sup>80</sup>, which stops being expressed in higher epidermal layers (Figure 13), it was a confirmatory finding that keratin 8/18 expression did not elevate in the same way as keratin 14. As a helpful reference to further boost these expression levels, I implemented parts of the methods tested by Kajiwara et al.<sup>68</sup> Their team aimed to find a therapy model for myelomeningoceles in human foeti with three-dimensional skin. I reduced the change of medium to every second day, after Day 4; I also simplified the coating to collagen I and IV from the start; used DKFS medium throughout the differentiation period; and implemented the use of EGF and Y-27632.

Kajikawa et al. introduced the use of calcium in the process of differentiation, which I further examined by gradually elevating the calcium concentration compared to an elevation of the calcium level in just one step. The first method was found to be superior (Figure 26) in terms of involucrin expression level and a plainer expression all over the cell. The expression of keratin 14 decreased, as expected in superficial layers of the skin. A possible reason why the successive elevation of calcium is superior is that it imitates the natural habitat of keratinocytes in the human epidermis. The calcium levels I used were comparable to those described by Bilousova et al.<sup>81</sup>, although they tested them on mouse-derived iPS cells.

Another aspect highlights my protocol's effectiveness compared with those of previous studies. The use of DAPT had previously been tested only in embryonic stem cells, not in human iPS cells, and with the single aim of improving p63 expression<sup>77</sup> rather than in the context of a keratinocyte differentiation protocol. Because iPS cells are stem cells and the p63 protein is characteristic of keratinocytes, the use of DAPT could logically accelerate the differentiation into dermal cells. As presented in Figure 23, I could not observe this predicted effect on p63 in my cells. However, I noted a slight elevation of keratin 14 in all cell lines, whereas keratin 8/18 expression remained stable or dropped; these are all signs of improvement for overall differentiation into keratinocytes. As DAPT was shown to have an elevating effect on the expression of p63, the biochemical interaction between DAPT and keratin 14 which I observed remains unclear. It requires further examination and verification.

The last new element I implemented was the use of CHIR. This is a small membrane-permeable molecule that is widely utilized for maintenance and differentiation of

---

embryonic stem cells of different species. It operates by activating the Wnt/ $\beta$ -catenin pathway<sup>82</sup>. My intent was not improvement in terms of differentiation; I had noted significant cell loss during the cultivating and passaging of the rather vulnerable iPS cell lines and wanted to strengthen them. A possible criticism is that by using CHIR, the protocol did not follow the natural flow of differentiation observed in nature. However, my results showed no obvious change in the genomic expression from its usage (Figure 25). The viability of the cells improved and I approved it for my protocol.

One chemical I would further examine in the future is calcipotriol, which I learned about as treatment for psoriasis by inhibiting proliferation but also accelerating differentiation of the dysregulated ceratinocytes<sup>83</sup>.

#### **4.2. Difficulties of gene knockdown in iPS cells**

A short comment about the cell line of XPA that I was unable to produce with my CRISPRi knockdown technique is required. Reasons I failed might be off-target effects, meaning unintended interactions with the gRNA on different sites, then the one actually targeted. I used the Basic Local Alignment Search Tool (BLAST)<sup>84</sup> to double-check the off-targets indicated by the Massachusetts Institute of Technology's gRNA design tool for CRISPRi<sup>59</sup> and found certain differences. Also, although unlikely considering my 25bps short gRNA, the hairpin structure of the dCas9-binding site might be influenced by the gRNA.<sup>85</sup> Furthermore, the database used to design the gRNA is not a result of a complete examination of the genome, but partly a product of stochastic calculation and therefore it holds a risk for slightly mistaken sequences. Another risk is possible variation between the genome of my C5 cells and the genome provided by the University of

California Santa Cruz, on which I based my analysis. Last, the area around the start of the first exon (I used -150bps) is not necessarily equal to the promotor of that gene<sup>86</sup>. In that case, attaching the dCas9 system via gRNA to that area would not effectively knock down the expression of the gene targeted.

The second and not yet completed aspect of my research aims to raise my basic research to a clinically applicable level.

#### **4.3. Translational medicine based on this research**

As summarized in Figures 33 and 36 my results showed different levels of viability and ROS expression under oxidative stress for each cell line, reacting to great extend accordingly to their actual clinical presentation, but also need to be viewed in the context of previous research. That is, UVSSA deficiency appears not to cause serious problems with lesions induced by oxidative stress, but will cause problems due to DNA helix-distortion lesions induced by UV light. It still has sufficient XP proteins and GG-NER that can repair most of the damage caused. XP-protein deficiency, depending on the subtype, can incur serious problems in repairing DNA helix-distortion lesions in exons as well as in introns because GG-NER is insufficient. However, CSB and other TC-NER related proteins can compensate for some of the damage-repair functions. Inherently this repair can occur only in lesions in transcribed exons. This compensation seems to be more effective in oxidative lesions than in helix-distortion lesions.

Last, CS-protein deficiency causes serious problems in oxidative lesions as well as in helix-distortion lesions. Oxidative stress seems to be a more fundamental and sensitive factor in DNA damage, causing more severe problems than helix-distortion lesions, even

though a helix distortion is generally seen as heavier damage. Despite CS-proteins deficiency would mainly affect the TC-NER while GG-NER should still have some capacity due to working XP-proteins, almost 80% of the CS patients (Figure 3) show clinical photosensitivity, which might be explained by the RNA polymerase II being stuck at the lesion and thus making the site of damage inaccessible for other repair mechanisms<sup>57</sup>.

By deepening the understanding of this group of diseases, I hope to optimize the current symptomatic treatment of patients. In addition, I hope to present new ideas that will not merely alleviate symptoms but rather treat the disease before symptoms occur. In terms of symptomatic treatment, I could suggest several chemicals to lower the stress level in cells. One is CHIR, for which I showed that – at least at a cell level *in vitro* – it strengthened the cells, without changing the keratinocyte character of the cell itself (Figures 25 and 32). This might imply a role for the Wnt/ $\beta$ -catenin pathway in the mechanism of NER. Other drugs said to prevent cells from being damaged by genomic stress and high ROS expression are 5H4PB<sup>87</sup> and nicotinamide mononucleotide (NMN)<sup>88,89</sup>. These should be further examined.

Regarding a complete cure, a comprehensive review on gene therapy for XP was conducted by Gonçalves-Maia et al. The authors suggested that despite promising results for retrovirus-mediated gene transfer *in vitro*, bona fide genetic correction with CRISPR technology (for example) is more promising for the future<sup>90</sup>. I used the CRISPRi (*interference*) method to knockdown specific genes in healthy iPS cells to create model cells for XP, CS and UVSS. Hence, it seems reasonable that an elevation of the expression level by CRISPRa (*activation*) might improve the robustness of the cells. Many patients

with XP, CS and UVSS do not have a complete absence of the corresponding proteins but rather very low expression<sup>91</sup>. Thus, CRISPR might be a promising approach to alleviate the phenotype of the patients, and to give young patients a normal life – including playing outside in the sunlight.

## 5. References

1. Menck CF, Munford V. DNA repair diseases: What do they tell us about cancer and aging? *Genet Mol Biol.* 2014;37(1 Suppl):220-233.
2. Wagener Cea. *Molekulare Onkologie.* Thieme; 2010.
3. Marnett LJ, Plataras JP. Endogenous DNA damage and mutation. *Trends Genet.* 2001;17(4):214-221.
4. Lankinen MH, Vilpo LM, Vilpo JA. UV- and gamma-irradiation-induced DNA single-strand breaks and their repair in human blood granulocytes and lymphocytes. *Mutat Res.* 1996;352(1-2):31-38.
5. Fromme JC, Banerjee A, Verdine GL. DNA glycosylase recognition and catalysis. *Curr Opin Struct Biol.* 2004;14(1):43-49.
6. Sancar A. DNA excision repair. *Annu Rev Biochem.* 1996;65:43-81.
7. Le May N, Egly JM, Coin F. True lies: the double life of the nucleotide excision repair factors in transcription and DNA repair. *J Nucleic Acids.* 2010;2010.
8. GeneCards®. <https://www.genecards.org>. Published 2018. Accessed 30.11.2018.
9. Ishino Y, Shinagawa H, Makino K, Amemura M, Nakata A. Nucleotide sequence of the iap gene, responsible for alkaline phosphatase isozyme conversion in Escherichia coli, and identification of the gene product. *J Bacteriol.* 1987;169(12):5429-5433.
10. Breakthrough Prize. <https://breakthroughprize.org/Laureates/2/P1/Y2015>. Published 2015. Accessed 30.11.2018.
11. New York Times. Chinese Scientist Claims to Use Crispr to Make First Genetically Edited Babies. <https://www.nytimes.com/2018/11/26/health/gene-editing-babies-china.html>. Published 2018. Accessed 30.11.2018.
12. Horvath P, Barrangou R. CRISPR/Cas, the immune system of bacteria and archaea. *Science.* 2010;327(5962):167-170.
13. Doudna JA, Charpentier E. Genome editing. The new frontier of genome engineering with CRISPR-Cas9. *Science.* 2014;346(6213):1258096.
14. Jinek M, Chylinski K, Fonfara I, Hauer M, Doudna JA, Charpentier E. A programmable dual-RNA-guided DNA endonuclease in adaptive bacterial immunity. *Science.* 2012;337(6096):816-821.
15. Chen B, Gilbert LA, Cimini BA, et al. Dynamic imaging of genomic loci in living human cells by an optimized CRISPR/Cas system. *Cell.* 2013;155(7):1479-1491.
16. Ji W, Lee D, Wong E, et al. Specific gene repression by CRISPRi system transferred through bacterial conjugation. *ACS Synth Biol.* 2014;3(12):929-931.

17. Gilbert LA, Horlbeck MA, Adamson B, et al. Genome-Scale CRISPR-Mediated Control of Gene Repression and Activation. *Cell*. 2014;159(3):647-661.
18. Gilbert LA, Larson MH, Morsut L, et al. CRISPR-mediated modular RNA-guided regulation of transcription in eukaryotes. *Cell*. 2013;154(2):442-451.
19. Kotin RM, Linden RM, Berns KI. Characterization of a preferred site on human chromosome 19q for integration of adeno-associated virus DNA by non-homologous recombination. *EMBO J*. 1992;11(13):5071-5078.
20. Mandegar MA, Huebsch N, Frolov EB, et al. CRISPR Interference Efficiently Induces Specific and Reversible Gene Silencing in Human iPSCs. *Cell Stem Cell*. 2016;18(4):541-553.
21. Lander ES, Linton LM, Birren B, et al. Initial sequencing and analysis of the human genome. *Nature*. 2001;409(6822):860-921.
22. University of California Santa Cruz. Genome Browser. <https://genome.ucsc.edu>. Published 2017. Accessed 2017.
23. Kraemer KH, Lee MM, Scotto J. Xeroderma pigmentosum. Cutaneous, ocular, and neurologic abnormalities in 830 published cases. *Arch Dermatol*. 1987;123(2):241-250.
24. McKay BC, Chen F, Clarke ST, Wiggin HE, Harley LM, Ljungman M. UV light-induced degradation of RNA polymerase II is dependent on the Cockayne's syndrome A and B proteins but not p53 or MLH1. *Mutat Res*. 2001;485(2):93-105.
25. Lehmann AR, McGibbon D, Stefanini M. Xeroderma pigmentosum. *Orphanet J Rare Dis*. 2011;6:70.
26. Kleijer WJ, Laugel V, Berneburg M, et al. Incidence of DNA repair deficiency disorders in western Europe: Xeroderma pigmentosum, Cockayne syndrome and trichothiodystrophy. *DNA Repair (Amst)*. 2008;7(5):744-750.
27. Mareddy S, Reddy J, Babu S, Balan P. Xeroderma pigmentosum: man deprived of his right to light. *ScientificWorldJournal*. 2013;2013:534752.
28. Kelly CM, Latimer JJ. Unscheduled DNA synthesis: a functional assay for global genomic nucleotide excision repair. *Methods Mol Biol*. 2005;291:303-320.
29. Cleaver JE. Diagnosis of Xeroderma Pigmentosum and Related DNA Repair-Deficient Cutaneous Diseases. *Curr Med Lit Dermatol*. 2008;13(2):41-48.
30. American Cancer Society. Cancer Statistic Center. [https://cancerstatisticscenter.cancer.org/?\\_ga=2.210845078.20531983.1543339164-1454720663.1543339164#!/cancer-site/Melanoma%20of%20the%20skin](https://cancerstatisticscenter.cancer.org/?_ga=2.210845078.20531983.1543339164-1454720663.1543339164#!/cancer-site/Melanoma%20of%20the%20skin) Published 2017. Accessed 27.11.2018, 2018.

31. Nance MA, Berry SA. Cockayne syndrome: review of 140 cases. *Am J Med Genet.* 1992;42(1):68-84.
32. Wilson BT, Stark Z, Sutton RE, et al. The Cockayne Syndrome Natural History (CoSynNH) study: clinical findings in 102 individuals and recommendations for care. *Genet Med.* 2016;18(5):483-493.
33. Genetics Home Reference. Xeroderma pigmentosum. Genetics Home Reference. <https://ghr.nlm.nih.gov/condition/xeroderma-pigmentosum> Published 2018. Accessed June 26, 2018.
34. Webb S. Xeroderma pigmentosum. *BMJ.* 2008;336(7641):444-446.
35. Oh KS, Khan SG, Jaspers NG, et al. Phenotypic heterogeneity in the XPB DNA helicase gene (ERCC3): xeroderma pigmentosum without and with Cockayne syndrome. *Hum Mutat.* 2006;27(11):1092-1103.
36. Fan L, Arvai AS, Cooper PK, Iwai S, Hanaoka F, Tainer JA. Conserved XPB core structure and motifs for DNA unwinding: implications for pathway selection of transcription or excision repair. *Mol Cell.* 2006;22(1):27-37.
37. Kubota M, Ohta S, Ando A, et al. Nationwide survey of Cockayne syndrome in Japan: Incidence, clinical course and prognosis. *Pediatr Int.* 2015;57(3):339-347.
38. Mala Cards® Human Gene Database. Uv-Sensitive Syndrome. Weizmann Institute of Science, Life Map Science. [http://www.malacards.org/card/uv\\_sensitive\\_syndrome](http://www.malacards.org/card/uv_sensitive_syndrome). Accessed October 20, 2017.
39. Gene Cards® Human Gene Database. ERCC6. Weizmann Institute of Science, Life Map Science. <https://www.genecards.org/cgi-bin/carddisp.pl?gene=ERCC6>. Published 2018. Accessed November 26, 2017.
40. Gene Cards® Human Gene Database. ERCC8. Weizmann Institute of Science, Life Map Science. <https://www.genecards.org/cgi-bin/carddisp.pl?gene=ERCC8>. Published 2018. Accessed November 27, 2017.
41. コケイン症候群研究会 (Cockayne Syndrome Research Group; National Center for Child Health and Development). コケイン症候群各論 (Detailed Description of Cockayne Syndrome). National Center for Child Health and Development. <http://www.cockayneresearchcare.jp/idea/journal1.html>. Accessed October 16, 2017.
42. Genetics Home Reference. ERCC6. Genetics Home Reference. <https://ghr.nlm.nih.gov/gene/ERCC6>. Accessed June 16, 2018.
43. Genetics Home Reference. ERCC8. Genetics Home Reference. <https://ghr.nlm.nih.gov/gene/ERCC8>. Published 2018. Accessed June 16, 2018.

44. Ogi T, Nakazawa Y, Sasaki K, et al. [Molecular cloning and characterisation of UVSSA, the responsible gene for UV-sensitive syndrome]. *Seikagaku*. 2013;85(3):133-144.
45. orphanet. UVSSA. [https://www.orpha.net/consor/cgi-bin/Disease\\_Search.php?lng=EN&data\\_id=638&Disease\\_Disease\\_Search\\_diseaseGroup=Cockayne-syndrome&Disease\\_Disease\\_Search\\_diseaseType=Pat&Disease\(s\)/group%20of%20diseases=Cockayne-syndrome&title=Cockayne%20syndrome&search=Disease\\_Search\\_Simple](https://www.orpha.net/consor/cgi-bin/Disease_Search.php?lng=EN&data_id=638&Disease_Disease_Search_diseaseGroup=Cockayne-syndrome&Disease_Disease_Search_diseaseType=Pat&Disease(s)/group%20of%20diseases=Cockayne-syndrome&title=Cockayne%20syndrome&search=Disease_Search_Simple). Published 2018. Accessed 30.11.2018.
46. Schwertman P, Vermeulen W, Marteiijn JA. UVSSA and USP7, a new couple in transcription-coupled DNA repair. *Chromosoma*. 2013;122(4):275-284.
47. Higa M, Zhang X, Tanaka K, Saijo M. Stabilization of Ultraviolet (UV)-stimulated Scaffold Protein A by Interaction with Ubiquitin-specific Peptidase 7 Is Essential for Transcription-coupled Nucleotide Excision Repair. *J Biol Chem*. 2016;291(26):13771-13779.
48. Nakazawa Y, Sasaki K, Mitsutake N, et al. Mutations in UVSSA cause UV-sensitive syndrome and impair RNA polymerase IIo processing in transcription-coupled nucleotide-excision repair. *Nat Genet*. 2012;44(5):586-592.
49. Graduate School of Biosciences Osaka University. DNA 損傷を修復する仕組みとその異常疾患とその分子病態を解明する . Tanaka Lab. <http://www.fbs.osaka-u.ac.jp/omoroiseimei/introduction/lab14-tanaka.html>. Accessed 13.12.2018.
50. Zhang X, Horibata K, Saijo M, et al. Mutations in UVSSA cause UV-sensitive syndrome and destabilize ERCC6 in transcription-coupled DNA repair. *Nat Genet*. 2012;44(5):593-597.
51. Gene Cards® Human Gene Database. UVSSA. Weizmann Institute of Science, Life Map Science. <https://www.genecards.org/cgi-bin/carddisp.pl?gene=UVSSA>. Accessed November 27, 2017.
52. National Center for Biotechnology Information. UVSSA UV stimulated scaffold protein A [ Homo sapiens (human) ]. <https://www.ncbi.nlm.nih.gov/gene/57654>. Published 2018. Accessed November 11, 2017.
53. Spivak G, Hanawalt PC. Host cell reactivation of plasmids containing oxidative DNA lesions is defective in Cockayne syndrome but normal in UV-sensitive syndrome fibroblasts. *DNA Repair (Amst)*. 2006;5(1):13-22.
54. El-Hattab AW, Adesina AM, Jones J, Scaglia F. MELAS syndrome: Clinical manifestations, pathogenesis, and treatment options. *Mol Genet Metab*. 2015;116(1-2):4-12.
55. Stevnsner T, Nyaga S, de Souza-Pinto NC, et al. Mitochondrial repair of 8-oxoguanine is deficient in Cockayne syndrome group B. *Oncogene*. 2002;21(57):8675-8682.

56. Scheibye-Knudsen M, Ramamoorthy M, Sykora P, et al. Cockayne syndrome group B protein prevents the accumulation of damaged mitochondria by promoting mitochondrial autophagy. *J Exp Med*. 2012;209(4):855-869.
57. Hanawalt PC, Spivak G. Transcription-coupled DNA repair: two decades of progress and surprises. *Nat Rev Mol Cell Biol*. 2008;9(12):958-970.
58. Lonza Cologne AG. Amaxa® Human CD34+ Cell Nucleofector® Kit. <http://bio.lonza.com/go/op/71>. Published 2009. Accessed April 1, 2018.
59. Massachusetts Institute of Technology. Guide Design Tool for CRISPR. <http://crispr.mit.edu>. Accessed.
60. GSL Biotech. Snapgene. <http://www.snapgene.com>. Published 2018. Accessed 2017-2018.
61. Molecular Research Center I. RNAzol® RT (RN 190). <https://www.mrcgene.com/wp-content/uploads/2017/04/RNAzolRTMarch2017.pdf>. Published 2017. Accessed June 28, 2017.
62. TAKARA. PrimeScript™ RT Master Mix (Perfect Real Time). [http://www.takara.co.kr/file/manual/pdf/RR036A\\_e.v1103Da.pdf](http://www.takara.co.kr/file/manual/pdf/RR036A_e.v1103Da.pdf). Published 2017. Accessed May 17, 2017.
63. TAKARA. Premix Ex Taq™ (Probe qPCR), ROX plus. [http://www.takara.co.kr/file/manual/pdf/RR39LR\\_e.v1209Da.pdf](http://www.takara.co.kr/file/manual/pdf/RR39LR_e.v1209Da.pdf). Published 2017. Accessed May 20, 2017.
64. Miyaoka Y, Chan AH, Judge LM, et al. Isolation of single-base genome-edited human iPS cells without antibiotic selection. *Nat Methods*. 2014;11(3):291-293.
65. Kogut I, Roop DR, Bilousova G. Differentiation of human induced pluripotent stem cells into a keratinocyte lineage. *Methods Mol Biol*. 2014;1195:1-12.
66. REPROCELL USA Inc. Stemgent Stemmolecule DAPT. <https://www.reprocell.com/small-molecules-c1/stemgent-stemmolecule-dapt-p240>. Published 2018. Accessed 19.12.2018.
67. Tadeu AM, Lin S, Hou L, et al. Transcriptional profiling of ectoderm specification to keratinocyte fate in human embryonic stem cells. *PLoS One*. 2015;10(4):e0122493.
68. Kajiwara K, Tanemoto T, Wada S, et al. Fetal Therapy Model of Myelomeningocele with Three-Dimensional Skin Using Amniotic Fluid Cell-Derived Induced Pluripotent Stem Cells. *Stem Cell Reports*. 2017;8(6):1701-1713.
69. Bikle DD, Xie Z, Tu CL. Calcium regulation of keratinocyte differentiation. *Expert Rev Endocrinol Metab*. 2012;7(4):461-472.
70. Logos Biosystems I. LUNA™ Automated Cell Counter. <https://logosbio.com/automated-cell-counters/brightfield/luna>. Published 2018. Accessed 19.12.2018.

71. Svobodova A, Walterova D, Vostalova J. Ultraviolet light induced alteration to the skin. *Biomed Pap Med Fac Univ Palacky Olomouc Czech Repub.* 2006;150(1):25-38.
72. Feldmeyer L, Keller M, Niklaus G, Hohl D, Werner S, Beer HD. The inflammasome mediates UVB-induced activation and secretion of interleukin-1beta by keratinocytes. *Curr Biol.* 2007;17(13):1140-1145.
73. Gentile M. Cell cycle arrest and apoptosis provoked by UV radiation-induced DNA damage are transcriptionally highly divergent responses. *Nucleic Acids Research.* 2003;31(16):4779-4790.
74. Niedernhofer LJ, Garinis GA, Raams A, et al. A new progeroid syndrome reveals that genotoxic stress suppresses the somatotroph axis. *Nature.* 2006;444(7122):1038-1043.
75. Schieber M, Chandel NS. ROS function in redox signaling and oxidative stress. *Curr Biol.* 2014;24(10):R453-462.
76. Li Y, Shelat H, Geng YJ. IGF-1 prevents oxidative stress induced-apoptosis in induced pluripotent stem cells which is mediated by microRNA-1. *Biochem Biophys Res Commun.* 2012;426(4):615-619.
77. Tadeu AM, Horsley V. Notch signaling represses p63 expression in the developing surface ectoderm. *Development.* 2013;140(18):3777-3786.
78. Tong C, Huang G, Ashton C, Li P, Ying QL. Generating gene knockout rats by homologous recombination in embryonic stem cells. *Nat Protoc.* 2011;6(6):827-844.
79. National Institutes of Health. ImageJ. <https://imagej.nih.gov/ij/>. Published 2004. Accessed July 20, 2017.
80. Cheng C, Tennenbaum T, Dempsey PJ, Coffey RJ, Yuspa SH, Dlugosz AA. Epidermal growth factor receptor ligands regulate keratin 8 expression in keratinocytes, and transforming growth factor alpha mediates the induction of keratin 8 by the v-rasHa oncogene. *Cell Growth Differ.* 1993;4(4):317-327.
81. Bilousova G, Chen J, Roop DR. Differentiation of mouse induced pluripotent stem cells into a multipotent keratinocyte lineage. *J Invest Dermatol.* 2011;131(4):857-864.
82. Wu Y, Liu F, Liu Y, et al. GSK3 inhibitors CHIR99021 and 6-bromoindirubin-3'-oxime inhibit microRNA maturation in mouse embryonic stem cells. *Sci Rep.* 2015;5:8666.
83. Kragballe K, Wildfang IL. Calcipotriol (MC 903), a novel vitamin D3 analogue stimulates terminal differentiation and inhibits proliferation of cultured human keratinocytes. *Arch Dermatol Res.* 1990;282(3):164-167.
84. National Center for Biotechnology Information. Basic Local Alignment Search Tool. <https://blast.ncbi.nlm.nih.gov/Blast.cgi>. Published 2018. Accessed 19.12.2018.

- 
85. Larson MH, Gilbert LA, Wang X, Lim WA, Weissman JS, Qi LS. CRISPR interference (CRISPRi) for sequence-specific control of gene expression. *Nat Protoc.* 2013;8(11):2180-2196.
  86. Zhang MQ. Computational analyses of eukaryotic promoters. *BMC Bioinformatics.* 2007;8 Suppl 6:S3.
  87. Tabei Y, Murotomi K, Umeno A, et al. Antioxidant properties of 5-hydroxy-4-phenyl-butenolide via activation of Nrf2/ARE signaling pathway. *Food Chem Toxicol.* 2017;107(Pt A):129-137.
  88. Guan Y, Wang SR, Huang XZ, et al. Nicotinamide Mononucleotide, an NAD(+) Precursor, Rescues Age-Associated Susceptibility to AKI in a Sirtuin 1-Dependent Manner. *J Am Soc Nephrol.* 2017;28(8):2337-2352.
  89. Tsubota K. Anti-Aging Approach for Ocular Disorders: from Dry Eye to Retinitis Pigmentosa and Myopia. *Nippon Ganka Gakkai Zasshi.* 2017;121(3):232-248.
  90. Goncalves-Maia M, Magnaldo T. Genetic therapy of Xeroderma Pigmentosum: analysis of strategies and translation. *Expert Opinion on Orphan Drugs.* 2017;5(1):5-17.
  91. Bowden NA, Tooney PA, Scott RJ. Gene expression profiling of xeroderma pigmentosum. *Hered Cancer Clin Pract.* 2006;4(2):103-110.

**6. List of abbreviations**

AAVS1	Adeno-Associated Virus Integration Site 1
ATP	Adenosine Triphosphate
BER	Base excision repair
bME	Basal Medium Egel
BMP4	Bone morphogenetic protein 4
bp	Base pair
C5	WTC with dCas9 activity
CD	Cluster of Differentiation
CnT-PR	CELLnTEC-Prime, Epithelial Culture Medium
Col I, IV	Collagen I, IV
CRISPRi	Clustered Regularly Interspaced Short Palindromic Repeats interference
CS	Cockayne Syndrome
Cy5 (Filter)	Cyan 5 (Filter)
DAPT	N-[N-(3,5-difluorophenacetyl)-1-alanyl]-S-phenylglycine t-butylester
DMEM, KO-DMEM	Dulbecco's modified Eagle's medium, Knockout DMEM
DMSO	Dimethyl Sulfoxide
DKSFM	Defined Keratinocyte Serum Free Medium
DOX	Doxycycline
DTT	Dithiothreitol
FBS	Fetal Bovine Serum
FcR	Fc Receptor
FGF	Fibroblast Growth Factor
FR (Filter)	Far Red (Filter)
E. coli	Escherichia coli

EcoRI	Restriction Enzyme EcoRI 5'-GAATTC-3'
EDTA	Ethylenediaminetetraacetic acid
EGF	Epidermal Growth Factor
EiIS	iPS cells derived from a patient with CS (subtype ERCC6 point mutation)
ES, h-ES	Embryotic Stem cell, Human ES
GFP	Green Fluorescent Protein
GRCh37/hg19	Genome Reference Consortium human genome build 37 with UCSC genomic annotations version 19
gRNA	Guided Ribonucleic Acid
H <sub>2</sub> DCFDA	2',7'-Dichlorodihydrofluorescein-Diacetate
HRP	Horseradish Peroxidase
ICU	Intensive Care Unite
IgG	Immunoglobulin Gamma
iPS cell	Induced Pluripotent Stem cell
K1/4/8/18	Keratin 1/4/8/18
KOD Plus	High fidelity DNA polymerase (obtained from hyperthermophilic Archaeon <i>Thermococcus kodakaraensis</i> )
KRAB	Krüppel-associated box
KSR	Knockout Serum Replacement
MACS	Magnetic-activated cell sorting
MMR	Mismatch repair
NaF	Sodium Fluoride
NEAA	Non Essential Amino acids
NER, TC-NER GG-NER	Nucleotide excision repair, Transcription-coupled NER Global genomic NER
NotI	Restriction Enzyme NotI 5'- GCGGCCGC -3'

p63	Tumor protein p63 or transformation-related protein 63
Pax6	Paired box protein Pax-6, also known as aniridia type II protein (AN2) or oculorhombin
PBS	Phosphate Buffered Saline
PBMC	Peripheral Blood Mononuclear Cell
PCR, rtPCR	Polymerase Chain Reaction, Reverse transcription PCR
PS	Phosphatidylserin
PVDF	Polyvinylidene fluoride
RCF	Relative Centrifugal Force
RA	Retinoic Acid
ROS	Reactive Oxidative Species
RT	Room Temperature
rtTA	Reverse transcriptional Activator
TFIIH	Transcription Factor IIH
SDS-PAGE	Sodium dodecyl sulfate–polyacrylamide gel electrophoresis
TBS	Tris-Buffered Saline
TRE	Transcriptional Response Element
Ub	Ubiquitin
UDS	Unscheduled DNA Synthesis
UV	Ultraviolet
UVSSA	Ultraviolet Sensitive Syndrome
WTC	Wild Type C human iPS cells derived by Miyaoka et al. <sup>64</sup>
XP	Xeroderma Pigmentosum

## 7. Appendix

### Permission for data usage



I, Michio Asahi, professor for pharmacology at the Osaka Medical School hereby permit the student Tobias Prell, born 15.03.1994 in Munich, to use the data acquired during his research at my laboratory for his doctoral thesis, to submit it to the Ludwig Maximilian University Munich, and to publish it on the university's websites and in its libraries.

24.01.2020 Osaka

Date, Place

\_\_\_\_\_  
Prof. Dr. Michio Asahi

## Danksagung

Vorab danke ich Ihnen, lieber Leser, für Ihr Interesse und das Durchlesen meiner Forschungsarbeit.

Mein Dank gilt weiterhin all denjenigen, die diese Arbeit überhaupt erst ermöglicht haben. Dass dieses in vielerlei Hinsicht mit Hürden versehene Projekt zu realisieren war, habe ich der großartigen Unterstützung und dem guten Willen vieler Personen zu verdanken.

Angeboten wurde mir das Projekt erstmalig während einer Famulatur am Osaka Medical College durch Prof. Dr. Michio Asahi, der in Kooperation mit der Abteilung für Dermatologie die Rahmenbedingungen festlegte. Da seit damals mein Hauptinteresse der Pädiatrie galt, war ich, abgesehen von der neuartigen Technik der iPS-Zellen und deren Potential, auch sehr davon angetan, dass die zu beforschenden Krankheitsbilder v.a. Kinder und Jugendliche betreffen. Dass ich in Professor Dr. Christoph Klein als Leiter des Dr. von Haunerschen Kinderspitals und Leiter einer Forschungsgruppe am Gene Center Munich daraufhin einen Experten der Pädiatrie und zugleich der Stammzellforschung an meiner Heimatuniversität finden und für die Schirmherrschaft meines Vorhabens begeistern konnte, war ein mehr als glücklicher Umstand. Obwohl die Betreuung auf die Entfernung sich schwierig gestaltete, haben die richtungsweisende Ratschläge von Prof. Dr. Klein und weiterhin die vielen konkreten Verbesserungsvorschläge durch Dr. Maximilian Witzel mir bei der Ausarbeitung sehr weitergeholfen.

Obleich meine Arbeit nicht als Teil einer Forschungsgruppe oder eines Teamprojekts konzipiert war, habe ich v.a. in der Anfangsphase viele wertvolle Hilfestellungen durch die Mitarbeiter des Asahi Labs in Form von Benutzungshinweisen zu den diversen Geräten, Teilen von Chemikalien, Medien u.v.m. erhalten, wofür ich mich an dieser Stelle explizit bei Prof. Asahi, Prof. Tetsuya Hayashi, Kiichiro Tomoda, Hirofumi Morihara, Atsuo Nomura, Shuichi Yokoe, Kazumasa Moriwaki, all den Laborassistenten und selbstverständlich auch dem Labor-Hamster Iemitsu bedanken will, der mir auch in später Stunde, wenn sonst niemand mehr im Labor war, immer beigestanden ist. Weiterhin bedanke ich mich bei dem Dekan der Universität Prof. Dr. Yoshinori Otsuki und dem Internationalen Office, hierbei explizit Megumi Kondo und Moe Fukuzaki, die v.a. auch im Hinblick auf mein Visum viel Aufwand auf sich genommen haben.

Für finanzielle Unterstützung will ich dem Max-Weber Programm und dem Tokushu-kai Scholarship Fund danken, sowie all den Leuten, die ich bei meinen verschiedenen Nebenjobs während des Jahres kennenlernen durfte.

Doch wäre trotz fachlicher, formeller und finanzieller Unterstützung diese Arbeit ebenso wenig vollendet worden, wie sie nicht ohne die viele menschliche Unterstützung möglich gewesen wäre.

Eine wunderbare Abwechslung wurde mir hierbei durch den Fußball-Verein der Universität zu teil, der mich ohne Vorbehalte für das Forschungsjahr bei sich mittrainieren ließ und mir so die nötige körperliche Auslastung neben der geistigen ermöglichte. Auch anderen neuen und alten Freunden in Japan und in der Heimat will ich für ihre Unterstützung und menschlichen Beistand danken, insb. meinen damaligen Mitbewohnern sowie Kyoichi, Akira, Yoshito, Kengo, Lukas, Daniel und so vielen anderen.

Selbstverständlich gilt ein ganz besonderer Dank auch meiner Familie, hierbei vor allem meiner Mutter und meinem Bruder, die mich in jeder Lebenslage unterstützen.

All diesen Personen widme ich hiermit aus tiefer Dankbarkeit heraus diese Dissertation.

## 謝辞

この場を借りて、この論文を可能にしてくださった皆様に感謝の気持ちを申し上げます。限られた日本語能力で自分の気持ちを十分に伝える自信がありませんが、完成までの3年間を渡り、本当にたくさんの方々のお世話になりました。

ご招待してくださった朝日教授、学位論文の主任を努めてくださった Klein 教授、留学を可能にしてくださった大槻学長、ビザ関係などしてくださった近藤先生と福崎さん、試薬と情報を共有してくださったラボの皆さん - 特に友田先生、森原先生、野村先生、横江先生、森脇先生、ラボの助手の皆さん、深夜にでも相手してくださったラボのハムスター家光、奨学金をくださった Max-Weber Programm と徳洲会国際奨学財団と楽しく様々なアルバイトをさせてくださった皆さん、身体を動かさせてくださったサッカー部の皆さんとその OB である鳴海教授、留学先で仲良くしてくださった浦上達、善杜達、映達、シェアハウスの同居人たち、いつでも気晴らしに相手してくださった教一、健吾、Daniel、Lukas などなど...

そして勿論、私をいつも支えてくれている母と兄。

上記に述べた方全員、そして他にもお世話になった方々には心底から深謝している印としてこの論文を献上いたします。